

**Removal of Thiophene and
Benzothiophenes from Diesel by Metal
Oxide Based Sorbents**

BY

ABDULLAH ABDULLAH NAJI ALSWAT

A Thesis Presented to the
DEANSHIP OF GRADUATE STUDIES

KING FAHD UNIVERSITY OF PETROLEUM & MINERALS

DHAHRAN, SAUDI ARABIA

In Partial Fulfillment of the
Requirements for the Degree of

MASTER OF SCIENCE

In

CHEMISTRY

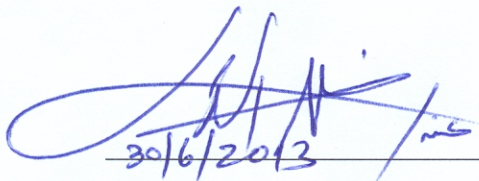
MAY, 2013

KING FAHD UNIVERSITY OF PETROLEUM & MINERALS

DHAHRAN- 31261, SAUDI ARABIA

DEANSHIP OF GRADUATE STUDIES

This thesis, written by **Abdullah Abdullah Naji Alswat** under the direction his thesis advisor and approved by his thesis committee, has been presented and accepted by the Dean of Graduate Studies, in partial fulfillment of the requirements for the degree of **MASTER OF SCIENCE IN CHEMISTRY**.


30/6/2013

Dr. Abdullah J. Al-Hamdan
Department Chairman



Dr. Salam A. Zummo
Dean of Graduate Studies





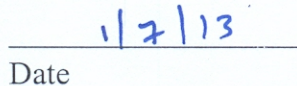
Dr. Khalid Alhooshani
(Advisor)



Dr. Mohammad Siddiqui
(Member)



Dr. Basheer Chanbasha
(Member)


Date

© Abdullah Abdullah Naji AlSwat

2013

DEDICATION

This work is dedicated to

My late father,

my mother, my beloved wife, and my children

ACKNOWLEDGMENTS

I am extremely grateful to Allah who gave me the health and ability to accomplish this work. Acknowledgment is due to the King Fahd University of Petroleum and Minerals for providing all facilities to finish this research.

I would like to express my deep thank to my thesis advisor Dr. Khalid Alhooshani for his supporting and guidance during this work. I also wish to thank the other members of my thesis committee, Dr. Mohammad Siddiqui and Dr. Basheer Chanbasha , for their valuable advises and comments.

Acknowledgment is due to Sana'a University for supporting me and giving me the opportunity to join to KFUPM to complete my MSc degree.

I would like to offer my deep appreciate to my family for their constant patient and supporting. Finally, I wish to thank all faculty members and staff of chemistry department at KFUPM.

TABLE OF CONTENTS

ACKNOWLEDGMENTS	V
TABLE OF CONTENTS	VI
LIST OF TABLES	IX
LIST OF FIGURES	X
ABSTRACT	XII
CHAPTER 1 INTRODUCTION	1
1.1 Sulfur compounds in transportation fuels.....	2
1.2 Effects of sulfur on the environment.....	7
1.3 Standards.....	7
1.4 PROBLEM STATEMENT	11
CHAPTER 2 LITERATURE REVIEW	12
2.1 Hydrodesulfurization (HDS).....	12
2.2 Oxidative desulfurization.....	13
2.3 Bio-desulfurization.....	14
2.4 Adsorptive desulfurization.....	15
2.4.1 Zeolites.....	15
2.4.2 Silica gel.....	17
2.4.3 Alumina.....	17
2.4.4 Metal Oxides.....	18
2.4.5 Activated carbon (AC).....	18
2.5 OBJECTIVES	25

3	CHAPTER 3 EXPERIMENTAL	26
3.1	Chemicals and materials	26
3.2	Preparation of the adsorbent.....	26
3.2.1	Preparation Activated Carbon (AC).....	26
3.2.2	Preparation of AC/NiO/ZnO	27
3.2.3	Preparation of AC/ZnO	27
3.2.4	Preparation of Alumina/ZnO	27
3.2.5	Preparation of Alumina/ NiO/ZnO.....	28
3.3	Characterization.....	28
3.3.1	Nitrogen Adsorption (BET).....	29
3.3.2	Fourier Transform Infrared spectroscopy (FT-IR)	29
3.3.3	X-ray diffraction (XRD).....	29
3.3.4	Energy Dispersive X-Ray Analysis (EDX)	29
3.4	Adsorption studies.....	30
3.4.1	Adsorption of model diesels in batch mode	30
3.4.2	Adsorption in a fixed-bed mode	30
3.5	Instrumentation.....	31
3.5.1	Gas Chromatography Sulfur Chemiluminescence Detector.....	31
3.5.2	Gas Chromatograph Linearity Response	33
3.6	GC- SCD Method of Analysis.....	35
3.7	Adsorption Kinetics	37
3.8	Adsorption Isotherms	38
3.9	Regeneration of the Adsorbents	38
	CHAPTER 4 RESULTS AND CONCLUSION	39
4.1	Characterizations	39

4.1.1	Surface area and pore size.....	39
4.1.2	Fourier transforms infrared (FT IR)	45
4.1.3	X-ray diffraction (XRD).....	49
4.1.4	Energy Dispersive X-Ray Analysis (EDX)	53
4.2	Adsorption studies	57
4.2.1	Comparison of adsorption desulfurization on the prepared adsorbents.....	57
4.2.2	Effect of dosage of the adsorbents	60
4.2.3	Effect of contact time	64
4.2.4	Adsorption experiments in a fixed-bed column	67
4.3	Adsorption kinetics	79
4.3.1	Pseudo-first-order	79
4.3.2	Pseudo-second-order	81
4.3.3	Intraparticle diffusion model.....	84
4.4	Adsorption isotherms	86
4.4.1	Langmuir isotherms.....	86
4.4.2	Freundlich isotherm	90
4.5	Regeneration of spent adsorbents	92
CONCLUSION		95
RECOMMENDATION FOR FUTURE WORK.....		96
REFERENCES.....		97
VITAE.....		109

LIST OF TABLES

Table 1.1 Typical sulfur compounds in petroleum fractions	3
Table 1.2 Arabian Crude Oils properties	6
Table 1.3 Maximum sulfur content in ppm	10
Table 3.1: Method optimum conditions.....	36
Table 4.1: BET Surface area and pore volume analysis	44
Table 4.2: Experimental q_e , pseudo-first-order, pseudo-second-order and Intraparticle diffusion models for adsorption of Thiophene, BT and DBT on AC, AC\ZnO and AC\NiO\ZnO.....	83
Table 4.3: Langmuir and Freundlich isotherm constants for Thiophene, BT and DBT onto AC, AC\ZnO and AC\NiO\ZnO	89

LIST OF FIGURES

Figure 1.1: Global trend on crude oil quality.....	8
Figure 2.1: Hydrodesulfurization (HDS) process used for removal of sulfur compounds	12
Figure 2.2: A typical reaction showing oxidative desulfurization (ODS) .	13
Figure 3.1: Gas chromatography sulfur chemiluminescence(355) Detector	32
Figure 3.2: Linearity response of GC- SCD for: a: thiophene , b:benzothiophene and c:dibenzothiophene	34
Figure 4.1a: Nitrogen adsorption/desorption isotherms for AC	40
Figure 4.1b: Nitrogen adsorption/desorption isotherms for AC\ ZnO.....	40
Figure 4.1c: Nitrogen adsorption/desorption isotherms for AC\ NiO\ZnO.....	41
Figure 4.1d: Nitrogen adsorption/desorption isotherms for Al ₂ O ₃ \ NiO\ZnO	41
Figure 4.1e: Nitrogen adsorption/desorption isotherms for Al ₂ O ₃ \ ZnO.....	42
Figure 4.2 a: FT-IR spectra of the prepared activated carbon	46
Figure 4.2 b: FT-IR spectra of AC\ ZnO	46
Figure 4.2 c: FT-IR spectra of AC\NiO\ZnO.....	47
Figure 4.2 d: FT-IR spectra of Al ₂ O ₃ \NiO\ZnO	47
Figure 4.2 e: FT-IR spectra of Al ₂ O ₃ \ ZnO.....	48
Figure 4.3 a: The XRD spectrogram of activated carbon prepared	50
Figure 4.3 b: The XRD spectrogram of AC\ ZnO	50
Figure 4.3 c: The XRD spectrogram of AC\NiO\ZnO	51
Figure 4.3 d: The XRD spectrogram of Al ₂ O ₃ \NiO\ZnO	51
Figure 4.3 e: The XRD spectrogram of Al ₂ O ₃ \ ZnO	52
Figure 4.4 a: EDX spectrum of the Activated Carbon (AC).....	54
Figure 4.4 b: EDX spectrum of AC\ZnO.....	54
Figure 4.4 c: EDX spectrum of AC\NiO\ZnO	55
Figure 4.4 d: EDX spectrum of Al ₂ O ₃ \NiO\ZnO.....	55
Figure 4.4 e: EDX spectrum of Al ₂ O ₃ \ ZnO.....	56
Figure 4.5: Percentage removal of thiophene, BT and DBT on AC, AC\NiO\ZnO, AC\ ZnO Alumina\NiO\ZnO and Alumina\ZnO.....	59
Figure 4.6: Effect of adsorbent dosage on the adsorption of thiophene, BT and DBT, on a: AC\NiO\ZnO and b: AC\ ZnO.....	61
Figure 4.6 c: Effect of adsorbent dosage on the adsorption of thiophene, BT and DBT, on AC.....	62
Figure 4.6 d: Effect of adsorbent dosage on the adsorption of thiophene, BT and DBT, on Alumina\NiO\ZnO.	63
Figure 4.7: Adsorption of sulfur compounds on a: AC\NiO\ZnO and b: AC\ ZnO at different time intervals.....	65
Figure 4.7: Adsorption of sulfur compounds on c: AC and d: Alumina\NiO\ZnO at different time intervals.....	66
Figure 4.8 a: Breakthrough curves of Thiophene on AC\NiO\ZnO, AC\ZnO and AC....	68

Figure 4.8 b: Breakthrough curves of BT on AC\NiO\ZnO , AC\ZnO and AC.....	70
Figure 4.8 c: Breakthrough curves of DBT on AC\NiO\ZnO , AC\ZnO and AC.....	72
Figure 4.9 a: GC-SCD chromatogram of the blank (hexan+toluene).....	73
Figure 4.9 b: GC-SCD chromatogram of sample (thiophene, BT and DBT) before adsorption processes	74
Figure 4.9 c: GC-SCD chromatogram of sample (thiophene, BT and DBT) after 10 min adsorption by AC	75
Figure 4.9 d: GC-SCD chromatogram of sample (thiophene, BT and DBT) after 10 min adsorption by AC\ZnO	76
Figure 4.9 e: GC-SCD chromatogram of sample (thiophene, BT and DBT) after 20 min adsorption by AC\ZnO	77
Figure 4.9 f: GC-SCD chromatogram of sample (thiophene, BT and DBT) after 10 min adsorption by AC\NiO\ZnO	78
Figure 4.10: First order Pseudo kinetics for adsorption of thiophene, BT and DBT by a: AC\NiO\ZnO, b: AC\ZnO and c: AC	80
Figure 4.11: Second order Pseudo kinetics for adsorption of thiophene, BT and DBT by a: AC\NiO\ZnO, b: AC\ZnO and c: AC	82
Figure 4.12: Plots for evaluating intraparticle diffusion rate constant for sorption of Thiophene, BT and DBT onto a: AC\NiO\ZnO, b: AC\ZnO and c: AC	85
Figure 4.13: plot of Langmuir isotherm for adsorption of thiophene, BT and DBT by a: AC\NiO\ZnO, b: AC\ZnO and c: AC	88
Figure 4.14: plot of Freundlich isotherm for adsorption of thiophene, BT and DBT by a: AC\NiO\ZnO, b: AC \ZnO and c: AC	91
Figure 4.15: amount of thiophene, BT and DBT desorbed from AC and AC\NiO\ZnO by toluene at different times	93
Figure 4.16: percentages of removal of thiophene, BT and DBT from model diesel by AC\NiO\ZnO, AC\ ZnO, and AC in three cycles	94

ABSTRACT

Full Name : Abdullah Abdullah Naji AlSwat
Thesis Title : Removal of Thiophene and Benzothiophenes from Diesel by Metal Oxide Based Sorbents
Major Field : Chemistry
Date of Degree : May, 2013

In this work, five different materials; Activated Carbon (AC) from waste rubber tire, Activated carbon\Nickel oxide\ Zinc oxide (AC\NiO\ZnO), Activated carbon \ Zinc oxide (AC\ ZnO), Alumina \Nickel oxide\ Zinc oxide (Al_2O_3 \NiO\ZnO) and Alumina \ Zinc oxide (Al_2O_3 \ ZnO) were prepared and used as adsorbents for removal of Thiophene, benzothiophen (BT) and dibenzothiophen (DBT) as a sulfur compounds from model diesel. The prepared materials were characterized by N_2 -adsorption, X-ray diffraction; Energy Dispersive X-Ray Analysis (EDX) and Fourier Transform Infrared spectroscopy (FTIR). The following adsorption capacity for the three compounds in the order: AC\NiO\ZnO > AC\ ZnO > AC > Alumina\NiO\ZnO > Alumina\ZnO, while the amount of compounds adsorbed follow the order DBT > BT > thiophene. Adsorption capacity is governed by chemical interaction and pore volume of the adsorbents. The results revealed that Freundlich isotherm provided a better fit to the experimental data while the adsorption kinetics followed the pseudo second-order. Obtained results indicate that the sorbents exhibited an efficient and economical way for removing sulfur compounds due to its low-energy consumption, ambient operation temperature and atmospheric pressure; rather, there was a simple regeneration method of the spent adsorbents.

ملخص الرسالة

الاسم الكامل: عبدالله عبدالله ناجي السوات

عنوان الرسالة: ازالة مركبات الثايوفين والبنزو ثايوفين من الديزل بواسطة أكاسيد المعادن مستندة على مميزات

التخصص: كيمياء

تاريخ الدرجة العلمية: مايو 2013

في هذا البحث تم تحضير خمسة نواع جديدة من المميزات ومن ثم تمت دراسة خصائصها وكذلك تطبيقاتها في مجال ازالة مركبات الثايوفين والبنزو ثايوفين كمركبات الكبريت من نموذج لزيت الوقود. المميزات الجديدة هي "الكربون المنشط" ذو مسامات نانوية الذي تم استخلاصه من اطارات السيارات القديمة, الكربون المنشط /أكسيد النيكل/أكسيد الزنك ، الكربون المنشط /أكسيد الزنك، الألومينا/أكسيد الزنك و الالومينا/أكسيد النيكل/أكسيد الزنك السعة الامتزازية للثلاثة المركبات كانت وفق الترتيب: الكربون المنشط /أكسيد النيكل/أكسيد الزنك < الكربون المنشط /أكسيد الزنك < الالومينا/أكسيد النيكل/أكسيد الزنك. بينما كانت المركبات الممتزة تتبع الترتيب : ثنائي بنزو ثايوفين < بنزو ثايوفين < ثايوفين. كما وجد أن سعة الامتزاز محكومة بواسطة التفاعل الكيميائي وحجم مسام المميزات. وكشفت النتائج أن فروندلنتش أيسوثرم أكثر مناسباً للنتائج العملية بينما حركية امتزاز تتبع الدرجة الثانية. النتائج التي تم الحصول عليها تشير إلى أن المميزات المحضرة تعتبر وسيلة فعالة واقتصادية لإزالة مركبات الكبريت نظراً لاستهلاكها المنخفض للطاقة كما انها تعمل تحت الظروف الطبيعية من درجة حرارة وضغط بالإضافة الى انه يمكن تجديدها بطريقة بسيطة وبالتالي اعادة استخدامها.

CHAPTER 1

INTRODUCTION

Producing energy is the most important issue in all over the world. While the global energy consumption in 2007 was about 12.0 billion toe (toe = tonnes of oil equivalent) it is expected to grow until 13.3 billion toe by 2015. Oil consumption rose from around 70 million barrels per day (bpd) in 1995 (1 barrel = 159 L) to over 80 (bpd) in 2005, and it is expected to grow to over 90 million barrels per day in 2020 [1]. Moreover, the demand for transportation fuels has been increasing in most countries for the past two decades, and the diesel fuel demand is expected to increase significantly in the early part of the 21st [2].

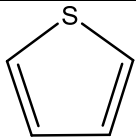
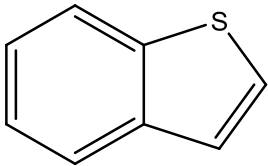
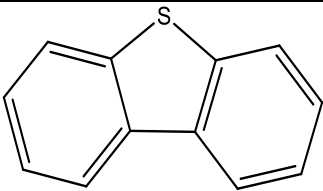
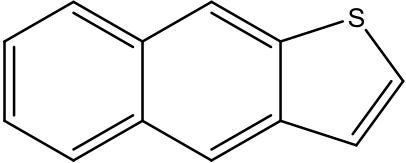
Crude oil, a complex mixture of organic liquids, is considered the largest source of energy and the major portions of the crude oils are used as transportation fuels such as gasoline, diesel and jet fuel. Aliphatic and aromatic hydrocarbons constitute the largest percentage of crude oils, ranging from 84 to 87 % weight of carbon and 11 to 14% weight of hydrogen. Hetero atoms include sulfur (0 - 5 %), nitrogen (0 – 0.2%), and other elements (e.g. oxygen, nickel, vanadium and iron) ranging from 0 to 0.1% weight and the sulfur content is expressed as a percentage of sulfur by weight and varies from less than 0.1% to greater than 5% depending on the type and source of crude oils [3].

1.1 Sulfur compounds in transportation fuels

There are four common types of sulfur compounds in liquid fuels the first type is Gasoline: naphtha, fluid catalytic cracking (FCC)–naphtha, Mercaptanes (RSH) like sulfides (R₂S); and disulfides (RSSR); Thiophene and its alkylated derivatives and Benzothiophene. Second type Jet fuel range which include heavy naphtha, middle distillate, (BT) and its alkylated derivatives.

Third type is diesel fuel range: middle distillate, light cycle oil (LCO), alkylated benzothiophenes; and (DBT) and its alkylated derivatives. The last type is boiler fuels feeds: heavy oils and distillation residues, \geq 3-ring polycyclic sulfur compounds, including DBT, benzonaphthothiophene (BNT); phenanthro[4,5-b,c,d]thiophene (PT), and their alkylated derivatives [4].

Table 1.1 Typical sulfur compounds in petroleum fractions [5]

Sulfur compounds	Chemical Structure
Thiols (mercaptans)	$R-S-H$
Sulfides	$R-S-R$
Disulfides	$R-S-S-R$
Thiophenes	
Benzothiophenes (BTs)	
Dibenzothiophenes (DBTs)	
Naphthothiophenes (NTs)	

In the past 30 years or so, a huge work has been made to comply with tightening refined product quality specifications. Throughout the 1980s and 1990s, regulators focused on lead content in gasoline. After a gradual shift to unleaded gasoline the process is still ongoing globally and the focus turned to sulfur content in the mid-1990s, especially in the EU, Japan, Canada and the US. This shift combined with the growing importance of diesel oil and gasoil, especially in road transportation, resulted in the tightening of quality requirements for these products too. In addition, the main goal of policymakers is to produce transportation fuels that have a sulfur content below 10 parts per million (ppm). The next step, which has already begun in a number of countries, is the extension of stricter sulfur specifications beyond on-road transportation to other products, particularly fuel oil, marine bunkers and jet fuel.

The measurement of crude oil quality typically depends on the terms of American Petroleum Institute API gravity and sulfur content, does, and will increasingly play an important role in determining future refining requirements [6]. Furthermore, the price differential between sour crude oil and sweet crude oil (crude oil having a relatively low level of sulfur compounds) favors sweet crude oil. Sweet crude oil commands a higher price than sour crude oil because it has fewer environmental problems and requires less refining to meet sulfur standards imposed on end-use product fuels [7].

In 2010, Saudi Arabia was the world's largest producer and exporter of total petroleum liquids and the world's second largest crude oil producer behind Russia. Saudi Arabia is the largest consumer of petroleum in the Middle East, particularly in the area of transportation fuels and direct burn for power generation [8]. The crude oils produced by the Saudi Arabian Oil Company (Saudi Aramco) are marketed under the following

names: Arabian Extra Light, which is a relatively high API gravity (38.50 °API) and low-sulfur, paraffinic-type crude oil. Arabian Light is produced from the Ghawar field, which is the largest onshore oil field in the world. Arabian Light is a moderately high-gravity (33.80 °API), medium-sulfur, and medium-paraffinic crude oil. Arabian Medium is produced from the Jurassic age Arab zone reservoirs as multistage separated oil from a blend of the following fields: 65% Khursaniya, 25% Qatif, and 10% Abu-Safah. This crude oil is a medium gravity (30.40 °API) paraffinic wax-containing crude oil [9].

Table 1.2 shows the Arabian crude oil characterization ,light crude oils or condensates contain in concentrations as low as 0.01 W%. In contrast, heavy crude oils contain as much as 5-6 W%. The nitrogen content of crude oils can range from 0.001 -1.0 W%.

Table 1.2 Arabian Crude Oils properties

Property	Super Light	Extra Light	Light	Medium	Heavy
Gravity	51.4	39.5	33.0	31.1	27.6
Sulfur, wt%	0.05	1.07	1.83	2.42	2.94
Nitrogen, ppm	70	446	1064	1417	1651
Ni+V	0.1	2.9	21	34.0	67

Where: wt% is percent by weight; ppm w is parts per million by weight [10]

1.2 Effects of sulfur on the environment

It is known that, sulfur compounds present in fuels lead to the emission of sulfur oxide gases (SO_x). These gases react with water in the atmosphere to form sulfates and acid rain which damages buildings, destroys automotive paint finishes, acidifies soil, and ultimately leads to loss of forests and various other ecosystems [11]. Traces of sulfur present in diesel fuels also poison the catalysts in the emission control system and reduce their effectiveness for the oxidation of harmful carbon monoxide, hydrocarbons and volatile organic matter. Sulfur emissions also cause several human health concerns such as, respiratory illnesses, aggravate heart disease, trigger asthma, and contribute to formation of atmospheric particulates [12], global warming and water pollution [13]. Moreover, the premature failure of combustion engines and poisoning the catalytic converters that used in automotive engines, as well as sulfur compounds can cause several corrosion problems in pipeline, pumping, and refining equipment [4,14].

1.3 Standards

Figure 1.1 shows the global trend on crude oil quality, moreover the strongest motivation for the reduction of sulfur in fuels today, is due to United State Environmental Protection Agency's (USEPA) regulation which is imposing stringent limits for sulfur levels in transportation fuels. Meanwhile, the demand for transportation fuels has been increasing in developed countries over the past two decades. Environmental regulations have been introduced in many countries around the world to reduce the sulfur content of diesel fuel to ultra-low levels of 10 ppm with the aim of lowering the diesel engine's harmful exhaust emissions and improving air quality [15].

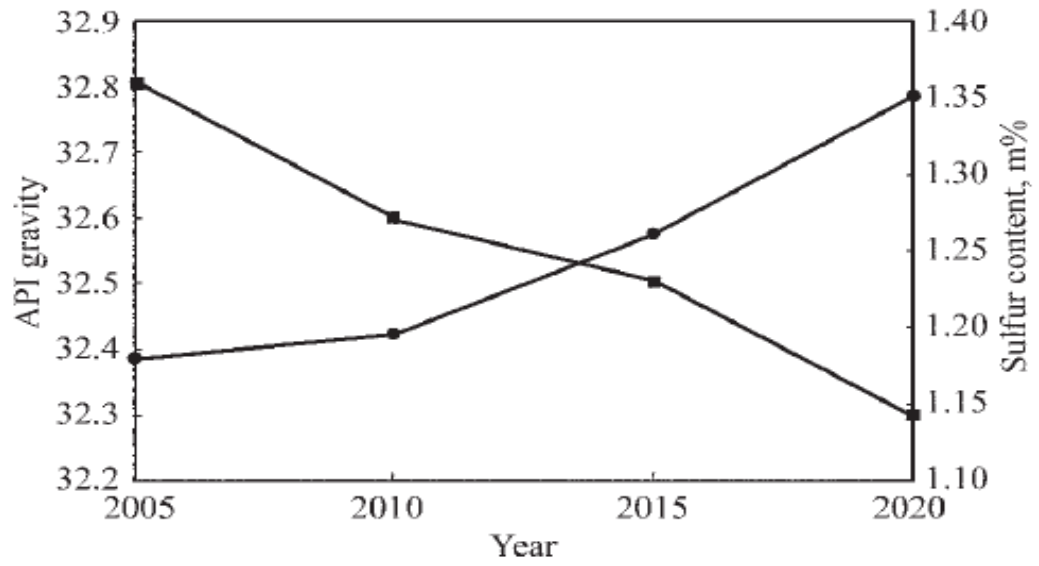


Figure 1.1 Global trend on crude oil quality [16]

- API gravity;
- Sulfur content, m%

Maximum sulfur content acceptable in the fuel around the world is summarized in Table 1.3. The primary focus of the new regulation is the reduction of sulfur in transportation fuels. In the United States of America (USA), the acceptable level of sulfur in highway diesel was first reduced from 2000 ppm to 500 ppm by the Clean Air Act (CAA) amendments in the nineties, then to 350 ppm, 50 ppm and 15 ppm in the years 2000, 2005, and 2006, respectively [17]. In the European Union (EU), Germany was the first country to adopt the 10 ppm sulfur limit for diesel as from January 2003. Other EU countries and Japan introduced diesel fuel with 10 ppm into the market from the year 2008 [18,19].

Table 1.3 Maximum sulfur content in ppm [20]

Region	Year			
	2010	2015	2020	2025
US/Canada	15	15	10	10
Europe	15	15	10	10
Asia-Pacific	230	150	100	100
Middle East	1,600	350	265	175

As a result, the problem of deep removal of sulfur has become more serious due to the lower limit of sulfur content in finished gasoline and diesel fuel. Therefore, desulfurization of fuels is extremely important in the petroleum industry and there is a need to research new desulphurization methods which are cost effective, more efficient and can meet the environmental regulations and refining requirements.

1.4 PROBLEM STATEMENT

Increasingly stringent environmental protection regulations mean that providing a clean fuel that meets the new emission control standards and environment friendly. Adsorptive desulfurization is a good challenge to remove sulfur compounds from the transportation fuels, because adsorption would be accomplished relatively at ambient temperature and pressure, cost effective adsorbents to be able to remove sulfur moieties to the lower level at ambient conditions without using hydrogen gas.

CHAPTER 2

LITERATURE REVIEW

Several trends are emerging toward minimizing sulfur content in transportation fuels to below 10 ppm. Various desulfurization techniques such as hydrodesulfurization (HDS), oxidative desulfurization (ODS), bio-desulfurization, and adsorptive desulfurization are being investigated to produce ultra-clean fuels.

2.1 Hydrodesulfurization (HDS)

The current industrial method for removal of sulfur from fuels is (HDS), for reducing of organic-sulfur in gasoline, diesel and other intermediate distillates where Co–Mo/Al₂O₃ or Ni–Mo/Al₂O₃, Ni–W/Al₂O₃ is used as the catalysts for the conversion of organic sulfur to H₂S (figure 2.1). This process successfully removes many sulfur compounds such as thiols, sulfides, disulfides and some thiophene derivatives, but to much lower extent removes dibenzothiophene derivatives due to the steric hindrance on the sulfur atom (refractory organosulfur compounds), such as 4,6-dimethyldibenzothiophene, which are present in diesel fuel with sulfur concentrations in the order 400 ppmw and high temperatures (300–400 °C) and pressure (20–100 atm of H₂), are needed which makes HDS a very costly option for deep desulfurization. [21,22].

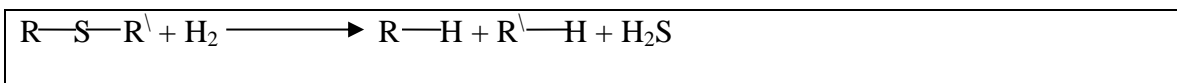


Figure 2.1 Hydrodesulfurization (HDS) process used for removal of sulfur compounds

2.2 Oxidative desulfurization

In the oxidation process, the sulfur containing compounds is oxidized to sulfone by chemical reaction (figure 2.2) using various types of oxidants namely H_2O_2 , H_2SO_4 , etc. The sulfone compound is then separated by way of adsorption on a solid adsorbent such as Al_2O_3 or by solvent extraction using extracting agents like acetonitrile because of its higher polarity [23–28].

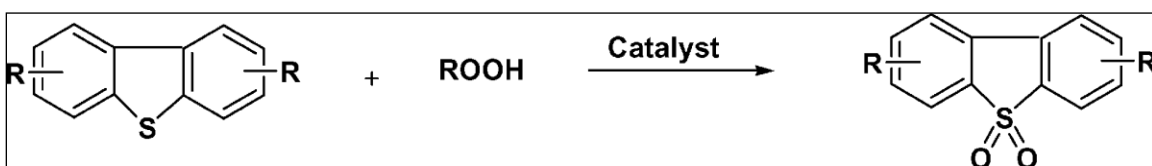


Figure 2.2 A typical reaction showing oxidative desulfurization (ODS) [29].

Though, they involve water in the reaction system which results in the biphasic problems of the mass transfer and oil phase recovery, peroxyacids and Hydrogen peroxide in aqueous solution used as oxidants for ODS [30,31]. Oxidative desulfurization process by homogeneous oxidation, Oil-soluble alkyl peroxides, such as tert-butyl hydroperoxide (BuOOH) [32,33] and cyclohexanone peroxide (CYHPO) [34,35], gave a simple ODS process but, their cost is still greatly concerned for developing an industrial feasible process. Zub et al. [36] took use of metal phthalocyanines as catalysts for direct oxidation of mercaptanes by O_2 , and similarly Aihua studied the oxidation of sulfides using O_2 in the presence of immobilized aluminum tetrasulfophthalocyanine in methanol–water solution [37]. However, the above oxidation does not deal with the refractory dibenzothiophenic compounds and was performed in polar solvent. Iron phthalocyanine attached with strong electron-withdrawing group, tetranitrophthalocyanine (FePc

(NO₂)₄), was employed as catalyst for direct oxidation of DBT using O₂ in non-polar hydrocarbon solvent under water-free condition [38].

Manganese and cobalt oxide catalysts supported on γ -Al₂O₃ used for catalyzing air oxidation of the sulfur impurities in diesel to corresponding sulfones at a temperature range of 130–200 °C and atmospheric pressure[39]. Di Giuseppe et al. Investigated oxidation of thiophene derivatives with homogeneous and heterogeneous MTO/H₂O₂ systems [40]. A Phosphotungstic acid/semi P coke catalyst was studied by wang for Oxidative desulfurization [41]. However, reaction selectivity, safety and cost are important concerns for the selection of oxidants, catalysts and operating conditions in ODS processing. The catalytic systems reported in literature are mostly toxic and expensive and some oxidants cause unwanted side reactions that reduce the quantity and quality of the light oil [42].

2.3 Bio-desulfurization

Bio-desulfurization has drawn wide attention over the past decade. Extensive research has been done for understanding of the enzymology and molecular genetics of the BDS system and to apply that into the design of the BDS bioreactor and bioprocesses [43-46]. Several species of bacteria metabolize organosulfur compounds in one of three ways: reductive C–S bond cleavage, oxidative C–S bond cleavage, and oxidative C–C bond cleavage [47]. Although, there is a lot of research going on in this area, Biological removal of sulfur has several limitations that prevent it from being applied today. The metabolism of sulfur compounds is typically slow compared to chemical reactions and ability of organic sulfur compounds [12,48].

However, to meet the challenges of producing ultra-clean fuels with sulfur content lower than 15 ppm, both capital investment and operational costs would increase due to more severe operating conditions. Consequently, advanced desulfurization technologies such as adsorption are needed [49].

2.4 Adsorptive desulfurization

Adsorption is a mass transfer process wherein molecules in a free phase become bound to a surface by intermolecular forces [50], it is often employed to remove trace impurities, such as the removal of trace amounts of aromatics from aliphatic [51] and it is the most common HDS alternative method currently used to achieve ultra-clean fuels [52]. Adsorptive desulfurization using porous materials is considered to be an efficient and economical way for removing organosulfur compounds due to its low-energy consumption, the ambient operation temperature and atmospheric pressure without using pressurized hydrogen gas and the availability of regeneration of the spent adsorbent and broad availability of adsorbents [53].

Various investigators have utilized adsorption technique for the removal of sulfur from various types of fuels and model oils by various types of adsorbents. Removal of sulfur compounds has been studied over zeolites, aluminosilicates, activated carbon (AC), alumina, and metal oxides.

2.4.1 Zeolites

Zeolites are crystalline aluminosilicates of alkali or alkali earth elements, such as sodium, potassium, and calcium. Many studies have been reported of using zeolites as adsorbents for sulfur removal. Weitkamp et al. examined the removal of thiophene from benzene

under dynamic condition using ZSM-5 and the adsorption capacity was 15-17 mg thiophene per gram zeolite [54]. Another study showed that ZSM-5 removed thiophene, 2-methyl thiophene and 2,5-dimethyl thiophene from toluene or xylene under static conditions [55]. Zeolite 13X reduced the sulfur level in non-HDS treated naphtha solution from 36.62 (mg/L) to 0.74 (mg/L) and a non-HDS treated naphtha solution from 412.2 (mg/L) to 287.3 (mg/L), but this sulfur level does not meet environmental regulation [56].

Hu et al. used a combination of ZSM-5/13X zeolites to extend the life of a reforming catalyst designed for portable power applications. The zeolite combination provided almost an additional 1 hr of life to the catalyst at 80% or better conversion. It shows that molecular sieves are promising options for onboard applications, particularly for unexploited options like the π -complexation adsorbents [57].

Ngamcharussrivichai et al. synthesized zeolites using coal fly ash. These zeolites were used for adsorption of thiophene and benzothiophene in n-hexane solution. It was shown that the introduction of different heteroatoms into the framework of zeolites leads to different catalytic and adsorption properties [58]. Tang et al. introduced gallium atoms into the framework of Y zeolite. Desulfurization of various model fuels containing about 500 mg sulfur/g was studied over the synthesized Y zeolite. The breakthrough capacity for the adsorption of sulfur compounds tested was found to be 7.0, 17.4 and 14.5 mg of sulfur/g of adsorbent, respectively [59].

Muzic et al. studied removal of dibenzothiophene from model fuel by adsorption on commercially available adsorbents including an activated carbon, aluminum oxide, 13X

and Y zeolite. The evaluation of the tested adsorbents showed that the best adsorptive performance was achieved by the Y zeolite [60].

2.4.2 Silica gel

Silica gel widely used as adsorbent as its surface can be readily modified by reacting (or grafting) with a monomolecular layer of organic ligand. Park et al. studied adsorption of sulfur compounds onto metallic nanosize Ni nanoparticles supported on mesoporous silica SBA-15 and KIT-6. The maximum Ni concentration achieved was 30 wt% for both the substrates. [61].

2.4.3 Alumina

Activated alumina is crystalline and has good adsorptive properties and has been used for the removal of organic compound from aqueous solutions [62]. Etemadi and Yen, studied the surface properties of two different phases of alumina (amorphous acidic alumina and nanopowder alumina) through SEM images. The effect of calcining on alumina particles was also investigated through SEM images. Adsorption capacity of amorphous acidic alumina was found to be 1.6 times lower than the nanopowder sample, though the surface area was 2.3 to 4.6 times smaller [63]. Srivastava, investigated the usage of commercial grade activated alumina (aluminum oxide) as adsorbent for the removal of DBT dissolved in n-hexane and they found that, the optimum adsorbent dose is 20g \L[42].

Recently, Manganese oxide was loaded on the surface of γ -Al₂O₃ by sub-critical water impregnation using manganese acetate and manganese nitrate precursors to synthesize Mn(A) and Mn(N) sorbents for removing H₂S from hot coal gas. The high desulfurization

activity of Mn(A) was better because of the dispersion of manganese on γ -Al₂O₃ and the higher Mn²⁺ and Mn³⁺ contents on the surface of sorbent [64].

2.4.4 Metal Oxides

Metal oxides are highly reactive towards sulfur compounds, especially thiols.

The process is based on thiophenes chemistry in which metal oxides react with thiophenes to form solid-metalthiolates. Study of comparative analysis of removing sulfur from crude oil was tested using activated manganese dioxide, and activated zinc oxide. The result showed that, activated manganese dioxide proved to be more efficient during the adsorption of sulfur compounds from crude oil when compared to activated zinc oxide [65]. Also, metal oxides demonstrated to be efficient adsorbents for the removal of dibenzothiophene and 4,6-dimethyldibenzothiophene from model diesel fuel and diesel fuel. Transition metals supported on base oxides are usually used as the adsorbents. Ni/ZnO is an ideal adsorbent, in which the ZnO acts not only as an acceptor of sulfur released during the regeneration of sulfided Ni species, but also acts as a co-catalyst for the hydrogenation of sulfur-containing compounds over the surface of Ni species [66,67].

2.4.5 Activated carbon (AC)

Activated carbon (AC) is one of the most important adsorbents dominating the commercial use of adsorption due to its porous structure with high surface area, large pore volume and they have high efficiency for the adsorption of various types of compounds [68]. It has widely been studied for the adsorptive removal of pollutants from both gas and liquid phases [69-71]. It was found that activated carbon was the best

adsorbent between the activated alumina and nickel-silica alumina to remove model sulfur compounds from n-hexadecane [72].

Salem and Hamid [56] studied removing of sulfur from naphtha with a 550 ppm initial sulfur level in a batch reactor using activated carbon, zeolite 5A, and zeolite 13X as solid adsorbents. They reported that, Activated carbon showed the highest capacity, but a low level of sulfur removal. Sano et al. reported that, activated carbon had an adsorption capacity of 0.098 g-sulfur/g-activated carbon and 0.039 g nitrogen/g-activated carbon [73]. Zhou, found that the surface properties of AC, especially oxygen functional groups, played an important role in adsorptive desulfurization, especially for the removal of the refractory sulfur compounds in diesel fuel, such as 4,6-dimethyldibenzothiophene which made it promising for adsorptive desulfurization from diesel fuel [74]. Seredych, synthesized polymer-derived carbons and reported that micropore volume and acidic groups located in larger pores of activated carbon affected the adsorption desulfurization capacity of diesel fuel [75]. The adsorption behavior of dibenzothiophene on an activated carbon fiber and a granular coconut-shell activated carbon in the solvents n-hexane, n-decane, toluene, and mixture of n-decane and toluene was investigated. The DBT adsorption onto both samples was more active in n-hexane than in n-decane. The lowest DBT adsorption was observed in toluene. Regardless of the type of activated carbons and solvents [76].

A study for the desulfurization of contaminated diesel with 72 ppmw sulfur using the CAA, CAB, CAC, and CAD commercial activated carbons was done. The adsorptive capacity increased as the amount of the adsorbent increased too [77].

Activated carbon was found to have much better adsorption characteristics than 13X type zeolite [78]. Activated carbon is also used for oxidative removal of DBT in presence of H_2O_2 as oxidant, where very low sulfur residual were left in the oxidized oil [79]. Bu et al. Studied the Adsorptive affinity of polycyclic aromatic sulfur heterocycles (PASHs) and polycyclic aromatic hydrocarbons (PAHs) on commercial activated carbons AC1 - to AC7. They concluded that the adsorption selectivity increases as follows: naphthalene < fluorene < dibenzothiophene < 4,6-dimethyl dibenzothiophene < anthracene < phenanthrene [49]. Granular activated carbon (GAC) was produced from dates' stones by chemical activation using $ZnCl_2$ as an activator. GAC samples were used in desulfurization of a model diesel fuel composed of n-decane and dibenzothiophene (DBT) as sulfur containing compound. More than 86% of DBT is adsorbed in the first 3 h which gradually increases to 92.6% in 48 h and no more sulfur is removed thereafter [80]. Adsorption of the organosulfurs was performed on four commercial activated carbons. The most porous granular carbon with acidic surface functional groups performed better than the other adsorbents at a high organosulfur concentration [81]. Study was employed for sulfur removal from model oil (dibenzothiophene; DBT dissolved in iso-octane) using commercial activated carbon (CAC) as an adsorbent. The highest removal of sulfur by CAC was obtained with adsorbent dosage 20 g/L, time of adsorption 6h, and temperature 308 °C) [82]. Trace amounts of oxygen-containing (Polyaromatics such as phenanthrene)diesel additives, nitrogen compounds, and moisture all have inhibiting effects on adsorptive desulfurization over commercial activated carbon AC-WPH, which can be attributed partly to hydrogen-bonding interaction between polar groups this was why activated carbons that show good

adsorption uptake for model diesel sulfur compounds are not effective for real diesel fuels [83]. Recently, Four types of carbons (activated carbon, Maxsorb superactivated carbon, mesoporous templated carbon CMK-3, and graphene) were investigated as selective sorbents for adsorption of thiophene from its solution in n-octane.

The adsorption capacities for thiophene followed the order: graphene >CMK-3> Maxsorb > AC. Surface area is not a critical factor influencing sulfur capacity of carbon sorbents in addition, the carbene-type zigzag edge sites and the carbyne-type armchair edge sites on graphene are among the possible sites for strong interactions with thiophene[84]. Al Zubaidy et al. reported that, diesel fuel of 410 ppm sulfur content was treated with commercial activated carbon and carbonized date palm kernel powder at room temperature in batch work. The addition of activated carbon caused reduction in sulfur content by more than 54% of the original sulfur content value while carbonized date palm kernel powder without any activation process showed lower performance toward sulfur recovery [85]. New study by Farzin, synthesized magnetic mesoporous carbon (Ni-CMK-3) as an adsorbent for removal of sulfur from model oil (dibenzothiophene, in n-hexane). The resulting magnetic mesoporous carbon afforded a maximum adsorption capacity of 62.0 mg DBT g⁻¹ of Ni-CMK-3 [86]. To further develop highly efficient desulfurization adsorbents for ultraclean fuels, the surface of activated carbons can be modified by using different methods like oxidation, impregnation with metal particle and so on.

Modifications of carbon surfaces by incorporation of metals and oxidation of carbon surface can have a positive effect on the adsorption of DBTs. Jiang et al found that, the modified activated carbon by concentrated H₂SO₄ at 250 °C has much higher adsorption capacities for dibenzothiophene than the unmodified AC but less adsorption capacities

for small molecules (e.g., iodine) [87]. Moreover, transitional metal ion-loaded ACs shows great application potential. Ania and Bandosz used metal-loaded carbon-based sorbents containing sodium, cobalt, copper, and silver as DBT removal media via reactive adsorption. The metals incorporated to the surface act not only as active sites for selective adsorption of sulfur-containing aromatic compounds but also as structural stabilizers of the carbon materials and as catalyst initiators in reactive adsorption. It was also reported that cobalt and copper loaded carbons showed the highest uptake, due to not-well defined catalytic synergistic effects [88]. CuCl/AC, PdCl₂/AC, and Pd/AC were used for the desulfurization of a model jet fuel by selective adsorption of thiophenic molecules. PdCl₂/AC presented higher sulfur adsorption capacity than that of CuCl/AC and Pd/AC [89]. Adsorption Desulphurization of Gasoline by Silver loaded onto modified Activated Carbons was studied by Cao, B. et al. The results showed that silver formed π -complexes with organic sulphides; the higher the silver loading, the greater the amount adsorbed, but the adsorption selectivity was poor [90].

The adsorption of benzothiophene and dibenzothiophene on transition-metal ion-impregnated activated carbons is investigated [91] and the equilibrium amounts adsorbed of BT and DBT on the modified ACs followed the order: AgI/AC > NiIII/AC > CuII/AC > ZnII/AC > AC > FeIII/AC. Zhou et al. reported that HNO₃ oxidation of AC was an effective method for improving adsorption performance of sulfur compounds, due to an increase in the acidic oxygen-containing functional groups, suggesting that the adsorption of sulfur compounds over the AC may involve an interaction of the acidic oxygen-containing groups on AC with the sulfur compounds [92]. Two commercially available activated carbons A and B and modified forms of the same by HNO₃ treatment and Ni

supported systems were used as adsorbents for, 4-methylbenzothiophene and 4,6-dimethyl-dibenzothiophene in Adsorptive desulfurization process. The results showed that, the trend for adsorption selectivity for various adsorbents increases in the order, carbon A (modified) > carbon B (modified) > Ni/carbon A > Ni/carbon B > Ni/silica > Ni/alumina > Ni/HY-zeolite [93]. Adsorption of dibenzothiophene and 4,6-dimethyldibenzothiophene from simulated diesel fuel with 20 ppmw total concentration of sulfur was investigated on polymer-derived carbon and its oxidized counterpart. The specific geometry of those pores in relation to the sizes of DBT and 4,6-DMDBT causes their adsorption to be stronger than that of arenes [94].

Metal species such as iron oxides or copper oxides/metallic copper were reported to have a positive effect on the performance of polymer derived carbon in the process of desulfurization of diesel fuel [95]. Zirconium dioxide was impregnated into a commercial activated carbon (AC) and tested as adsorbents for dibenzothiophene (DBT) from a model diesel fuel. The results indicated that surface acidic sites on the impregnated ZrO_2 may play an important role in the improved desulphurization performance of the composite [96]. Fallah, and Azizian, studied the adsorption behavior of benzothiophene, dibenzothiophene and 4,6-dimethyldibenzothiophene from n-heptane onto activated carbon cloth (ACC) and its modified forms at 30 °C in batch condition. ACC was modified by HNO_3 , $(NH_4)_2S_2O_8$, H_2SO_4 , HCl and NaOH at ambient temperature. Among the tested adsorbents, they found that, modified ACC with HNO_3 (ACC- HNO_3) had the highest capacity for adsorption of DBT [97]. Cerium-loaded activated carbon was tested for dibenzothiophene adsorption from model fuels. This adsorbent showed much better adsorption capacity and selectivity towards DBT than the virgin carbon due to the

changes in surface chemistry of the adsorbent, in which the increased acidic sites and cerium ion may play important roles [98].

Furthermore, loaded nanoparticle adsorbents showed high efficiency for organosulfur compounds adsorption. Karvan et al. reported that mesoporous composite of nanosize CuO and amorphous SiO₂ were effective in H₂S adsorption [99]. Nickel nanoparticles were incorporated inside the mesopores of MCM-41 via a modified in situ approach and tested for adsorptive desulfurization of gas oil contains 300 ppmw of refractory sulfur compound (MDBT). The results indicated that, the smaller size of nanoparticles exhibited higher adsorption capacity toward refractory sulfur compounds like MDBT. This is due to two major factors, decrease of space hindrance during the interaction of nickel nanoparticles with sulfur atoms that are surrounded by benzene and methyl groups in MDBT molecules and increase in the number of active sites for adsorption [100]. Vu and coworkers used composite of multiwalled carbon nanotubes (MWNTS) and titanium oxide (IV) (TiO₂), for the photocatalytic oxidative desulfurization of dibenzothiophene and 4,6-dimethyl dibenzothiophene [101]. Fallah et al. studied the activity of dispersed carbon nanoparticles in aqueous solution (CNPs) as adsorbent for the removal of (BT), DBT, and DMDBT from an n-heptane model fuel solution. They found that, the higher adsorption selectivity for BT and DBT was due to their smaller size and the acidic surface of CNPs. while the presence of aromatics in the model diesel fuel only slightly reduced the desulfurization performance of CNPs [102].

2.5 OBJECTIVES

The major objectives of this work are as follows:

- Synthesis of different adsorbent materials.
- Characterization and morphological studies of synthesized adsorbents.
- Development of an experimental setup for desulfurization process.
- Investigation of desulfurization using model diesel; thiophene, benzothiophene (BT) and dibenzothiophene (DBT) followed by gas chromatography sulfur chemiluminescence detector (GC-SCD).
- Optimization of the desulfurization process to achieve higher selectivity and capacity.

CHAPTER 3

EXPERIMENTAL

3.1 Chemicals and materials

The Sulfur compounds used in this work are: (Thiophene (C_4H_4S , 99%, 84.14 g/mol), Benzothiophene (BT) (C_8H_6S , 99%, 134.2 g/mol), Dibenzothiophene (DBT) ($C_{12}H_8S$, 99%, 184.26 g/mol)) and they were obtained from Sigma Aldrich. Activated alumina (Al_2O_3), Zinc Oxide (ZnO) and N-Hexane (C_6H_{14} , 97%, 86.18g/mol) were obtained from Sigma Aldrich also, while the Toluene (C_7H_8 , 99.7%, 92.14 g/mol) was obtained from Merck (Germany).

3.2 Preparation of the adsorbent

3.2.1 Preparation Activated Carbon (AC)

Activated Carbon (AC) was synthesized from waste materials as described by Chan et al. [103]. Briefly, a waste rubber tire was cleaned and ground. The granules were heated up to 300 °C to separate the produced oil; then to 500 °C for 3h for carbonization. For the development of the porosity of tire carbon the sample heated to 900 °C for 2h, following this, surface modification was accomplished via H_2O_2 and HNO_3 treatment in order to develop oxygen surface groups on the rubber tire carbon. Finally, the product AC was washed and dried at 100°C.

3.2.2 Preparation of AC/NiO/ZnO

The adsorbent AC/NiO/ZnO (12:1:4 %) was prepared via thermal co-precipitation. Briefly, 6.0 g of AC was dispersed in 150 mL of deionized water by the use of sonicator. Then, 50 mL solution containing 1.763 g of $\text{Ni}(\text{NO}_3)_2 \cdot 6\text{H}_2\text{O}$ was added into the dispersed AC. This mixture was stirred for 2. The pH of the mixture was maintained at 8-9 followed by heating up to 90 °C for 6h under stirring. The precipitate was then filtrated, washed and dried at 110 °C overnight. The material was dispersed in 150 mL deionized water. Then, a 50 mL solution containing 6.975 g of $\text{Zn}(\text{NO}_3)_2 \cdot 6\text{H}_2\text{O}$ was drop-wise added into that. This mixture was stirred for 2. The pH of the mixture was maintained at 8-9 followed by heating up to 90 °C for 6h under stirring. The precipitate was then filtrated, washed and dried at 110 °C overnight. The product was calcined at 350 °C for 4h.

3.2.3 Preparation of AC/ZnO

Similarly, the adsorbent AC/ZnO was prepared in the absent of NiO solution. Briefly, the adsorbent AC/ZnO was prepared via thermal co-precipitation where 6.0 g of AC was dispersed in 150 mL of deionized water by the use of sonicator. A 50 mL solution containing 6.975 g of $\text{Zn}(\text{NO}_3)_2 \cdot 6\text{H}_2\text{O}$ was drop-wise added. This mixture was stirred for 2. The pH of the mixture was maintained at 8-9 followed by heating up to 90 °C for 6h under stirring. The precipitate was then filtrated, washed and dried at 110 °C overnight. The product was calcined at 350 °C for 4h.

3.2.4 Preparation of Alumina/ZnO

The composite adsorbent (Alumina/ZnO) was prepared via thermal precipitation method. This was realized by dispersion of 5.0 g of alumina in a solution of water and ethanol 1:1

v: v. On the other side, 5.0 g of $\text{Zn}(\text{NO}_3)_2 \cdot 6\text{H}_2\text{O}$ was dissolving in water and its pH was shifted up. Then this solution was added into the dispersed alumina, and mixed under sonication for 60 min. Then, the mixture was heated at 90 °C for 12 h. Then, it was cooled to room temperature and filtered. The sample was finally dried in oven at 50 °C. Calcination of the material was conducted for 2h.

3.2.5 Preparation of Alumina/ NiO/ZnO

The composite adsorbent (Alumina/NiO/ZnO) was prepared via thermal precipitation method. This was realized by dispersion of 5.0 g of alumina in a solution of water and ethanol 1:1 v: v. On the other side, a mixed solution of 5.0 g of $\text{Zn}(\text{NO}_3)_2 \cdot 6\text{H}_2\text{O}$ and 5.0g g of $\text{Ni}(\text{NO}_3)_2 \cdot 6\text{H}_2\text{O}$ was dissolving in water and its pH was shifted up. Then this solution was added into the dispersed alumina, and mixed under sonication for 60 min. Then, the mixture was heated at 90 °C for 12 h. Then, it was cooled to room temperature and filtered. The sample was finally dried in oven at 50 °C. Calcination of the material was conducted for 2h.

3.3 Characterization

The synthesized adsorbents were characterized by different techniques such as, N_2 adsorption (BET), X-ray diffraction spectroscopy (XRD), Energy Dispersive X-Ray Analysis (EDX) and Fourier Transform Infrared spectroscopy (FT-IR).

3.3.1 Nitrogen Adsorption (BET)

Nitrogen sorption isotherms were performed using liquid nitrogen temperature ($-196\text{ }^{\circ}\text{C}$) on a Micromeritics ASAP 2020 volumetric instrument (Micromeritics, USA) to determine surface area (BET), pore volume and pore size distribution of tested sorbents.

3.3.2 Fourier Transform Infrared spectroscopy (FT-IR)

The experiments were done on the powdered samples, with KBr addition. Spectra for samples were recorded using a Nicolet 6700 spectrometer (Thermo electron, USA) equipped with OMNIC program and Deuterated triglycine sulfate (DTGS) detector.

The spectra of the samples were recorded in transmission mode and the wavenumber range ($4000\text{-}400\text{cm}^{-1}$). FTIR spectra were obtained by adding 64 scans with a resolution of 2 cm^{-1} and corrected for the background noise.

3.3.3 X-ray diffraction (XRD)

X-ray diffraction data were obtained on a (Shimadzu XRD Model 6000, Japan) diffractometer using $\text{K}\alpha$ radiation of Cu. The machine was operated at 40 kV and 30 mA.

3.3.4 Energy Dispersive X-Ray Analysis (EDX)

Energy dispersive X-ray spectroscopy (EDX) is an analytical technique used for the elemental analysis or chemical characterization of a sample. EDX obtained using Oxford Instrument (England) and X-Max detector.

3.4 Adsorption studies

The adsorption of DBT, BT and Thiophene from model fuel onto the derived sorbents was performed using both batch and fix bed modes.

3.4.1 Adsorption of model diesels in batch mode

Typically, various amounts, in the range between 0.05 to 0.75g of adsorbent was introduced into 50 mL of the fuel solution. The total DBT, BT and Thiophene initial concentrations was 500 mg/L, prepared by dissolving 166.5mg DBT, 166.5mg BT and 166.5mg Thiophene in 1L solvent (762 ml toluene + 238 ml hexane). Thus, the amount of sulfur calculated in the fuel was 63.435ppm, 39.783ppm and 28.975ppm, respectively. The resulting mixture was continuously shaken at room temperature until equilibrium. Aliquots were taken from the system at the pre-determined time intervals and analyzed by GC-SCD method.

3.4.2 Adsorption in a fixed-bed mode

Dynamic adsorption experiments were carried out by passing the fuel sample through a fixed bed at ambient temperature and constant flow rate in order to determine the adsorption capacity. The dimensions of the adsorption column used were: 1 cm (diameter)×8cm (length) with total volume of 120 ml. In brief, a column was packed with the adsorbent. Model fuel was passed through the column packed with adsorbent by peristaltic pump with a controlled flow rate. Once the adsorption process was started, aliquots of the outlet were collected at different time intervals and injected in the GC for analysis. The process was stops once the breakthrough point has been reached.

3.5 Instrumentation

Analysis of the sulfur compounds in the model diesel were separated and analyzed on gas chromatography- sulfur chemiluminescence detector (GC-SCD) (Model 7890A)system (Agilent) equipped with autosampler (7693) and splitless injector with part number (1581-1267). It was operated through DB-1 column 30 m × 0.32 mm dimensions and a film thickness of 1 μm DB-1 100% dimethyl siloxane stationary phase were used. High purity helium flowing at a rate of 1.1 mL min⁻¹ was the carrier gas, the other operating conditions are listed in (table 3.1).

3.5.1 Gas Chromatography Sulfur Chemiluminescence Detector

The Sulfur Chemiluminescence Detector (355) (figure 3.1) is a sulfur selective detector for gas chromatography. Operation of the SCD is based on the detection of sulfur from the reaction of ozone with sulfur monoxide (SO) produced from combustion of the analyte:



A vacuum pump pulls the combustion products at low pressure into a reaction cell, where excess ozone is added. The sulfur dioxide and oxygen produced from this reaction are filtered and detected with a blue-sensitive photomultiplier tube, and the signal is amplified for display or output to a data system [104-107].

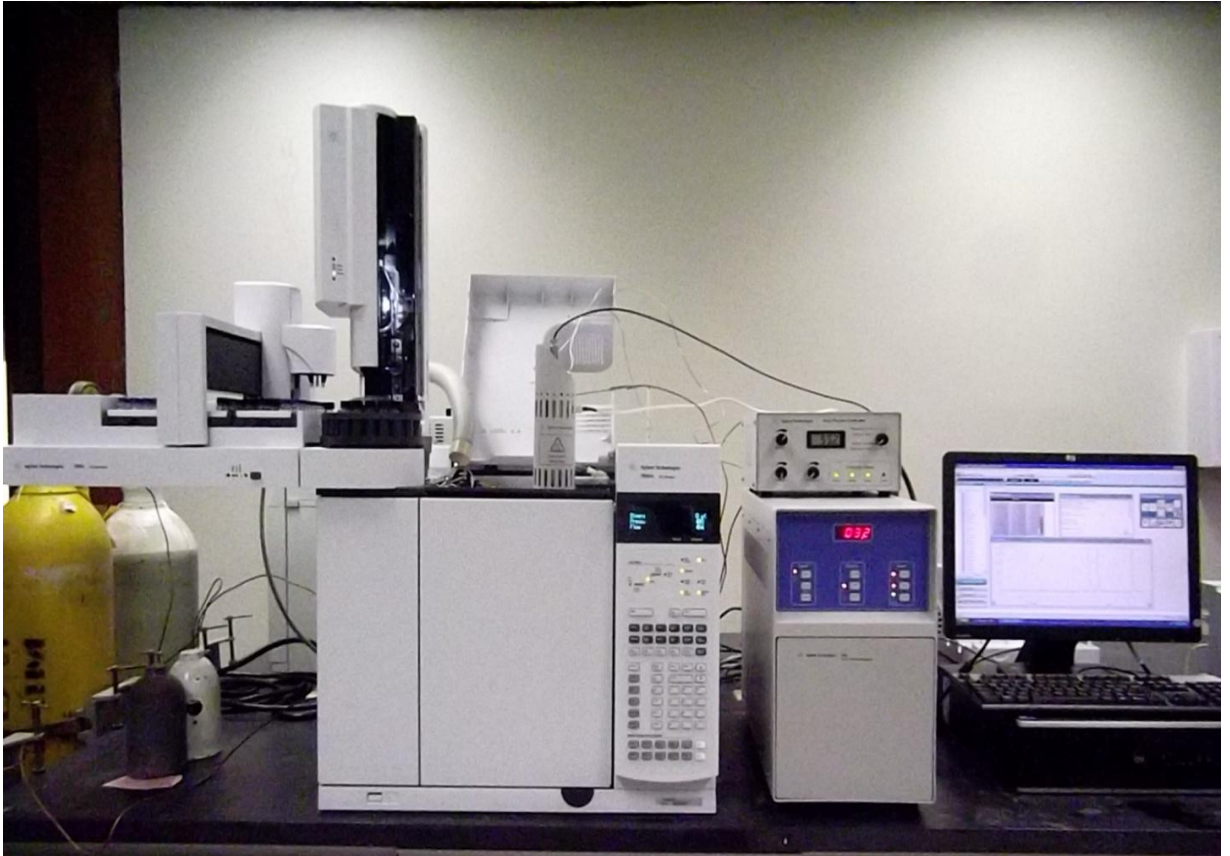


Figure 2.1: Gas chromatography sulfur chemiluminescence(355) Detector

3.5.2 Gas Chromatograph Linearity Response

The GC- SCD was calibrated by using certified standards of thiophene, BT, and DBT, then a dynamic linear range was established of thiophene (0.68-106 ppm), BT (0.66-100 ppm) and DBT(0.66-100 ppm) Figure (3.2 a,b and c) , Isopropyl sulfide 7 ppm sulfur was used as internal standard.

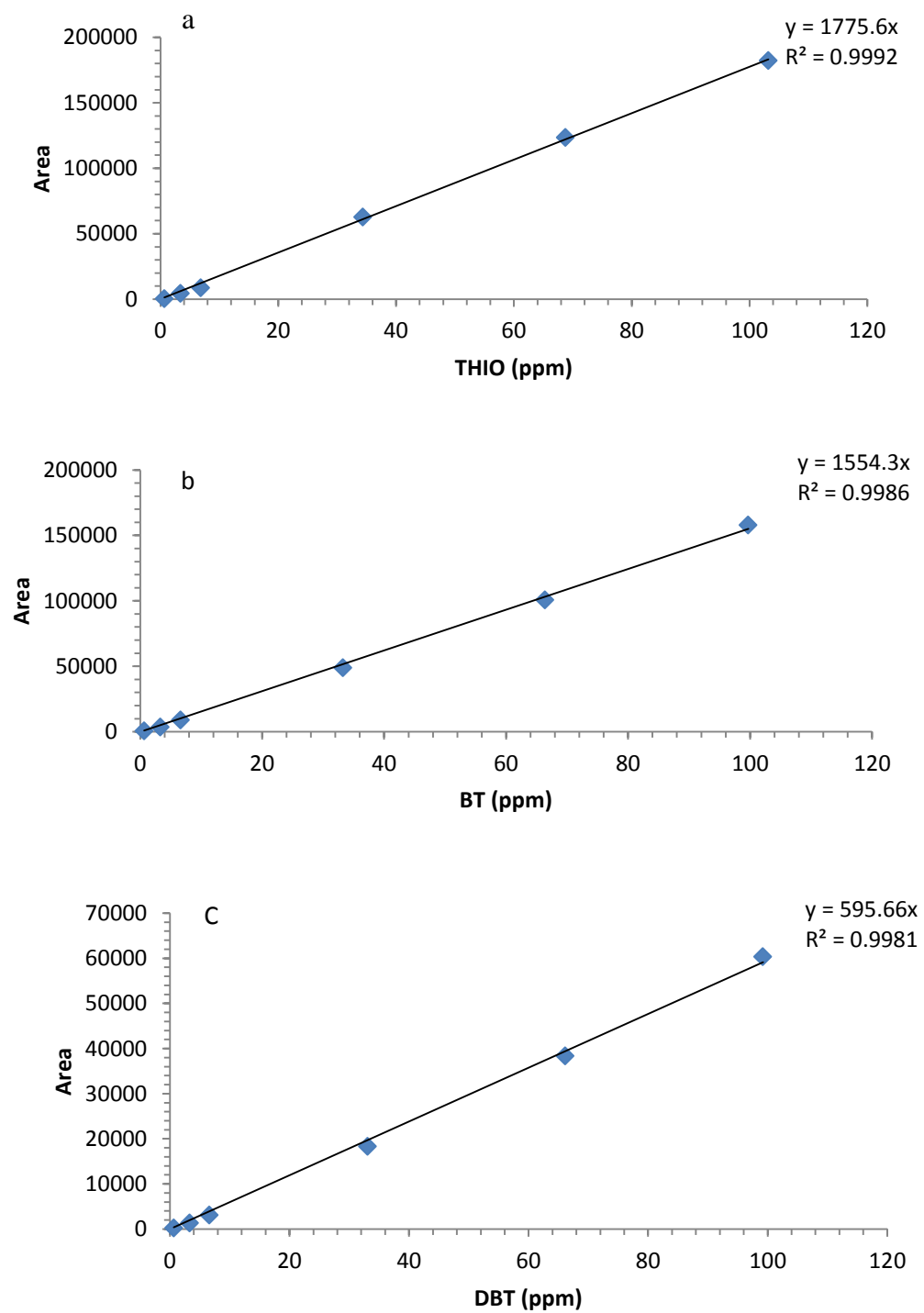


Figure 2.2: Linearity response of GC- SCD for: a: thiophene , b:benzothiophene and c:dibenzothiophene

3.6 GC- SCD Method of Analysis

The concentration of DBT, BT and thiophene in solution was analyzed by Agilent Gas Chromatograph with a Sulfur Chemiluminescence Detector (GC-SCD). The GC was equipped with splitless injection port and operated using splitless mode.

Separated done in DB-1 column with 30m length and 0.32mm diameter and the injection volume was 0.1ul with flow rate 1.1 ml\min, oven (column) temperature 280 °C Table 3.1.

Since the detector detect the sulfur we used the following equation to calculate the relative amount of analyte

ppm of sulfur = amount of thiophenic compound (mg) X [molar mass of sulfur \ molar mass of thiophenic compound]

Table 3.1: Method optimum conditions

Column Description :	DB-1	
Inventory# :	1447.44357	
Model# :	123-1033	Manufacturer: J&W
Diameter :	320.00 μm	Length : 30.0 m
Film thickness :	1.00 μm	Void time : 2.368 min
Maximum Temperature:	325.0 $^{\circ}\text{C}$	
Front SS Inlet He		
Mode	Splitless	
Heater	On 280 $^{\circ}\text{C}$	
Pressure	On 6.1629 psi	
Total Flow	On 19.1 mL/min	
Septum Purge Flow	On 3 mL/min	
Gas Saver	On 20 mL/min After 2 min	
Purge Flow to Split Vent	15 mL/min at 0.75 min	
Initial)	60 $^{\circ}\text{C}$	
Pressure	6.1629 psi	
Flow	1.1 mL/min	
Average Velocity	21.111 cm/sec	
Holdup Time	2.3685 min	
Flow Program	On 1.1 mL/min for 1 min	
Run Time	28 min	
3 min (Post Run)	3 mL/min	

The percentage removal of sulfur was calculated using the following equation:

$$\text{Percentage sulfur removal} = [(C_0 - C_e) / C_0] * 100$$

Where C_0 is the initial sulfur concentration (mg/L), C_e is the sulfur concentration (mg/L) at equilibrium.

The analyte adsorption (q_e , mg/g) at equilibrium, was calculated using the following equation:

$$q_e = (C_0 - C_e) \frac{V}{w}$$

Where, C_0 (mg/L) and C_e (mg/L) are the sulfur compound concentrations contained in the initial solution and at equilibrium, respectively; V (L) is the volume of the fuel solution; and w (mg) represents the weight of adsorbents.

3.7 Adsorption Kinetics

Adsorption kinetics demonstrates the solute uptake rate at the solid–solution interface and evidently provides valuable information about mechanism of the reactions and the reaction pathways. Two parameters, namely, adsorbent dosage and contact time, have a pronounced effect on the adsorption kinetics of thiophene, BT and DBT from model fuel. The kinetics of organosulfur compounds adsorption on AC/NiO/ZnO, AC/ZnO and AC were analyzed using pseudo first- order, pseudo-second-order and intraparticle diffusion models. The conformity between experimental data and the model predicted values was expressed by the correlation coefficients (R^2). A relatively high correlation coefficients value indicated that the model successfully describes the kinetics adsorption process.

3.8 Adsorption Isotherms

In this study, for investigation of the adsorption of Thiophene, BT and DBT onto AC\NiO/ZnO, AC/ZnO and AC, the adsorption equilibrium data were fitted using Langmuir and Freundlich models, which correspond to homogenous and heterogeneous adsorbent surfaces respectively.

3.9 Regeneration of the Adsorbents

The regeneration of the sorbents was investigated after they were saturated by thiophenic compounds. For the regeneration, Used sorbents were treated by Toluene and heating at 300 °C for 3 h. The desorbed amounts of thiophenic compounds were analyzed as a function of time with GC-SCD. Also, the used adsorbents were regenerated thermally only by heating at 350° for 3h.

CHAPTER 4

RESULTS AND CONCLUSION

4.1 Characterizations

4.1.1 Surface area and pore size

All sorbents show major nitrogen uptake at relative pressures less than 0.25 (Figures 4.1a, b, c, d and e). This means that the adsorbents are microporous. As well as, a small hysteresis loop can also be observed at high relative pressures indicating the presence of mesopores [108].

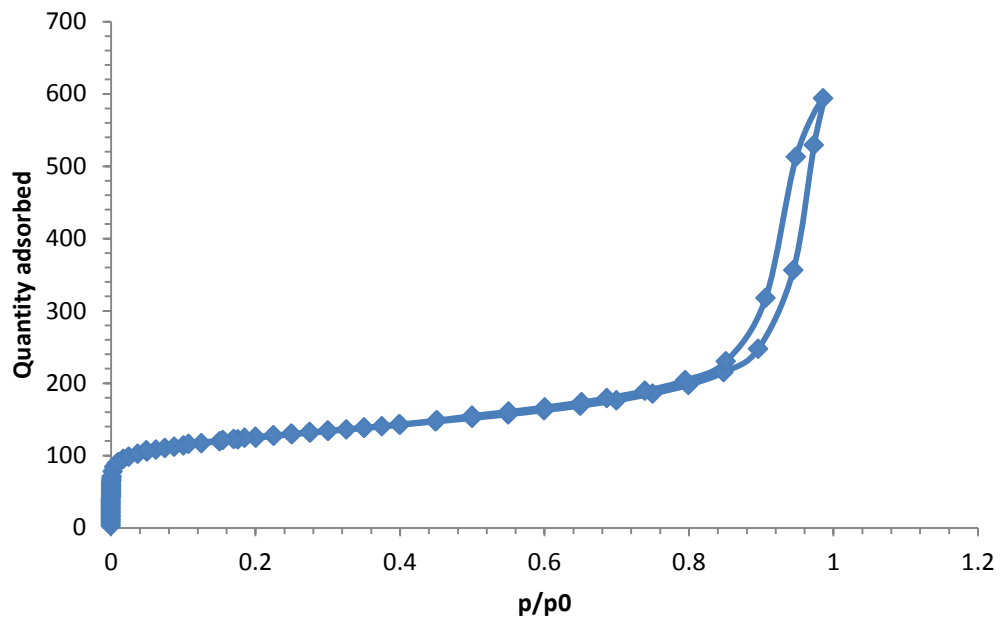


Figure 4.1a: Nitrogen adsorption/desorption isotherms for AC at -196°C

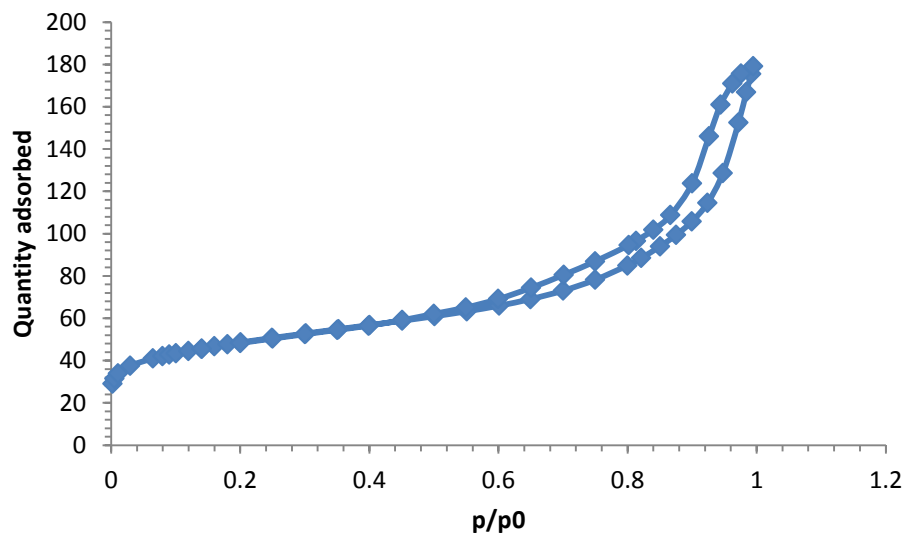


Figure 4.1b: Nitrogen adsorption/desorption isotherms for AC\ ZnO at -196°C

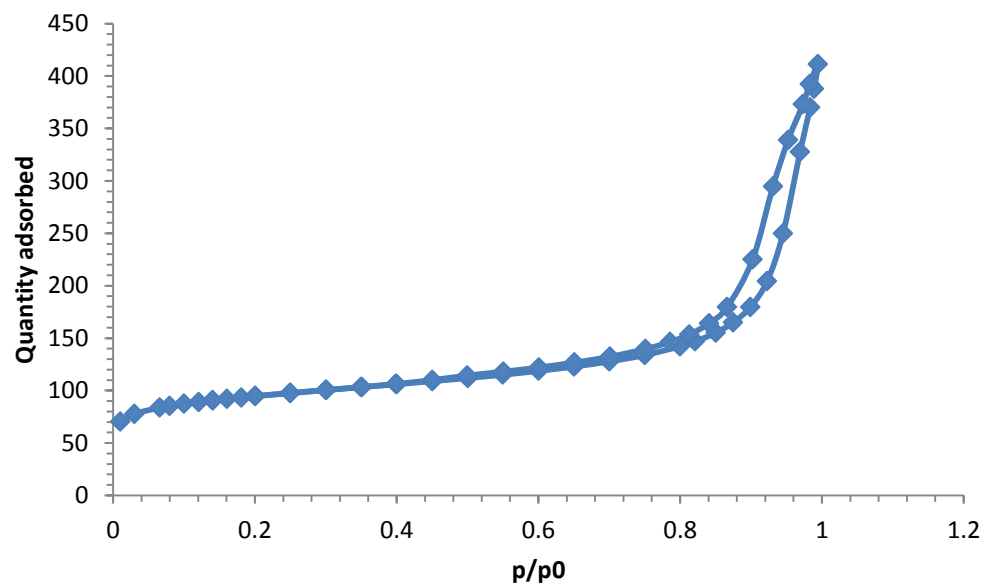


Figure 4.1c: Nitrogen adsorption/desorption isotherms for AC\ NiO\ ZnO at -196 °C

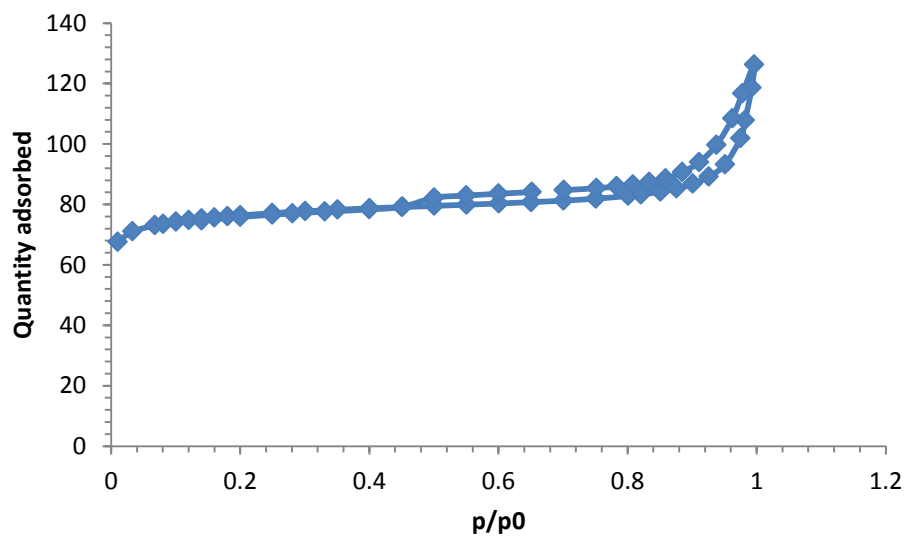


Figure 4.1d: Nitrogen adsorption/desorption isotherms for Al₂O₃\ NiO\ ZnO at -196 °C

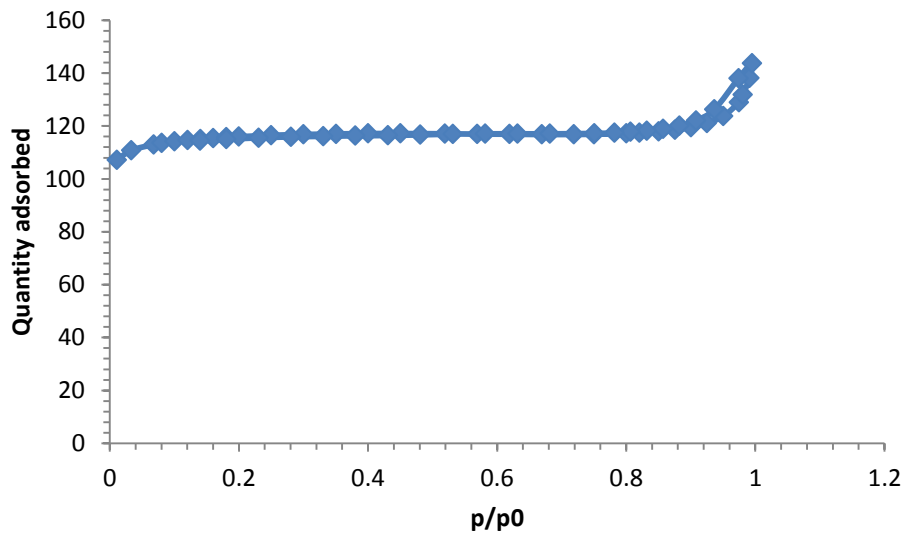


Figure 4.1e: Nitrogen adsorption/desorption isotherms for Al₂O₃\ ZnO at -196 °C

From (table 4.1) pore volume of the prepared adsorbents follow the order AC > AC\NiO\ZnO > AC\ZnO > Alumina\ ZnO > Alumina\NiO\ZnO. This could be attributed to occupied the pore volume by loaded NiO and ZnO species. In addition, BET surface area a follow the order AC > AC\NiO\ZnO > AC\ZnO > Alumina\ ZnO > Alumina\NiO\ZnO. This means that, the specific surface area (BET) and the total pore volumes decreased upon loaded NiO and ZnO functional groups which were introduced as the chemical modification (Seredych, et al 2010)and (Jiang et al 2003)[87].

This suggests factors other than pore volume and surface area should be involved to account for the higher adsorption capacity of AC\NiO\ZnO as we will discuss it latter.

Table 4.1: BET Surface area and pore volume analysis

Adsorbents	BET surf. area (m ² /g)	pore vol (cm ³ /g)	Adsorption average pore width Å
AC	62.3489	0.959211	615.3830
AC\NiO\ZnO	38.8997	0.506763	521.0974
AC\ ZnO	15.1786	0.304183	801.6115
Alumina\NiO\ZnO	12.4481	0.161860	520.1114
Alumina\ZnO	15.523	0.20944	539.679

4.1.2 Fourier transforms infrared (FT IR)

Fourier transform infrared spectroscopy is the useful tool to show the presence of any functional group in organic compounds.

For AC the intensity of the band centered around 1640 cm^{-1} indicating enhancement in the aromatic C=C groups (carbonization). Absorption bands at 3400 cm^{-1} represent O-H mode while the band at 2900 cm^{-1} are C-H mode; band at 1054 cm^{-1} may be attributed to C-O stretching vibration (figure 4.2 a).

For AC\NiO\ZnO and AC\ ZnO spectra (figures 4.2 b and c) in addition to the above bands there are bands at 490 cm^{-1} and $\sim 455\text{ cm}^{-1}$ that may attributed to the stretching mode of ZnO and of NiO stretching vibrational mode respectively.

On the other hand, for the spectra of Alumina\NiO\ZnO and Alumina\ ZnO (Figures 4.2 d and e). It is reported that the peak at 3500 cm^{-1} is attributed to the atmospheric water vapor. Alumina presents an absorption band at $\sim 1625\text{ cm}^{-1}$. The peak at $\sim 1040\text{ cm}^{-1}$ corresponds to the Al-O stretching vibration (Tsuchida,et al 1993 and Zhareslu et al 2003) [109,110].

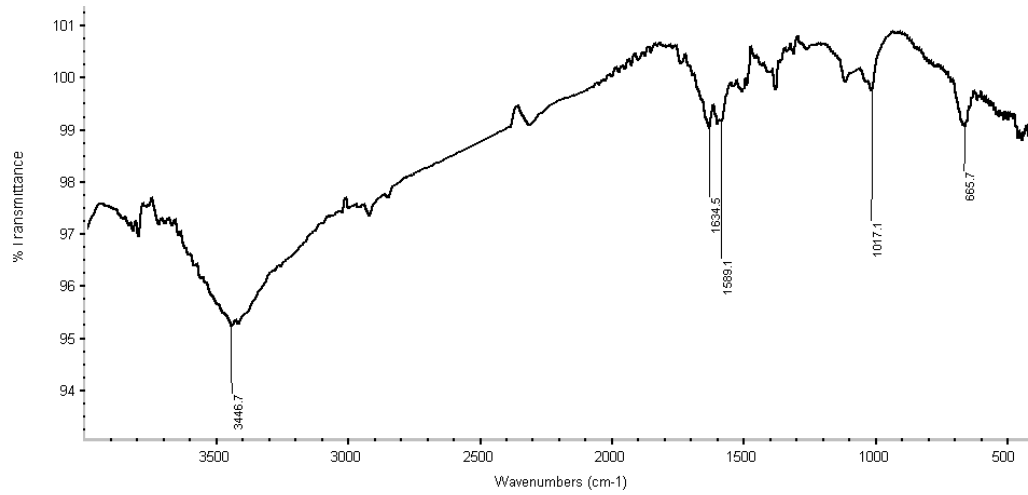


Figure 4.2 a: FT-IR spectra of the prepared activated carbon

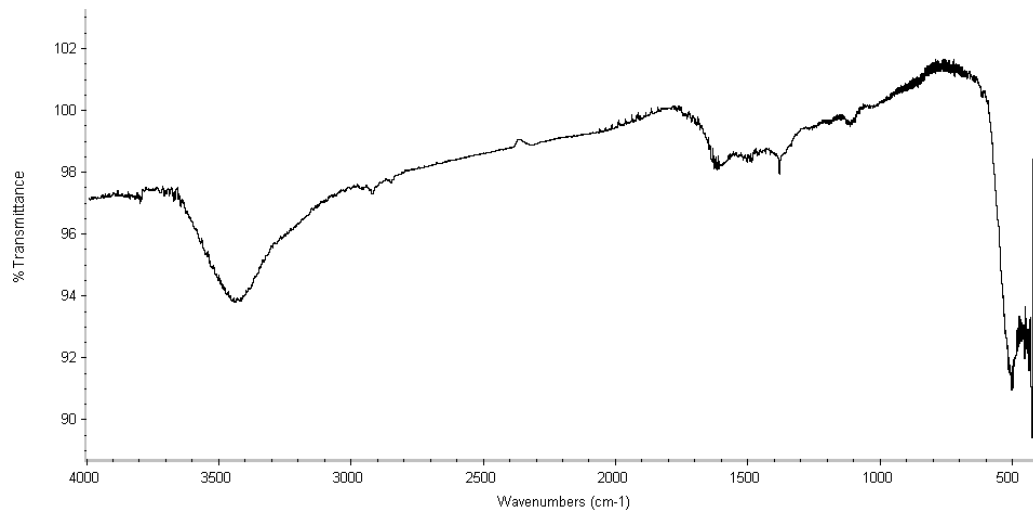


Figure 4.2 b: FT-IR spectra of AC\ ZnO

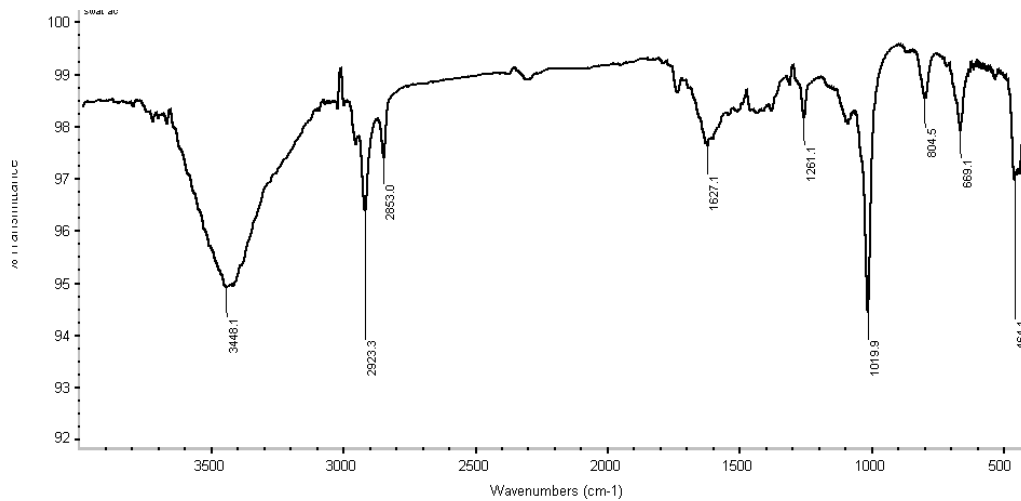


Figure 4.2 c: FT-IR spectra of AC\NiO\ZnO

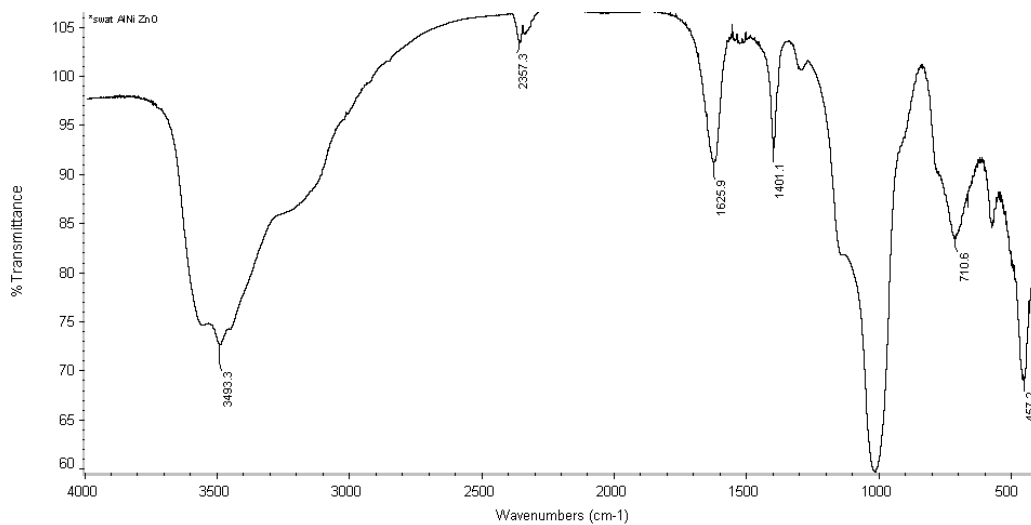


Figure 4.2 d: FT-IR spectra of Al₂O₃ \NiO\ZnO

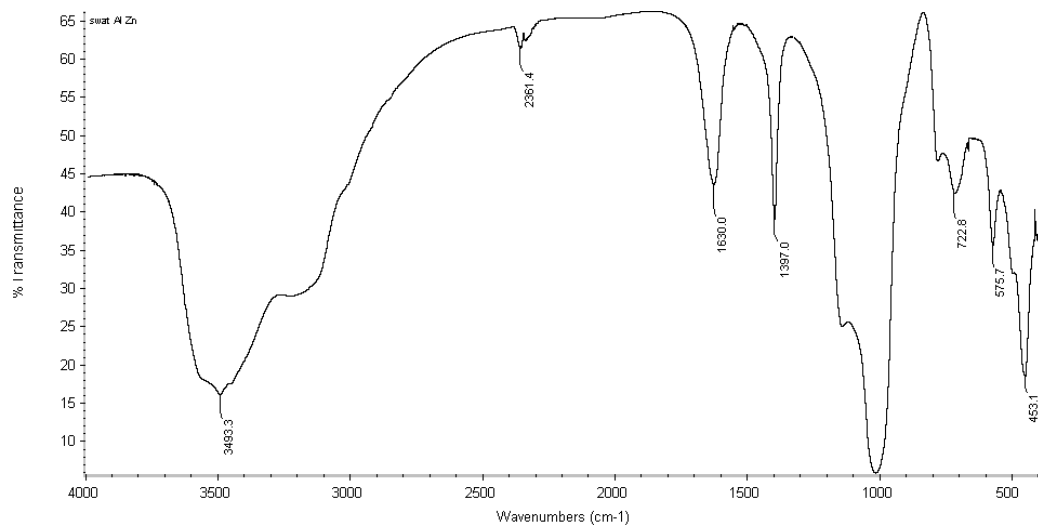


Figure 4.2 e: FT-IR spectra of Al₂O₃ \ ZnO

4.1.3 X-ray diffraction (XRD)

From the XRD spectra of the activated carbon sample shown in (Figure 4.3 a), we can see three broad diffraction peaks located at $2\theta = 20\text{--}30$ and $40\text{--}50$, revealing the presence of amorphous carbon which is disorderly stacked up by carbon rings (Tang et al 2012) [111]. For the other adsorbents new peaks are appeared in different 2θ with different intensity as show in (figures 2.3 a, b, c, d and e).

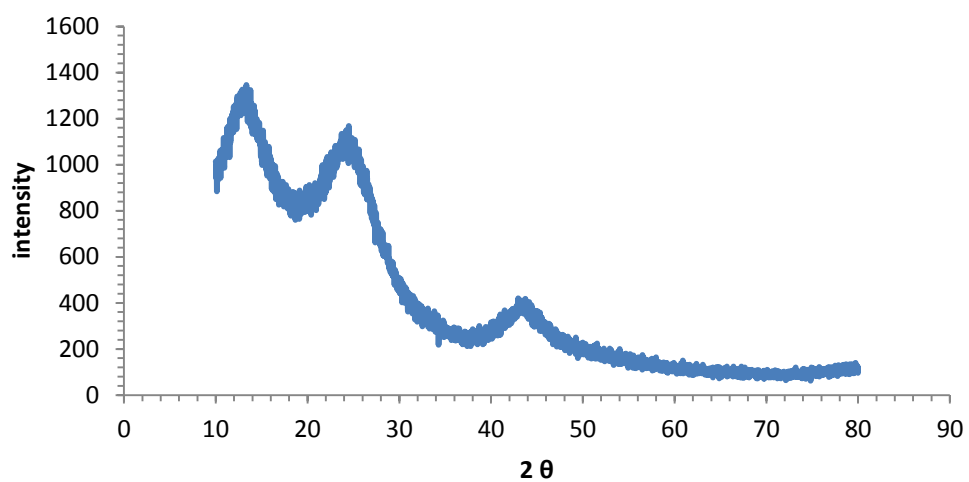


Figure 4.3 a: The XRD spectrogram of activated carbon prepared

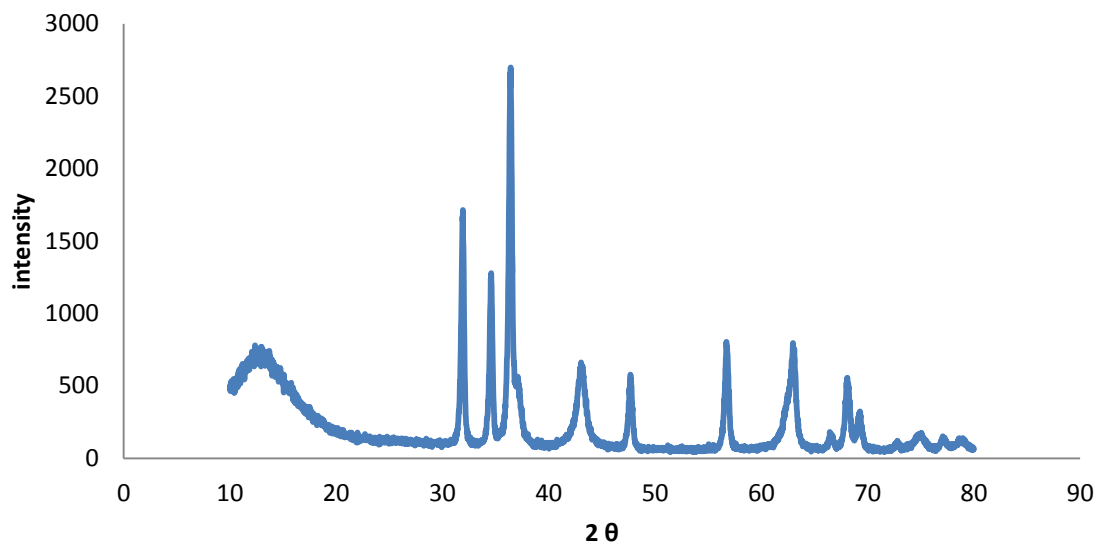


Figure 4.3 b: The XRD spectrogram of AC\ ZnO

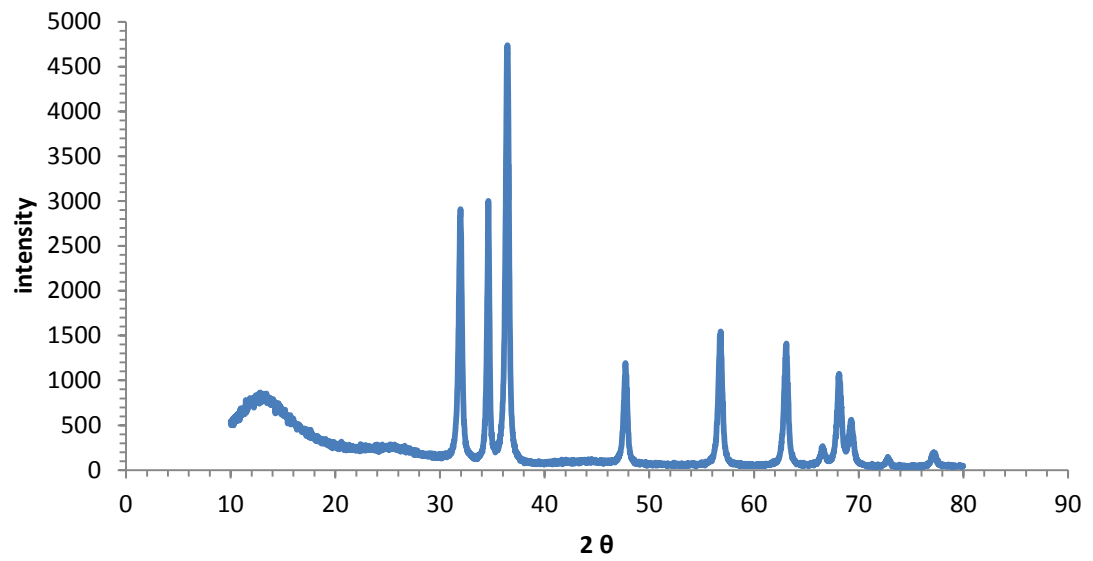


Figure 4.3 c: The XRD spectrogram of AC\NiO\ZnO

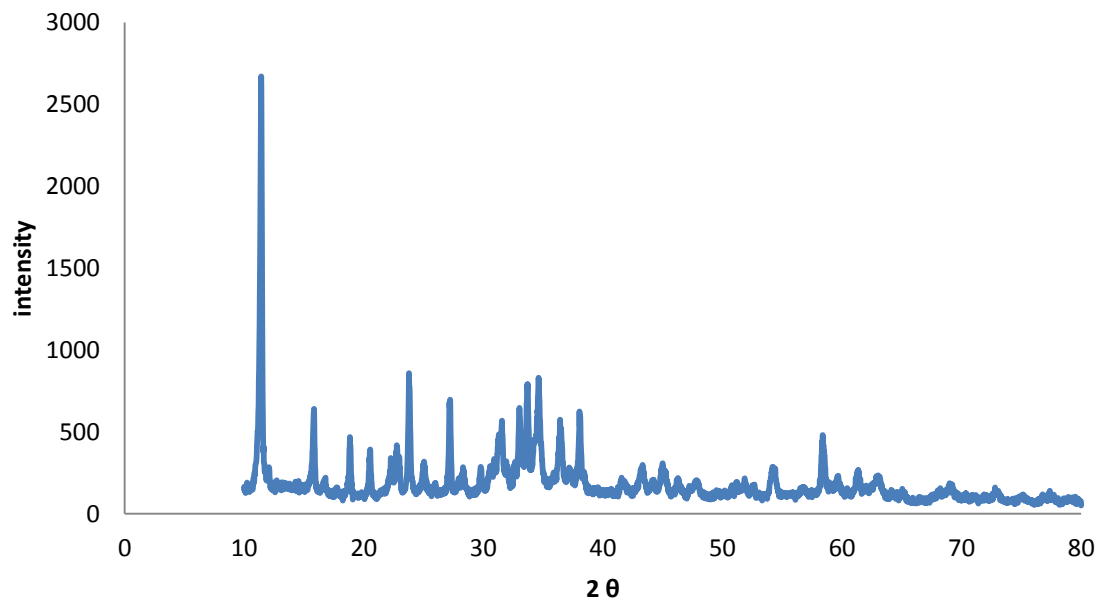


Figure 4.3 d: The XRD spectrogram of Al₂O₃\NiO\ZnO

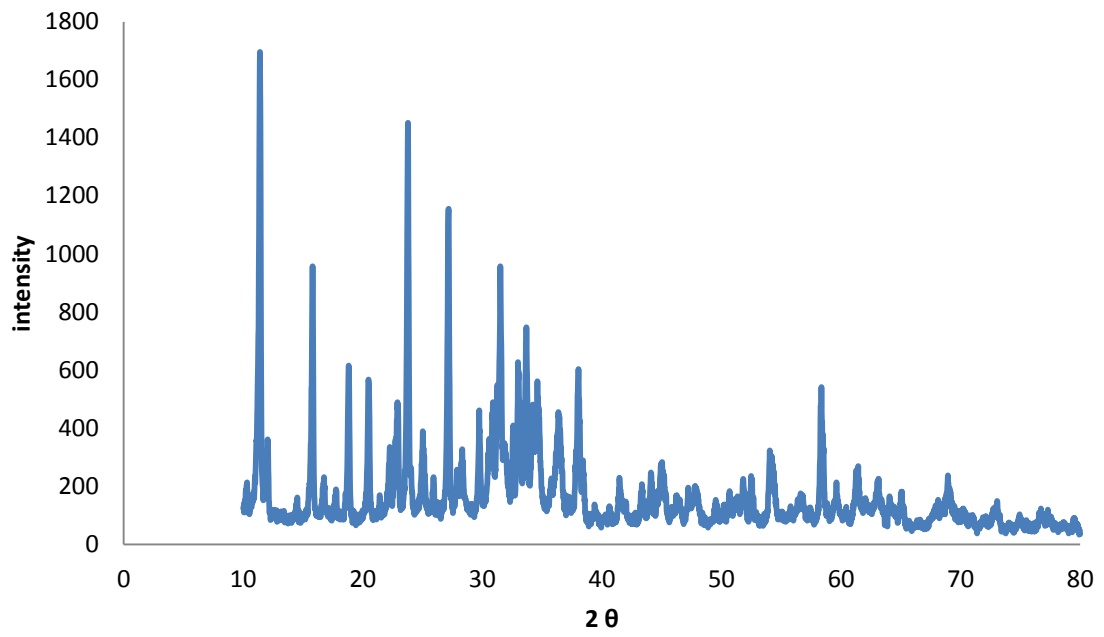


Figure 4.3 e: The XRD spectrogram of Al₂O₃/ZnO

4.1.4 Energy Dispersive X-Ray Analysis (EDX)

(EDX), technique used to identify the elemental composition of materials. EDX spectrum of AC (figure 4.4 a) indicates that the major elements present were carbon, and oxygen, while the EDX spectrum of AC\ ZnO and shows the present of Zn and AC\NiO\ZnO spectrum shows the present of Ni in addition to the C, O, Zn (Figures 4.4 b, c).

For Alumina\NiO\ZnO and Alumina\ ZnO the EDX spectrum represent the present of Al, O, Zn, Ni and it is clear that no carbon peak (Figures 4.4 d, e).

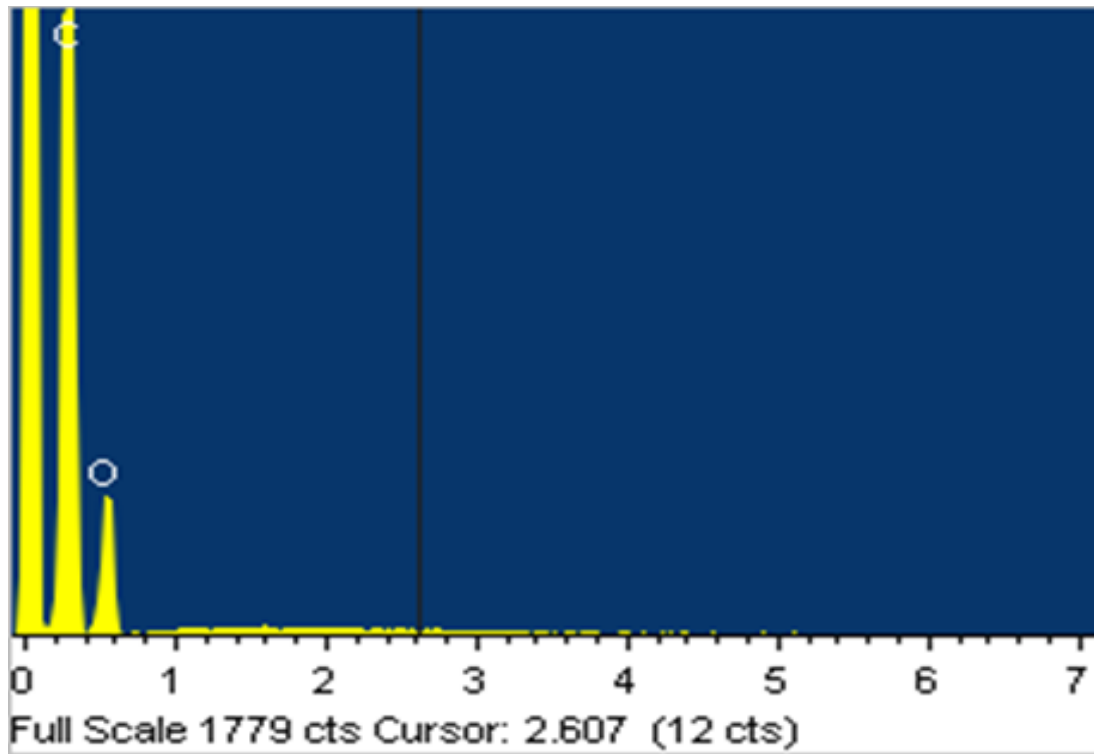


Figure 4.4 a: EDX spectrum of the Activated Carbon (AC)

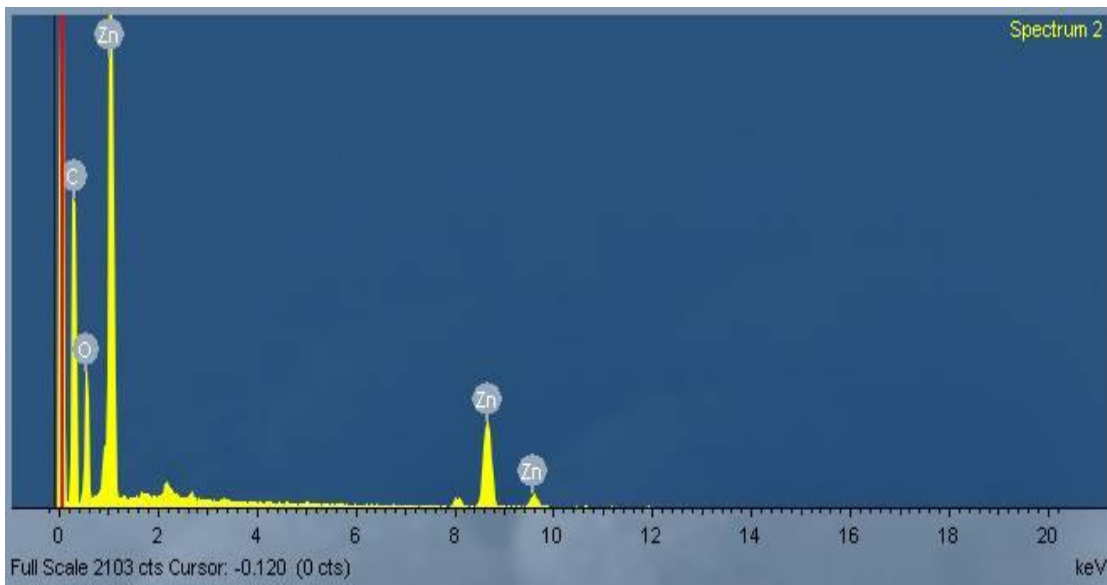


Figure 4.4 b: EDX spectrum of AC/ZnO

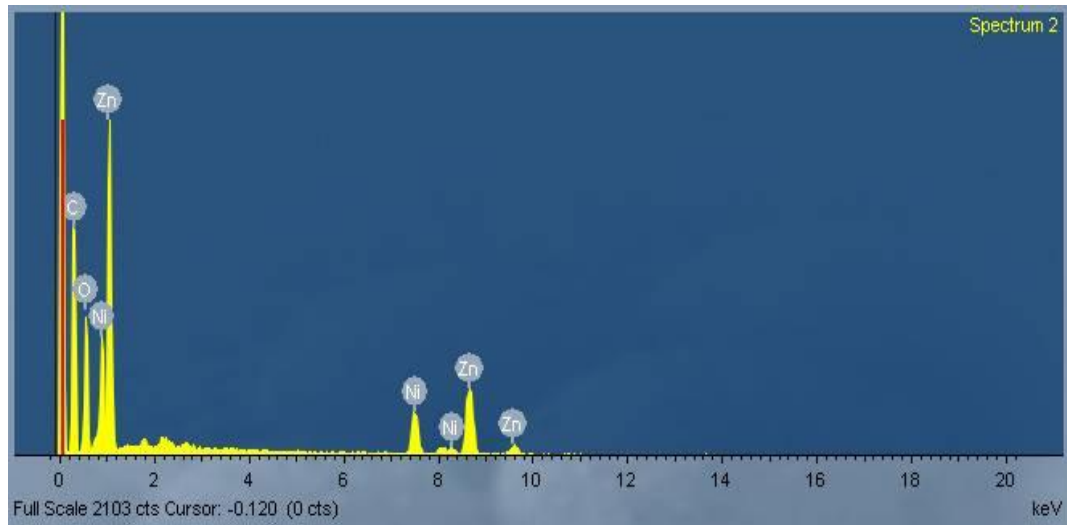


Figure 4.4 c: EDX spectrum of AC\NiO\ZnO

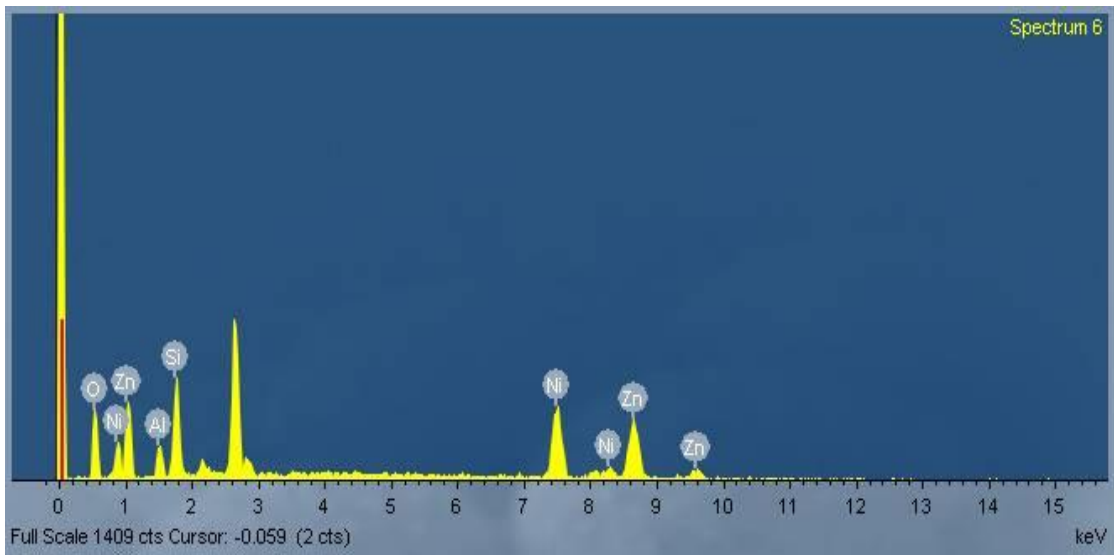


Figure 4.4 d: EDX spectrum of Al₂O₃\NiO\ZnO

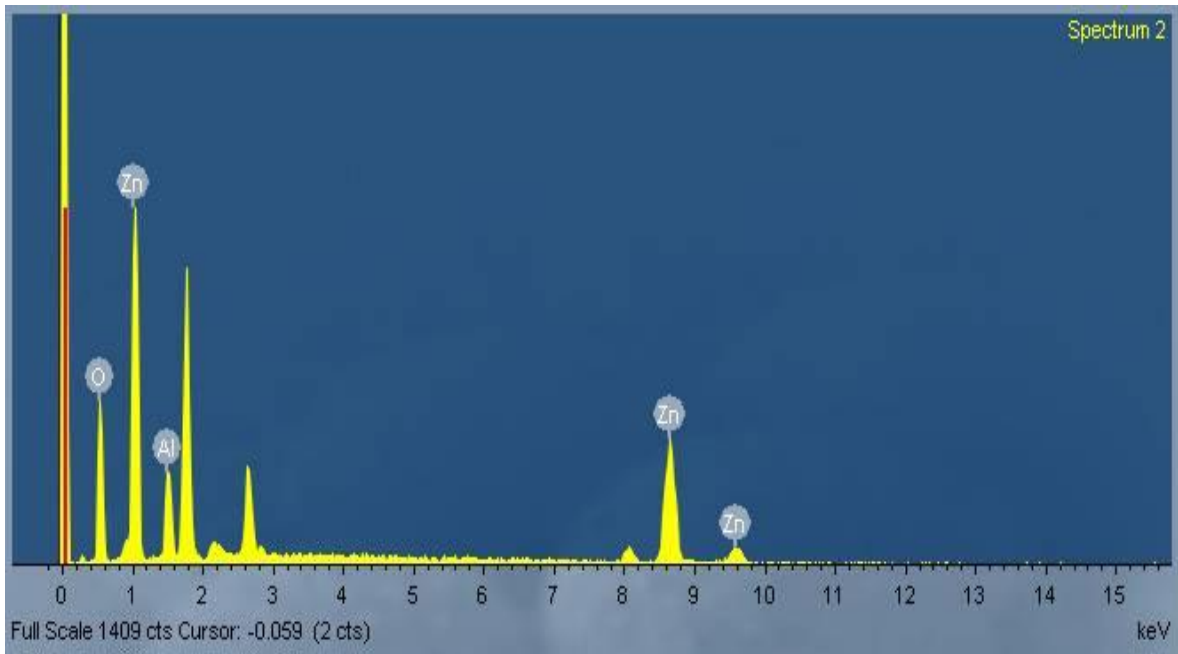


Figure 4.4 e: EDX spectrum of Al₂O₃/ ZnO

4.2 Adsorption studies

4.2.1 Comparison of adsorption desulfurization on the prepared adsorbents

For comparing constant amount (0.75g) from each adsorbent was added to five different flasks each one contains the same concentration of sample (500 ppm in 50 ml solvent). The flasks were stirred for 80 minutes then samples were taken from each one and analyzed by GC-SCD. The results given in (Figure 4.5) present the percentages of removal for thiophene, BT and DBT using five different adsorbents. It is obvious that AC has higher percentage of removal than Alumina\NiO\ZnO and Alumina\ZnO this can be attributed to the porosity where AC has larger pore volume adsorption and surface area than Alumina\NiO\ZnO and Alumina\ZnO. On the other hand, Although, AC has larger BET surface area and pore volume than AC\NiO\ZnO, AC\ ZnO (table 4.1) , they exhibited higher adsorption capacity and percentages of removal , this could be attributed to another factor which is S-M interaction between sulfur and Ni and Zn (Song et al 2003) [112].

In addition, it is clear that AC\NiO\ZnO exhibited higher adsorption capacity for the three compounds which means that, the metal species located contribute to enhanced interactions. These results agree with previous reported that Nickel has an affinity to the organic sulfur compounds and it is the active sites on Ni/ZnO for desulfurization process(Kim et al 2006 and Moosavi et al 2010)[113].

The following adsorption capacity in the order: AC\NiO\ZnO > AC\ZnO > AC > Alumina\NiO\ZnO > Alumina\ZnO.

From the above we can conclude that, the adsorption properties (adsorption capacity and selectivity) of the adsorbents did not determined by their porosity (adsorption pore volume) but also affected by the chemical property of their surfaces, which is corresponded to the previous studies also (Xiao et al 2008 and Li et al 2006) [114].

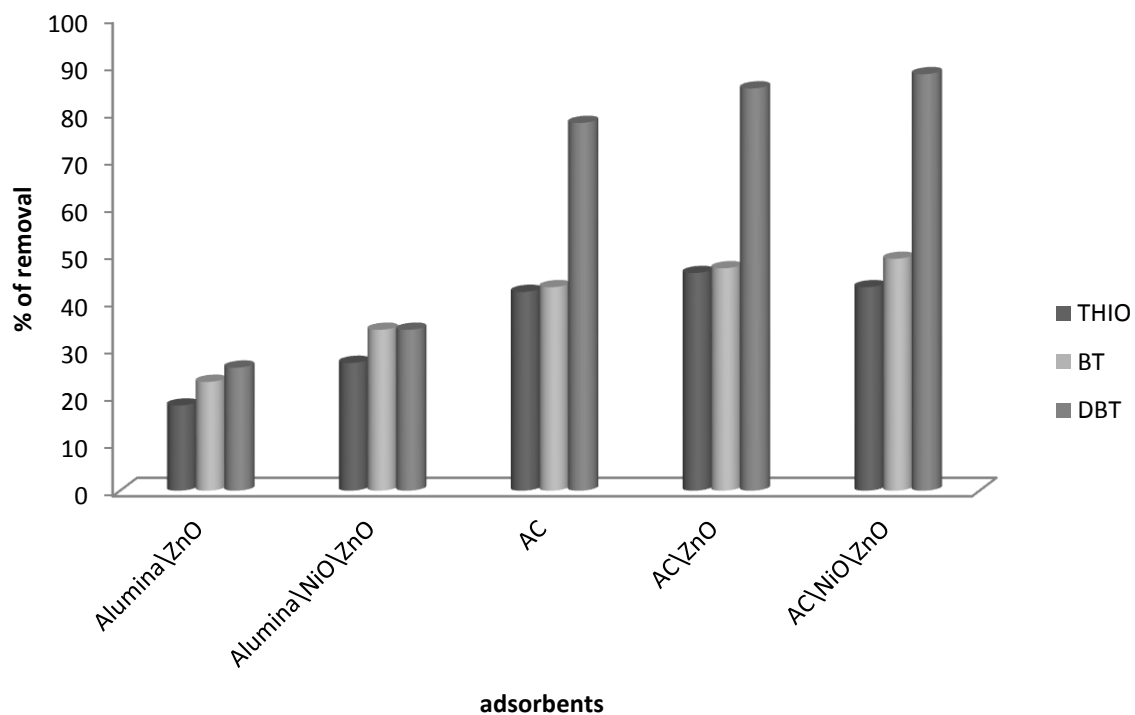


Figure 4. 5: Percentage removal of thiophene, BT and DBT (initial concentration of each on is 166.6 ppm) on AC, AC\NiO\ZnO, AC\ ZnO, Alumina\NiO\ZnO and Alumina\ZnO (dosage 0.75 g, 50 ml and time 50 min)

4.2.2 Effect of dosage of the adsorbents

The efficiency of sulfur removal is significantly influenced by the amount of adsorbent used. Since the adsorbent Alumina/ZnO did not exhibited good efficiency for removal of thiophene, BT and DBT, The effect of the mass of adsorbents as well as the Effect of contact time versus percentages of sulfur adsorbed was investigated for the other adsorbents. The amounts of thiophene, BT and DBT adsorbed onto the adsorbents are depicted in (Figure 4.6 a, b, c and d). A trend of increment in adsorption capacity with increment in adsorbent dose was observed from 0.1 to 0.75 g. The results indicate that the amount of sulfur compounds adsorbed by the adsorbent increased with increasing the amount of the adsorbent. The initial increase in adsorption capacity with increase in adsorbent dosage was expected because the increase in the number of adsorbent particles results in more surface area and more adsorption sites (Srivastav et al 2009) available for sulfur compounds attachment.

DBT exhibits higher percentage of removal for each dosage and on all adsorbents due to the ability of DBT to form π - π dispersive interactions between the aromatic ring in DBT and the graphene layers on AC. This also can explain that the molecules with three-aromatic rings (DBT) showed a significantly higher adsorptive affinity than two-ring aromatics (BT) and higher than one ring (thiophene) (Bu et al 2011).

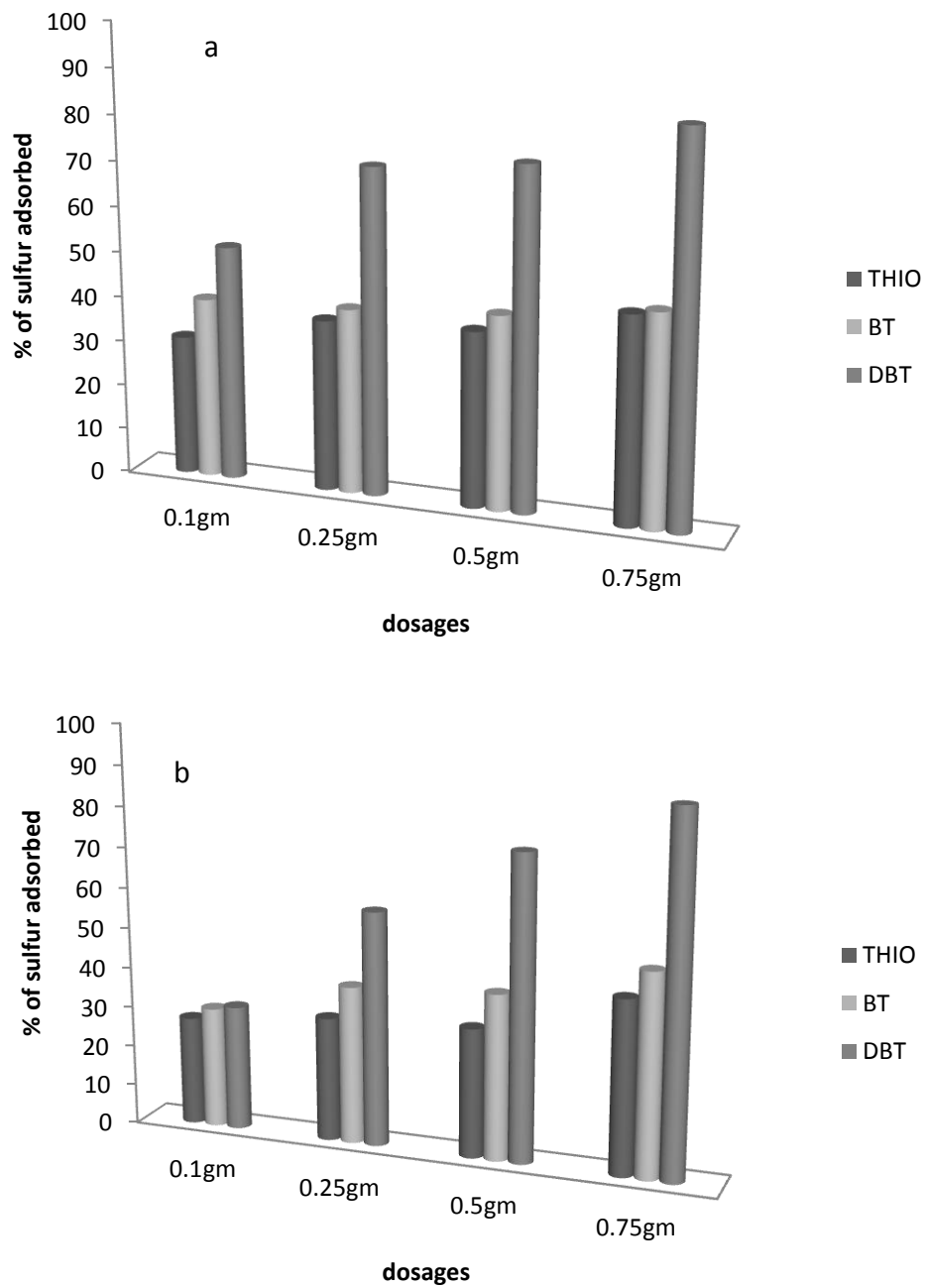


Figure 4. 6: Effect of adsorbent dosage on the adsorption of thiophene, BT and DBT, on a: AC\NiO\ZnO and b: AC\ ZnO (in 50 ml solution with initial concentration 190,190 and 197 ppm respectively) contact time 50 min.

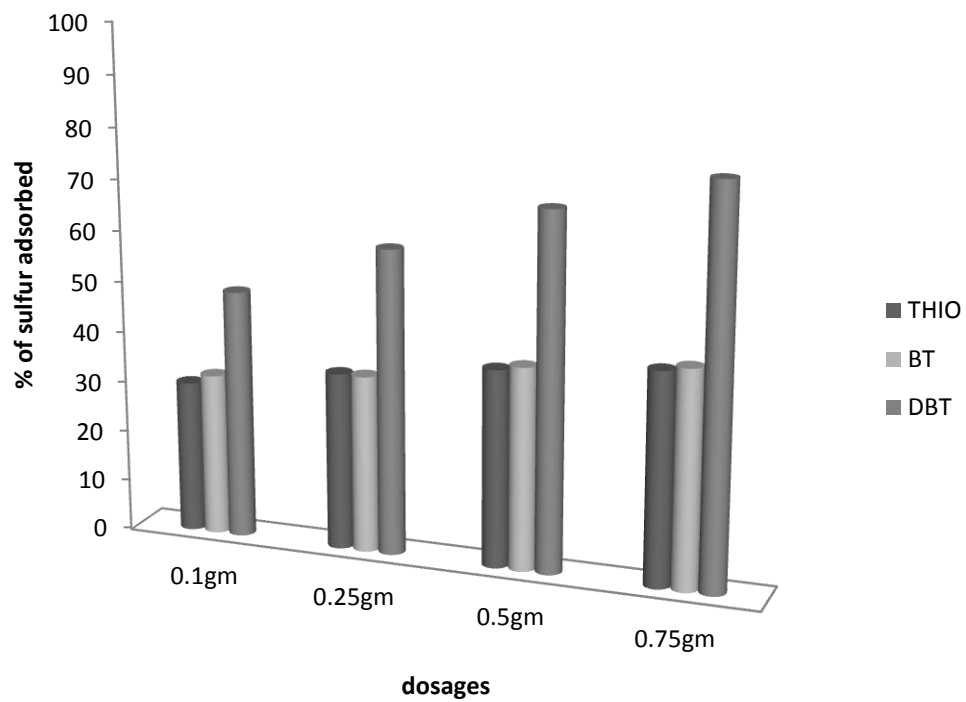


Figure 4.6 c: Effect of adsorbent dosage on the adsorption of thiophene, BT and DBT, on AC (in 50 ml solution with initial concentration 190,190 and 197 ppm respectively) contact time 50 min.

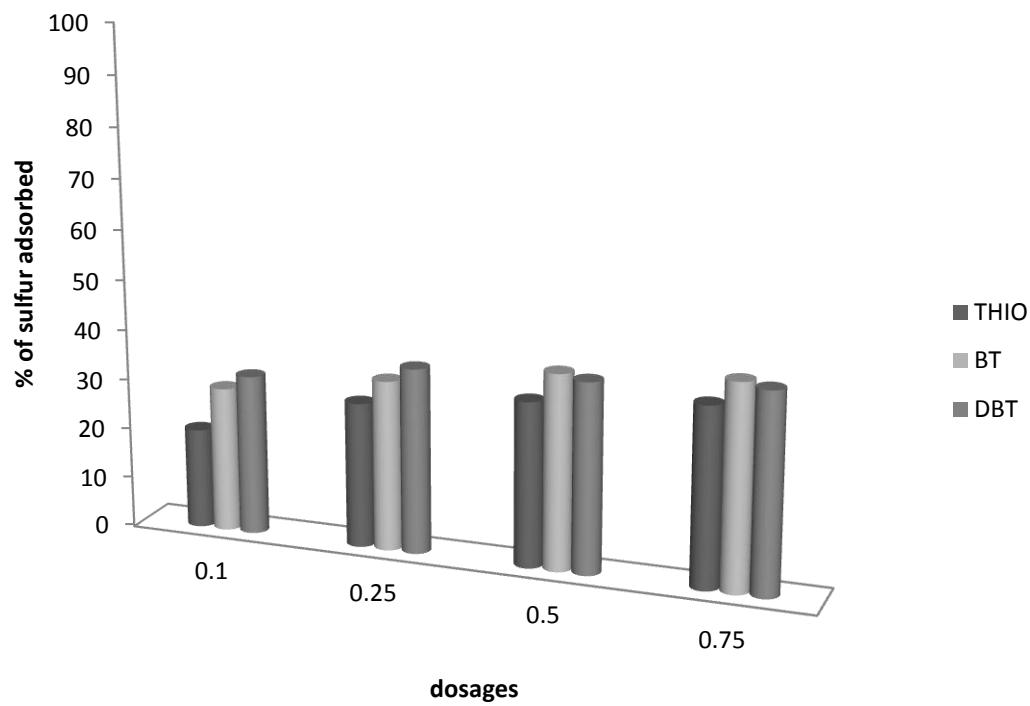


Figure 4.6 d: Effect of adsorbent dosage on the adsorption of thiophene, BT and DBT, on Alumina\NiO\ZnO (in 50 ml solution with initial concentration 190,190 and 197 ppm respectively) contact time 50 min.

4.2.3 Effect of contact time

The effect of contact time on the amount of sulfur compounds adsorbed was investigated and the data are presented in (Figure 4.7 a, b, c and d).

The extent of removal of sulfur by AC/NiO/ZnO, AC/ZnO, AC and Alumina/NiO/ZnO was found to increase, reach a maximum value with increase in contact time. In some cases it decreases with the increase in contact time after, 50 min which may be due to a desorption process. The rate and quantity of sulfur adsorbed by the adsorbent is limited by the size of adsorbent molecules, concentration of adsorbate and its affinity towards the adsorbent, diffusion coefficient of the adsorbent in the bulk and solid phase and the degree of mixing. With increasing contact time, the number of available adsorption sites decreased as the number of sulfur ions adsorbed increased.

A large number of vacant surface sites are available for adsorption during the initial stage, and after a lapse of time, the remaining vacant surface sites are difficult to be occupied due to repulsive forces between the solute molecules on the solid and bulk phases (Kumar et al 2011)[115].

Besides, the DBT, BT, thiophene (as sulfur) are absorbed into the micro- and meso-pores that get almost saturated with DBT, BT, thiophene during the initial stage of adsorption. Thereafter, the DBT, BT, Thiophene molecules have to traverse further and deeper into the micro-pores encountering much larger resistance. This results in the slowing down of the adsorption rate during later period.

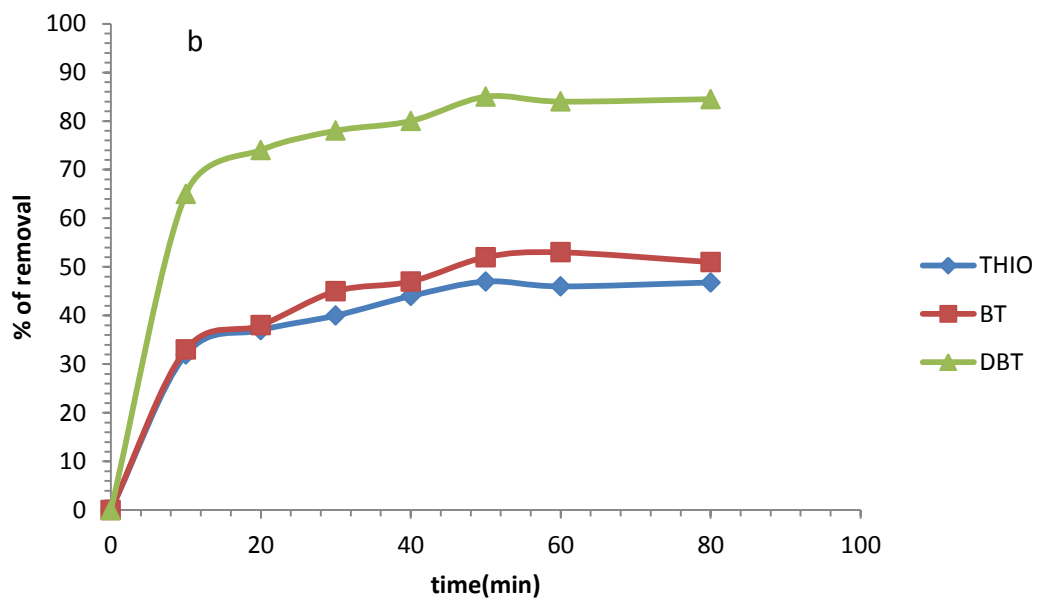
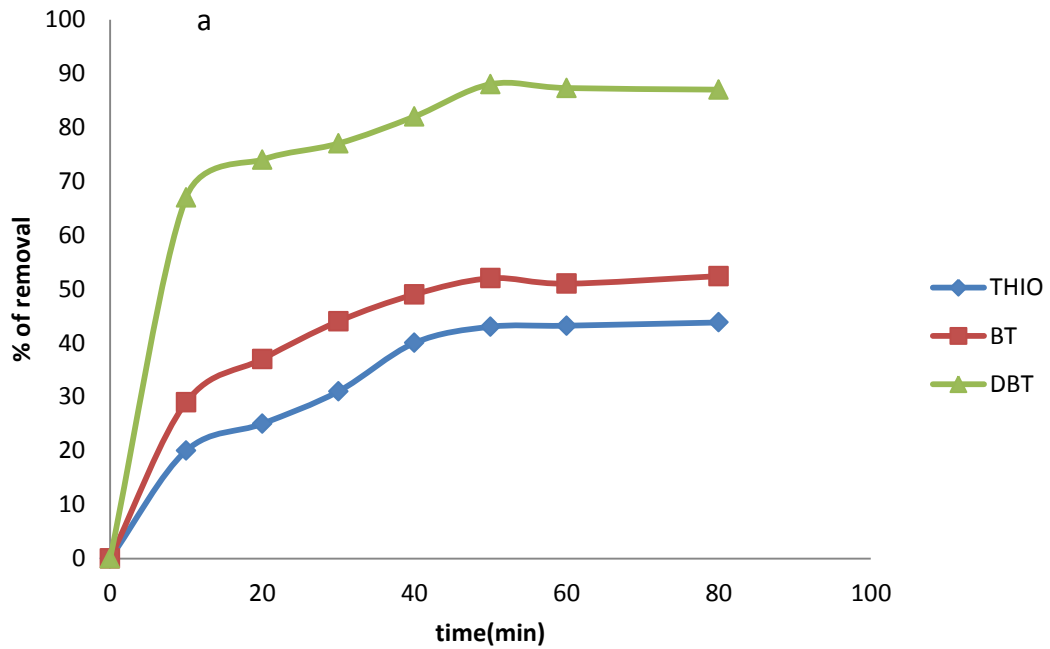


Figure 4.7: Adsorption of sulfur compounds on a: AC\NiO\ZnO and b: AC\ZnO at different time intervals; conditions dosage is 0.75g, (with initial concentration 190,190 and 197 ppm respectively), batch mode

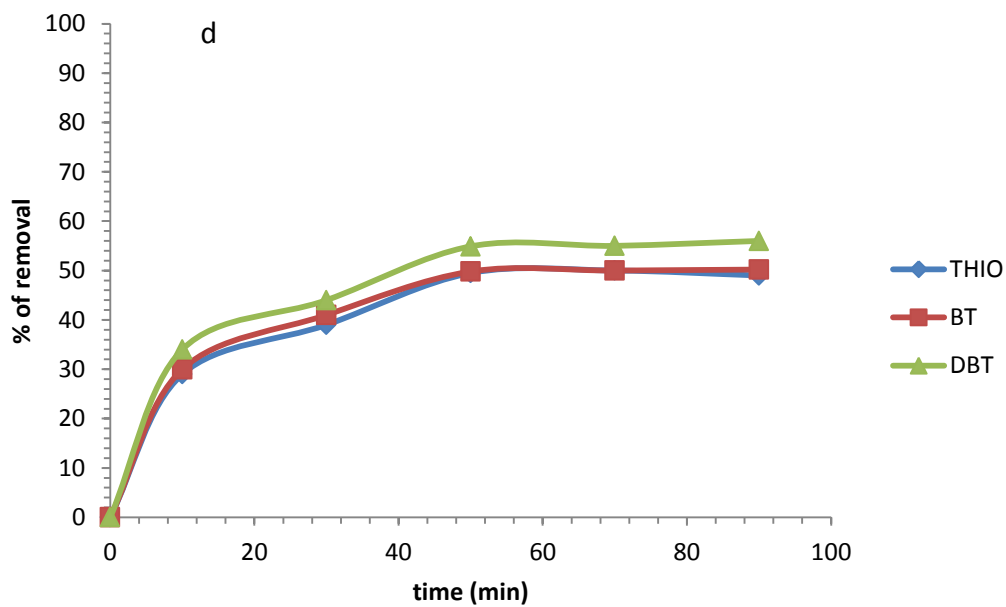
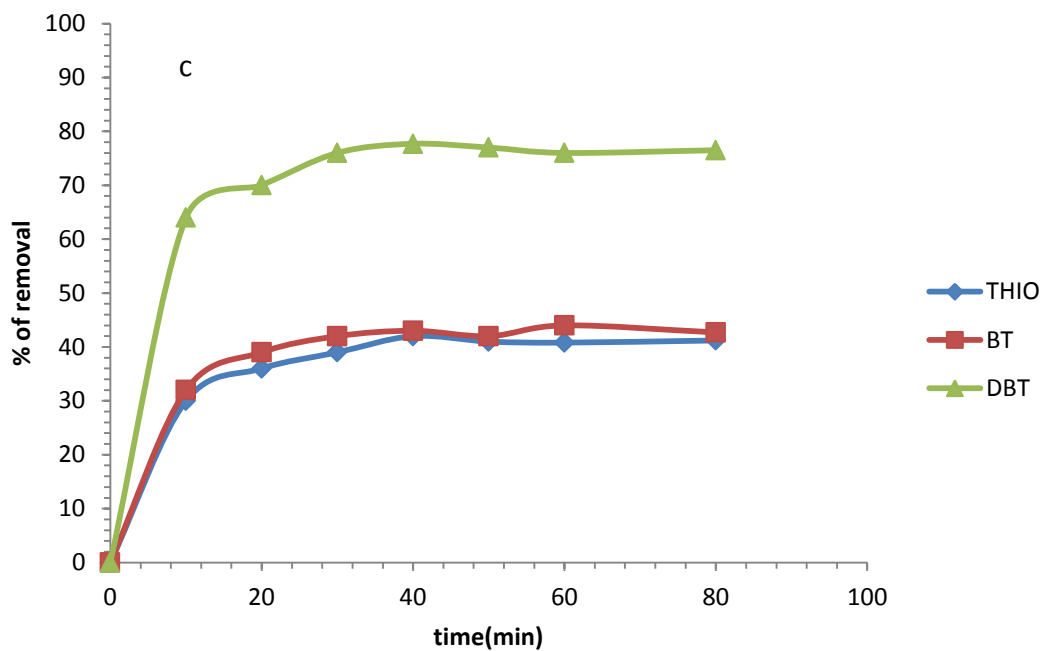


Figure 4.7: Adsorption of sulfur compounds on c: AC and d: Alumina/NiO/ZnO at different time intervals; conditions dosage is 0.75g, (50 ml with initial concentration 190,190 and 197 ppm respectively), batch mode

4.2.4 Adsorption experiments in a fixed-bed column

From the Batch mode and the effect of contact time and adsorbents dosage, AC\NiO\ZnO, AC\ ZnO and AC have significantly higher adsorption activities toward thiophene, BT and DBT. The effectiveness of these sorbents was further investigated in a continuous flow mode.

Adsorption break through curves were generated by plotting the transient total sulfur concentration normalized by the feed total sulfur concentration (C_t/C_o) vs. cumulative time. The results are given in (Figure 4.8 a). Show the breakthrough for thiophene on AC\NiO\ZnO, AC\ ZnO and AC. The initial concentration was 166 ppm and it decreased to 50, 55 and 110 ppm in the first 10 minutes by AC\NiO\ZnO, AC\ZnO and AC respectively and it came back to the initial concentration after three hours this means that no more adsorption happened after three hours.

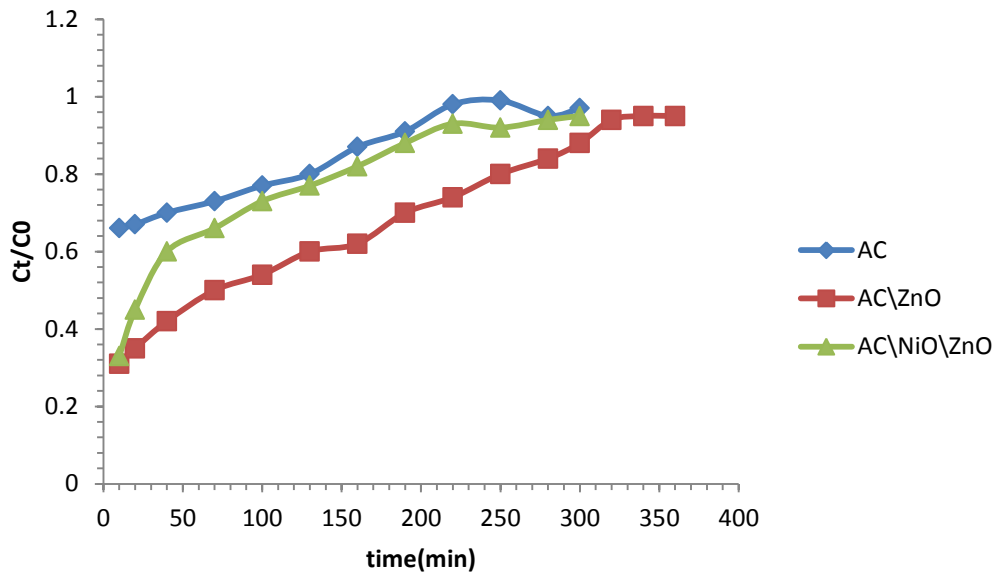


Figure 4.8 a: Breakthrough curves of Thiophene with initial concentration 166 ppm on AC/NiO/ZnO, AC/ZnO and AC (column mode).

AC\NiO\ZnO, AC\ ZnO and AC exhibited better capacity for BT than thiophene, and though the initial concentration of BT was 166 PPM it declined significantly to less than 0.05 PPM in the first 10 min treatment by AC, AC\ ZnO and AC\NiO\ZnO respectively and then increased gradually for 300 min until it returned to the initial concentration. (Figure 4.8 b) the absorption capacity for BT in column mode follow the order AC\NiO\ZnO > AC\ZnO > AC.

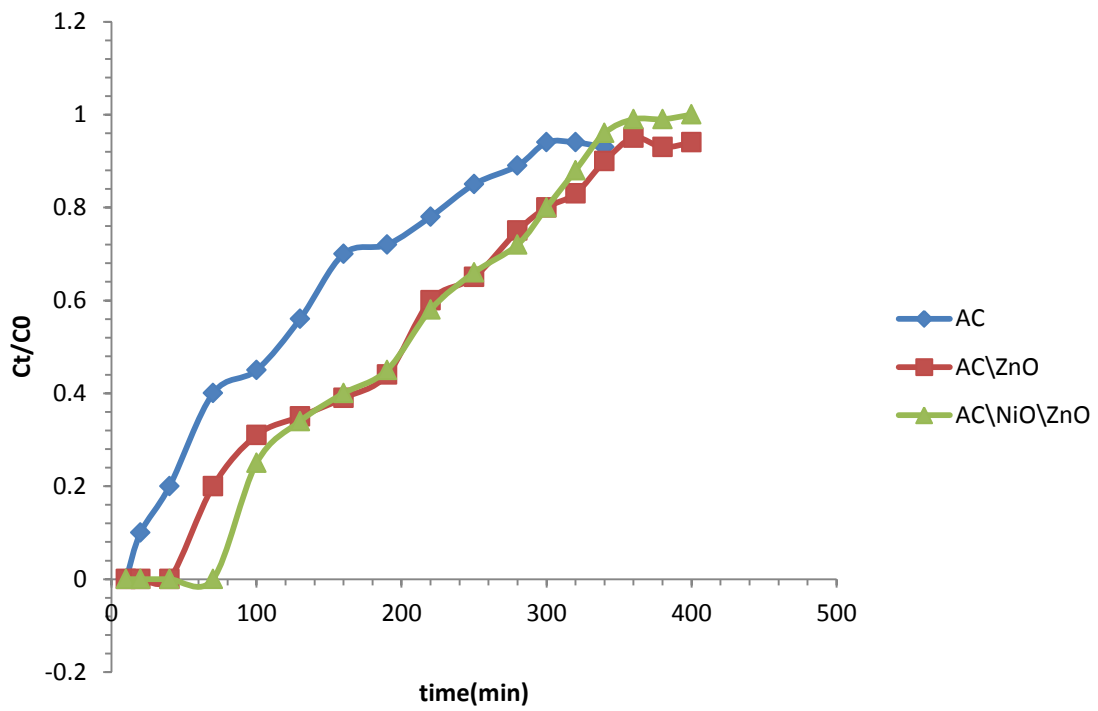


Figure 4.8 b: Breakthrough curves of BT with initial concentration 166 ppm on AC\NiO\ZnO , AC\ZnO and AC (column mode).

The best results were observed for DBT adsorption (Figures 4.9 c, d, e and f), there is no peak appears for DBT and the DBT became zero during the initial 10 min. The initial concentration was 166 mg/l and it remains at the same level (zero) during the treatment.

The adsorption capacity of the adsorbent decreased slowly with time. On AC after 180 minutes sulfur appeared in the sample with low concentration and returned to the initial concentration after five hours. AC\ ZnO exhibited higher adsorption capacity where the sulfur appeared in samples after longer time than AC the break through started after 270 minutes. The highest adsorption capacity for DBT was on AC\NiO\ZnO adsorbent where there was no peak appears for DBT and the DBT became zero during the initial 320 min (Figure 4.8 c). After 320 minutes sulfur appeared in the sample with low concentration and returned to the initial concentration after six hours.

As depicted in the (Figures 4.8 a,b and c), the breakthrough points are of the order

DBT > BT > thiophene and the order of adsorbents are: AC\NiO\ZnO > AC\ZnO > AC.

These results indicated that AC\NiO\ZnO > AC\ZnO > AC are suitable for removal of thiophene, BT and DBT in both modes. However, the column mode exhibited better removal toward thiophene, BT and DBT than the batch mode.

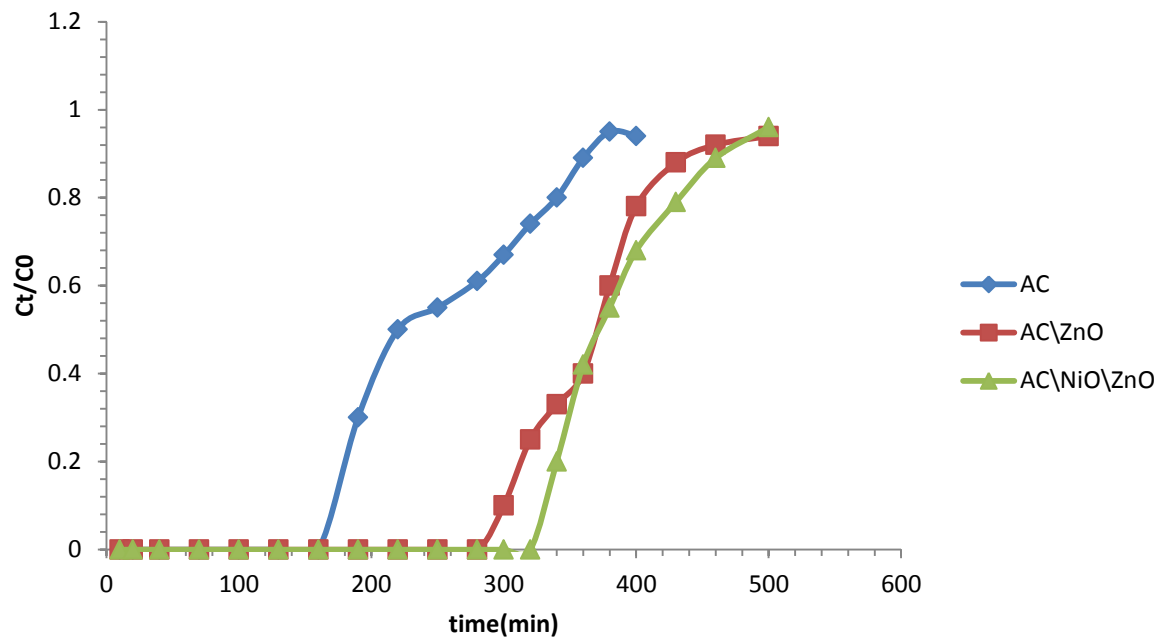


Figure 4.8 c: Breakthrough curves of DBT with initial concentration 166 ppm on AC\NiO\ZnO , AC\ZnO and AC (column mode).

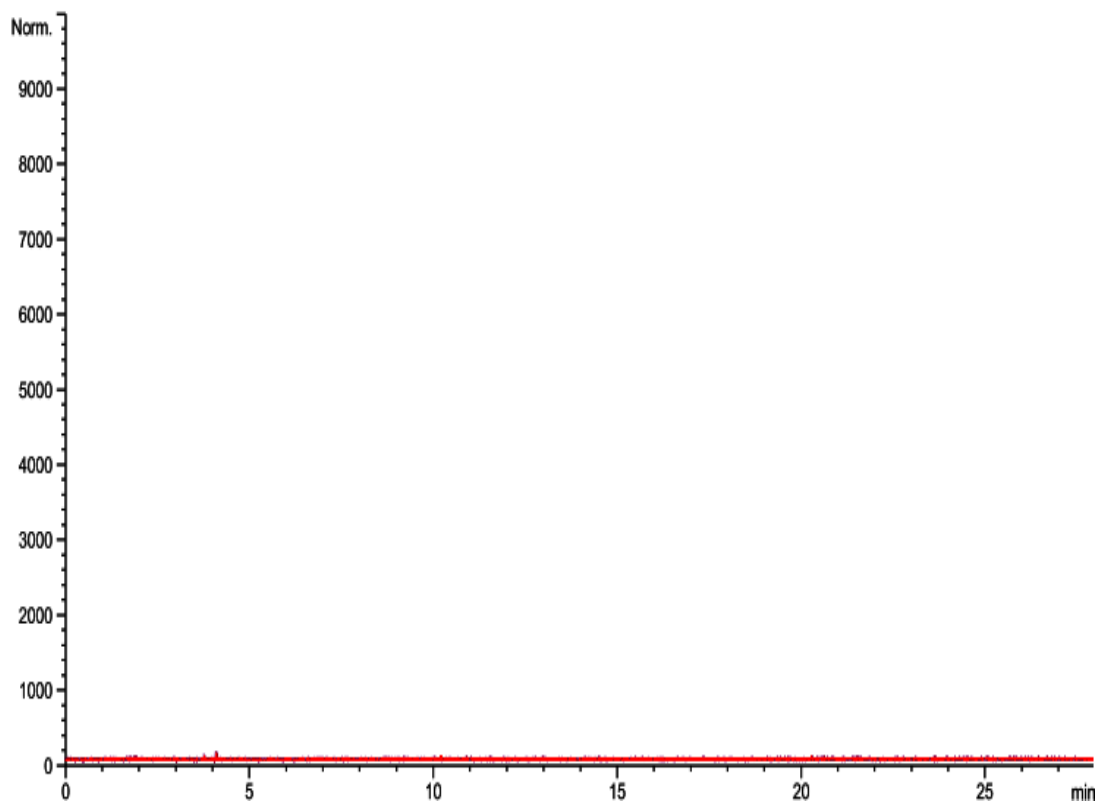


Figure 4.9 a: GC-SCD chromatogram of the blank (hexan+toluene)

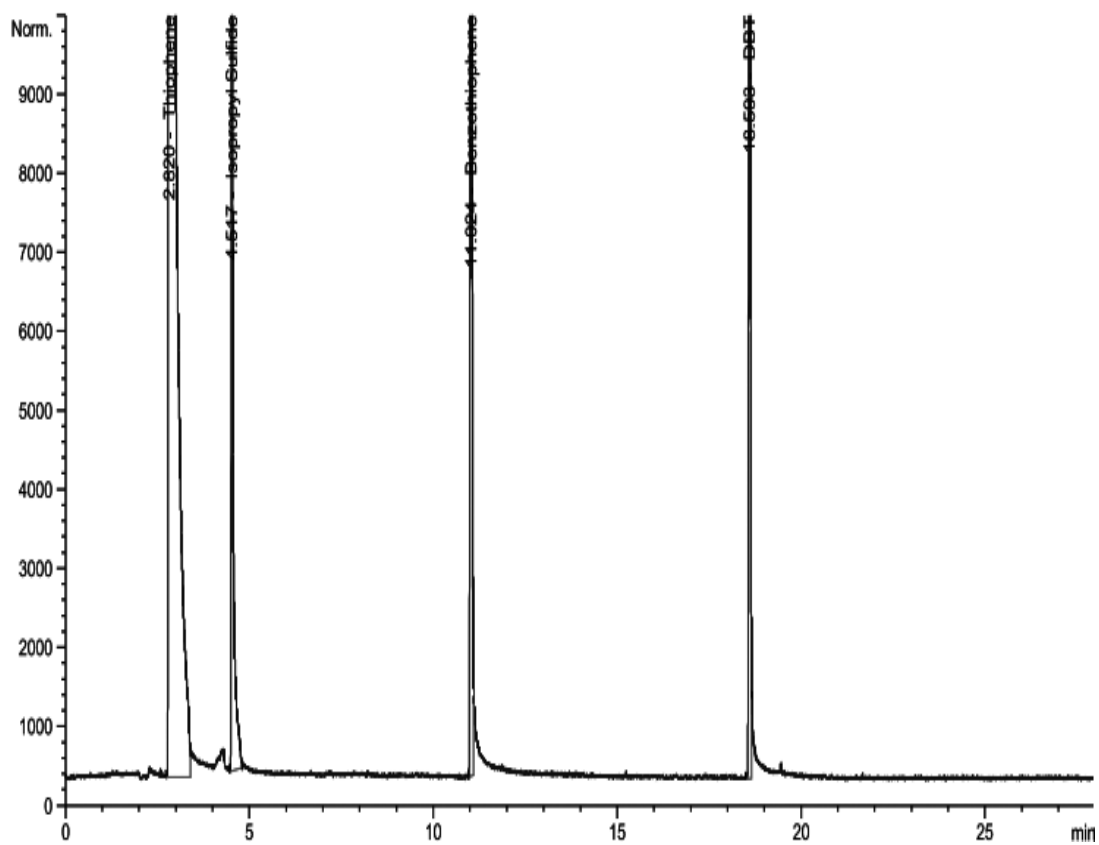


Figure 4.9 b: GC-SCD chromatogram of sample (thiophene, BT and DBT) before adsorption processes

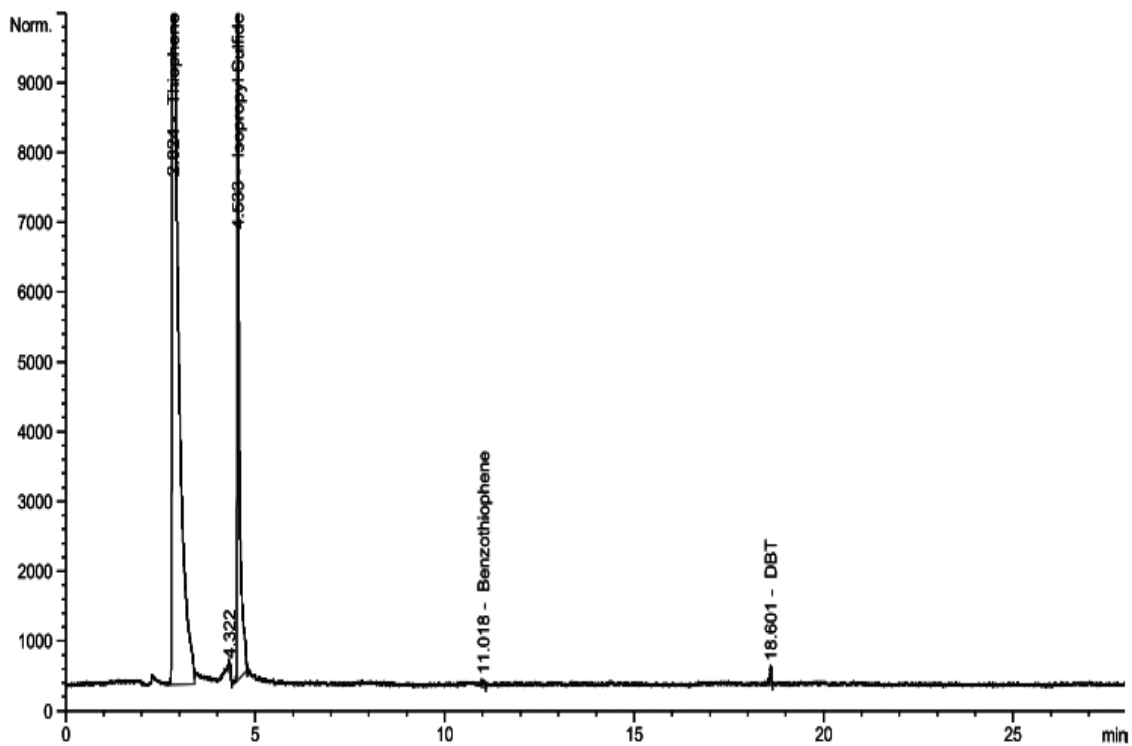


Figure 4.9 c: GC-SCD chromatogram of sample (thiophene, BT and DBT) after 10 min adsorption by AC (column)

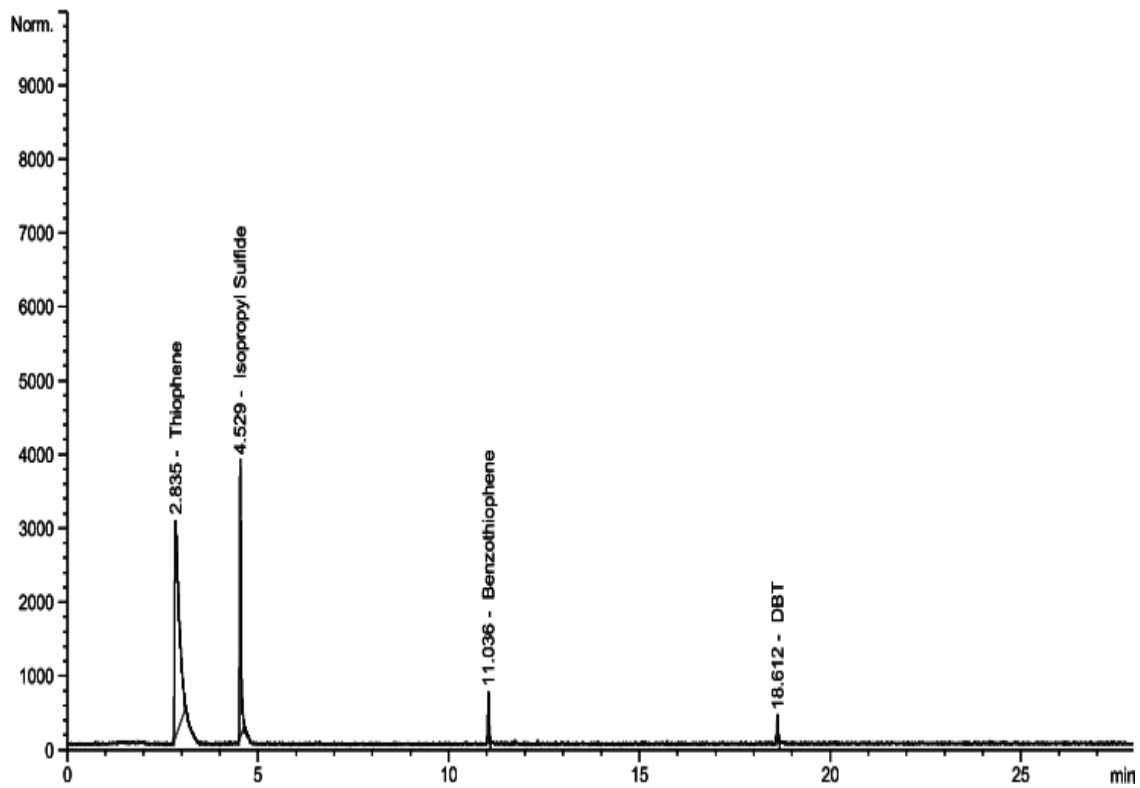


Figure 4.9 d: GC-SCD chromatogram of sample (thiophene, BT and DBT) after 10 min adsorption by AC/ZnO (column)

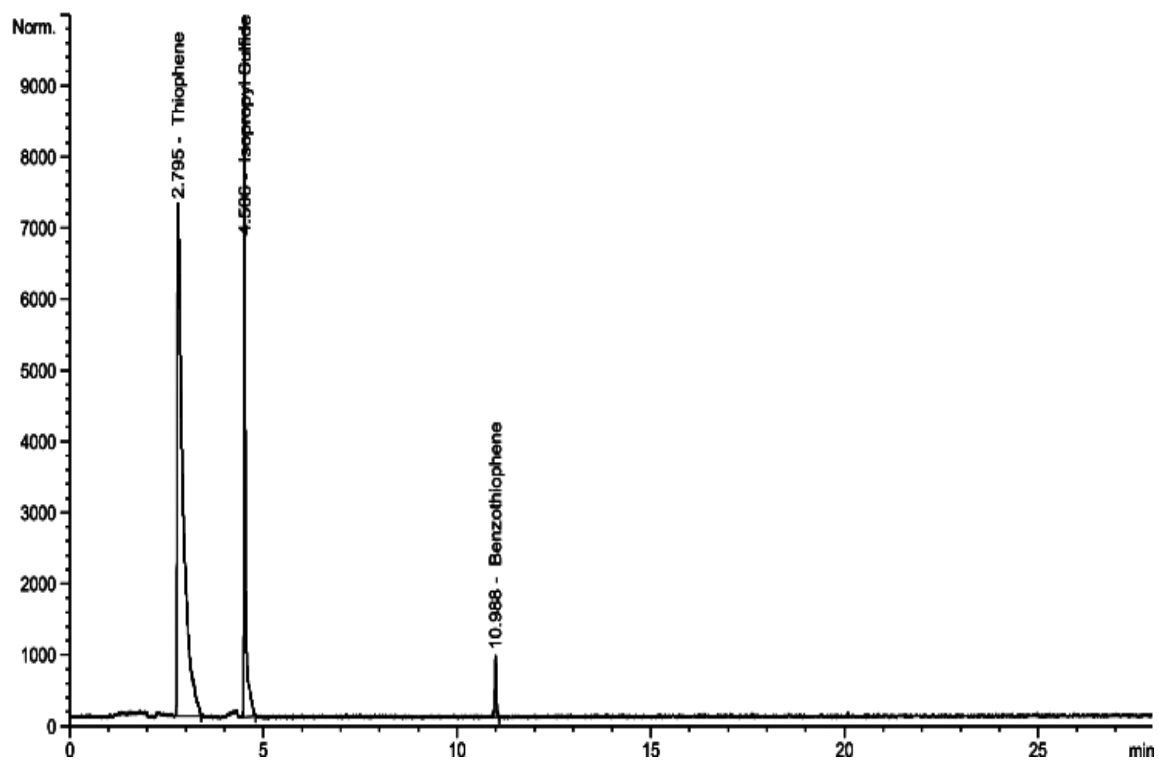


Figure 4.9 e: GC-SCD chromatogram of sample (thiophene, BT and DBT) after 20 min adsorption by AC/ZnO (column)

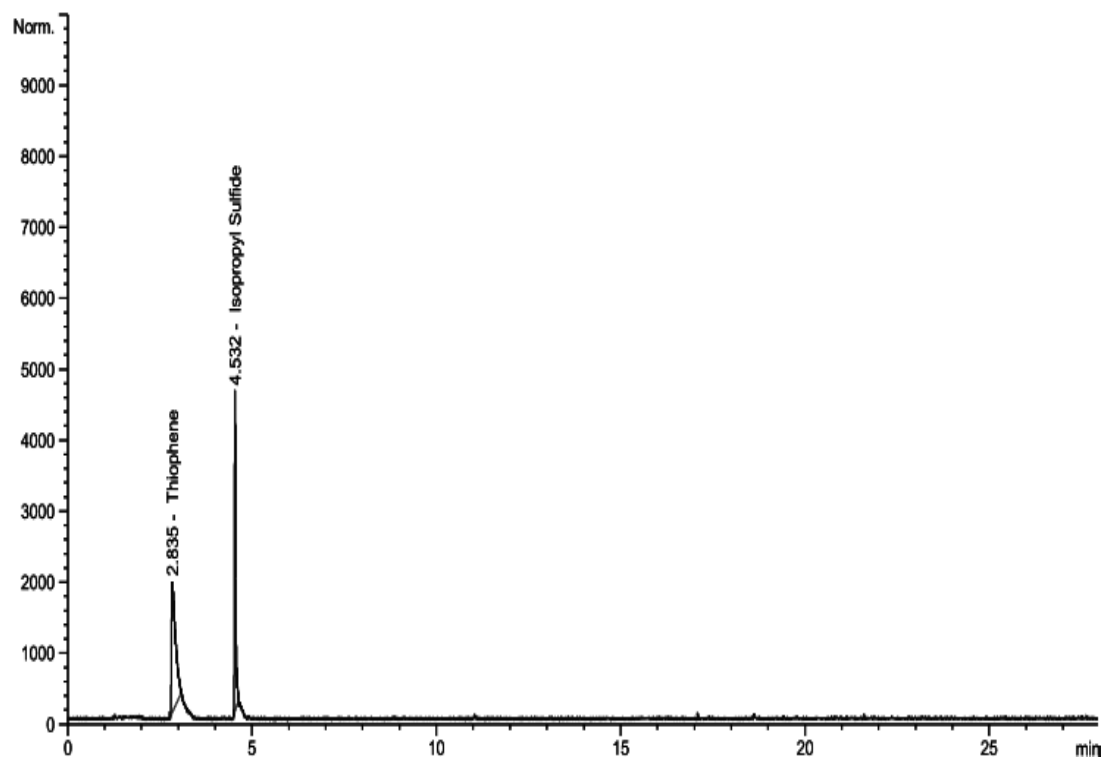


Figure 4. 9 f: GC-SCD chromatogram of sample (thiophene, BT and DBT) after 10 min adsorption by AC\NiO\ZnO (column)

4.3 Adsorption kinetics

Three kinetic models were applied for analysis of experimental kinetic data. In general, pseudo-first order kinetics is usually used to describe the initial stage of the adsorption process whereas, pseudo-second-order kinetics is based on the adsorption capacity, which usually gives good description of the whole adsorption process (Mansoor et al 2011) [116].

The adsorption process was described by pseudo first-order and pseudo-second-order kinetics and intraparticle diffusion models.

4.3.1 Pseudo-first-order

Pseudo-first-order equation was first given by Lagergren [117].

The Lagergren rate equation is the one generally used It is expressed in the following equation:

$$\ln(q_e - q_t) = \ln q_e - k_1 t$$

Where, q_e (mg/g) and q_t (mg/g) are the amounts of analyte adsorbed at equilibrium and time t (min), respectively; and k_1 (min^{-1}) is the rate constant of the Lagergren-first-order kinetics model.

The k_1 and q_e were calculated from the slope and intercept The plot of $\ln(q_e - q_t)$ versus t , respectively (Figures 4.10 a ,b and c) . The calculated q_e shown in (table 4. 2) are lower than the experimental values. As well as, The R^2 of the pseudo first order model are lower than the pseudo second order model, indicating that the adsorption of thiophene, BT and DBT on AC\NiO\ZnO , AC\ ZnO and AC do not obey the pseudo first order kinetic.

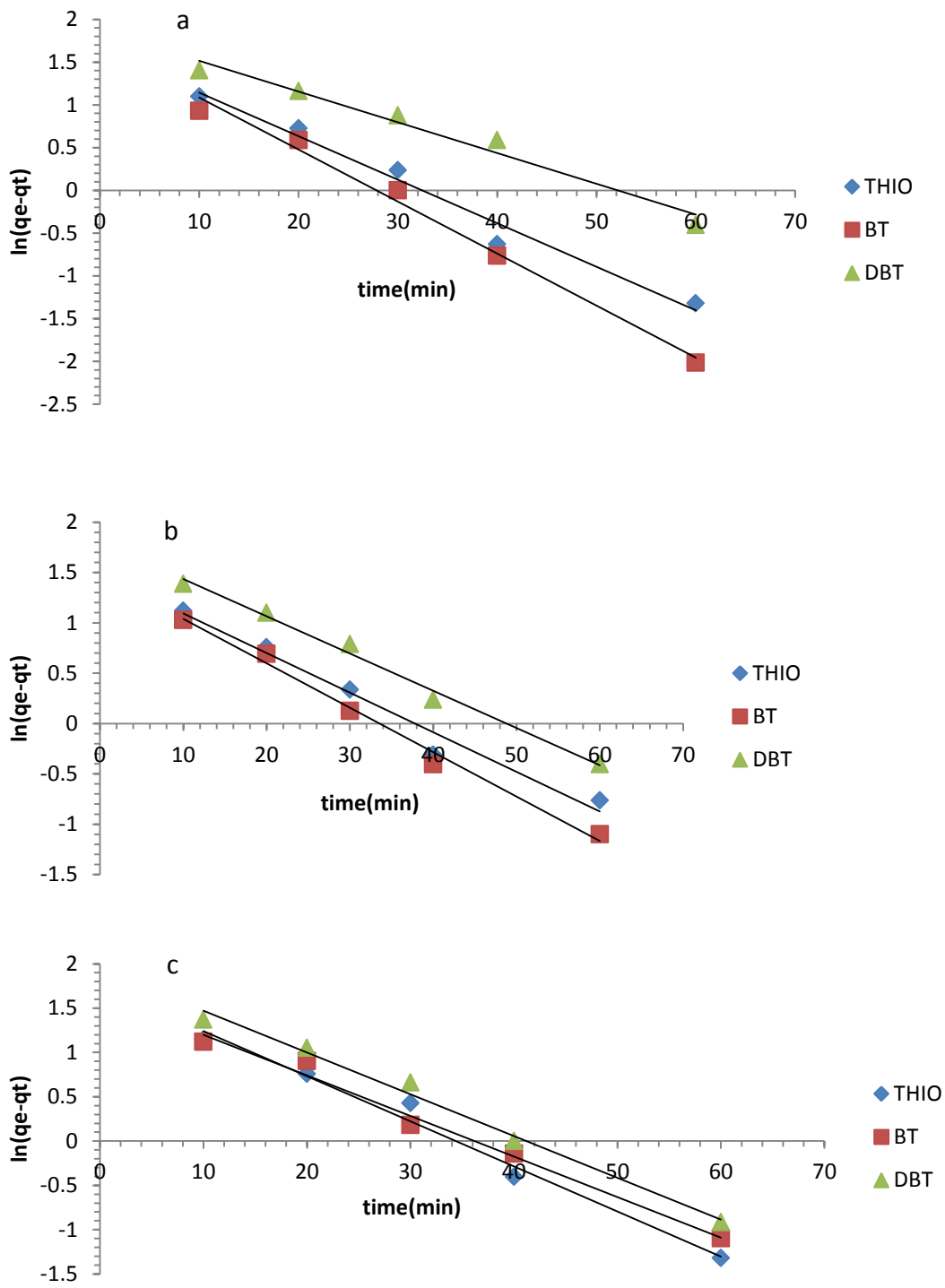


Figure 4.10: First order Pseudo kinetics for adsorption of thiophene, BT and DBT by a: AC/NiO/ZnO, b: AC/ZnO and c: AC

4.3.2 Pseudo-second-order

The pseudo-second-order kinetics can be expressed as the following equation [(McKay and Ho, 1999) [118].

$$\frac{t}{q_t} = \frac{1}{k_2 q_e^2} + \frac{t}{q_e}$$

Where q_t is the amount of adsorption thiophene, BT and DBT (mg/g) at time (min) and k_2 (g/ (mg min)) is the adsorption rate constant of pseudo-second-order adsorption.

The slope and intercept of the linear plots of t/q_t against t yield the values of $1/q_e$ and $1/k_2 q_e^2$. Where $k_2 q_e^2$ (mg/g.min) term is the initial adsorption rate at $t = 0$.

The k_2 and q_e can be obtained from the slope and intercept of plot of t/q_t versus t (Figures 4.11 a, b and c). The values of the rate constants, maximum amount adsorbed and the correlation coefficients are given in (table 4.2). The pseudo second order model is based on the assumption that the rate limiting step may be chemisorption which involves valence forces by sharing or electron exchange between the adsorbent and the adsorbate (Wang, et al 2008) [119].

The maximum adsorption capacities q_e calculated from the pseudo second order model are in accordance with the experimental values and higher correlation coefficient (R^2) indicate that the adsorption obeys a pseudo second order model.

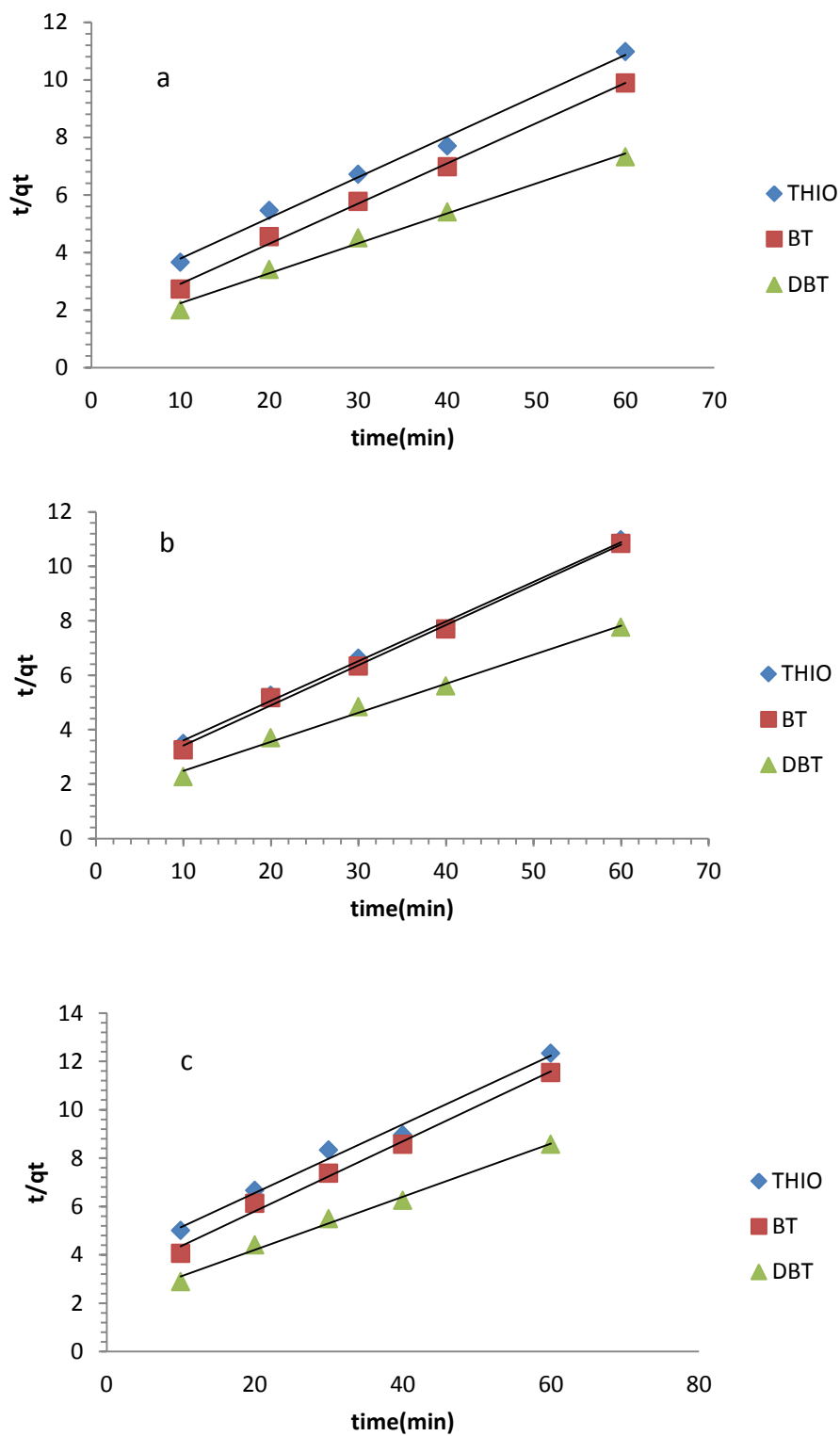


Figure 4.11: Second order Pseudo kinetics for adsorption of thiophene, BT and DBT by a: AC/NiO/ZnO, b: AC/ZnO and c: AC

Table 4.2: Experimental q_e , pseudo-first-order, pseudo-second-order and Intraparticle diffusion models for adsorption of Thiophene, BT and DBT on AC, AC\ZnO and AC\NiO\ZnO

adsorbent	compound	$q_{e,exp}$ (mg/g)	Pseudo-first order			Pseudo-second order			Intraparticle diffusion model		
			k1	q_e, cal	R^2	k2	q_e, cal	R^2	ki	C	R^2
AC	THIO	5.13	0.05	5.4	0.98	0.006	6.6	0.99	0.64	0.06	0.97
	BT	5.5	0.045	4.9	0.99	0.01	5.5	0.99	0.61	0.96	0.98
	DBT	7.4	0.047	6.6	0.98	0.008	7.5	0.99	0.8	0.98	0.97
AC\ZnO	THIO	5.9	0.039	4.4	0.97	0.01	6.2	0.99	0.59	1.4	0.95
	BT	5.8	0.04	4.3	0.98	0.012	6.1	0.99	0.56	1.4	0.95
	DBT	8.4	0.037	6	0.99	0.008	9	0.99	0.75	2	0.98
AC\NiO\ZnO	THIO	5.7	0.05	4.9	0.97	0.009	6.1	0.99	0.62	0.86	0.95
	BT	6.2	0.06	5.4	0.98	0.016	6.4	0.99	0.55	0.96	0.96
	DBT	9.06	0.36	6	0.98	0.01	9.3	0.99	0.7	1	0.99

4.3.3 Intraparticle diffusion model

The kinetic experimental results were also fitted to the Weber's intraparticle diffusion mechanism to gain insight understanding to the mechanisms and rate controlling steps affecting the adsorption kinetics (Weber 1963)[120].

The kinetic results were analyzed by the intraparticle diffusion model to elucidate the diffusion mechanism. The following equation was applied:

$$qt = k_{id}t^{1/2} + C$$

where C is the intercept (mg/g) which is related to the boundary layer thickness and k_{id} is the slope which represents the intraparticle diffusion rate constant ($\text{mg/g h}^{1/2}$), which can be evaluated from the slope of the linear plot of q_t versus $t^{1/2}$ (Figures 4.12 a ,b and c) .

Our results indicate that the three adsorbents have higher adsorption efficiency toward DBT over the other two sulfur compounds. This can be concluded from the intercept as presented in (table 4.2). The correlation coefficient (R^2) and intercept of DBT is higher than that of thiophene and BT table (4.2) indicating greater contribution of the surface sorption in the rate controlling step in case of DBT adsorption. If the regression of qt versus $t^{1/2}$ is linear and passes through the origin, then intraparticle diffusion is the sole rate-limiting step. However, the linear plots at each dosage did not pass through the origin. This indicates that the intraparticle diffusion was not only rate controlling step [Hameed 121].

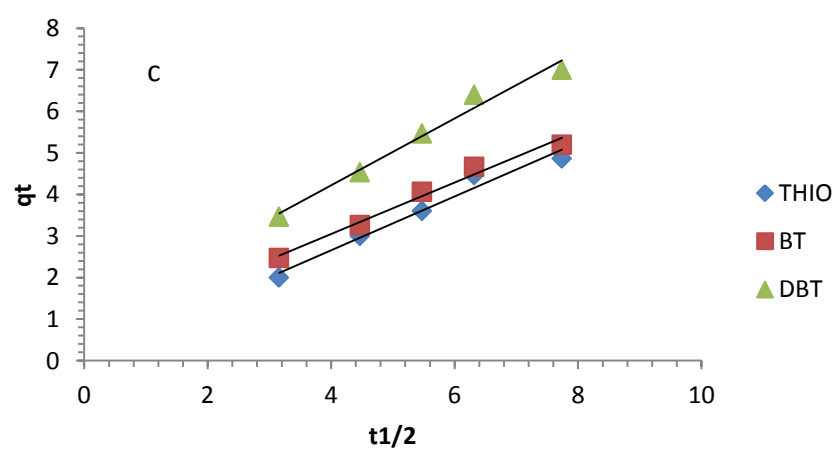
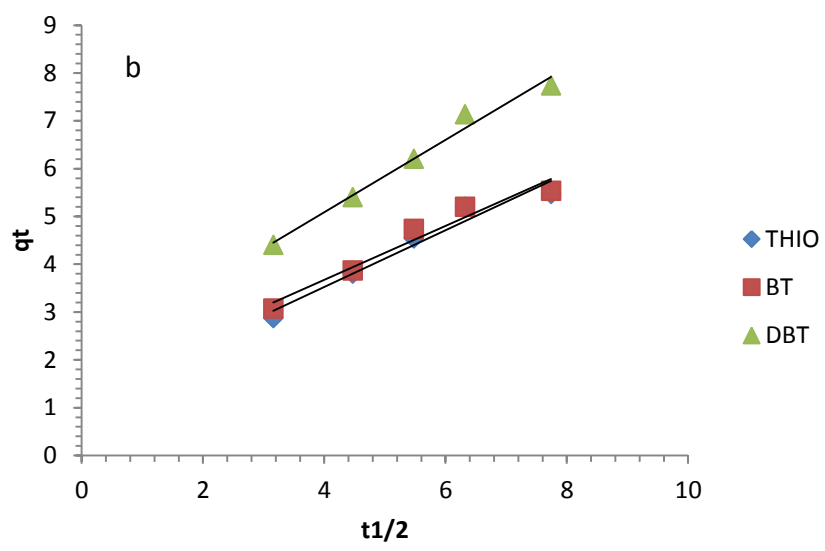
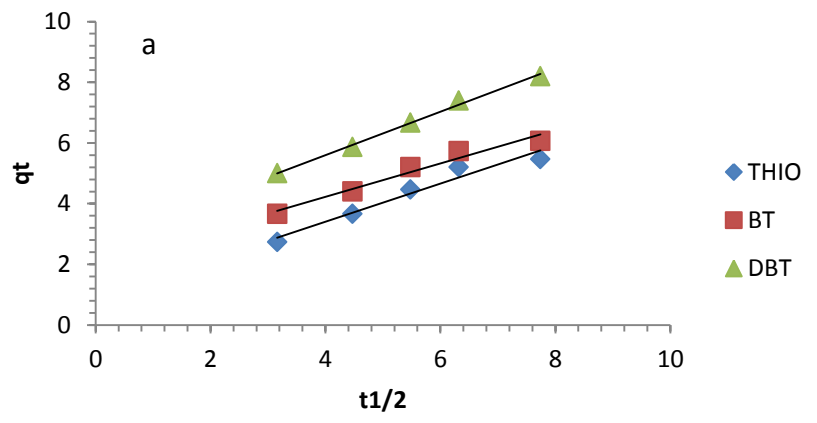


Figure 4.12: Plots for evaluating intraparticle diffusion rate constant for sorption of Thiophene, BT and DBT onto a: AC\NiO\ZnO, b: AC\ZnO and c: AC

4.4 Adsorption isotherms

The adsorption capacity is an important factor because it determines how much of an adsorbent is required for quantitative enrichment of adsorbates from a given solution. In addition, the distribution of Thiophene, BT and DBT between the liquid and solid phases at equilibrium can be expressed by adsorption isotherms.

In this study, for investigation of the adsorption of Thiophene, BT and DBT onto AC\NiO\ZnO , AC\ ZnO and AC the adsorption equilibrium data were fitted using Langmuir and Freundlich models, which correspond to homogenous and heterogeneous adsorbent surfaces respectively. The Langmuir model assumes that adsorption takes place at uniform energy sites on the surface of the adsorbent while; the Freundlich model is an empirical equation that assumes multilayer adsorption due to the diversity of adsorption sites.

4.4.1 Langmuir isotherms

The Langmuir equation (Suna Erses et al., 2005) [122] governs the amount of DBT, BT and Thiophene adsorbed and its linear equation is given in the following equation:

$$\frac{C_e}{q_e} = \frac{1}{bq_m} + \frac{C_e}{q_m}$$

Where q_e (mg g^{-1}) is the amount adsorbed at equilibrium concentration C_e (mg L^{-1}), q_m (mg g^{-1}) is the Langmuir constant representing maximum monolayer capacity and b is the Langmuir constant related to the energy of adsorption.

The slope and intercept of linear plots of C_e/q_e against C_e (Figures 4.13 a, b and c) yield the values of $1/q_m$ and $1/bq_m$.

The adsorption capacity q_m of thiophene increased from 39 mg/g on AC to 43 mg/g onto AC/ZnO to 47 mg/g onto AC/NiO/ZnO. As well as, the highest maximum monolayer capacity q_m for BT and DBT was obtained onto AC/NiO/ZnO also (table 4.3)

The dimensionless constant separation factor R_L considers an essential characteristic of the Langmuir isotherm [123 Hall].

$$R_L = \frac{1}{1 + bC_0}$$

Where C_0 is the highest initial concentration of adsorbate (mg/L), and b (L/mg) is Langmuir constant. The shape of the isotherm can better be represented by the R_L value where $R_L > 1$ indicates unfavorable process $R_L = 1$ indicates linearity and $0 < R_L < 1$ indicates favorable process. Our results represent in (table 4.3) show the value of R_L between 0 and 1 which indicate that the adsorption of DBT, BT and Thiophene on AC/NiO/ZnO, AC/ZnO and AC is favorable process.

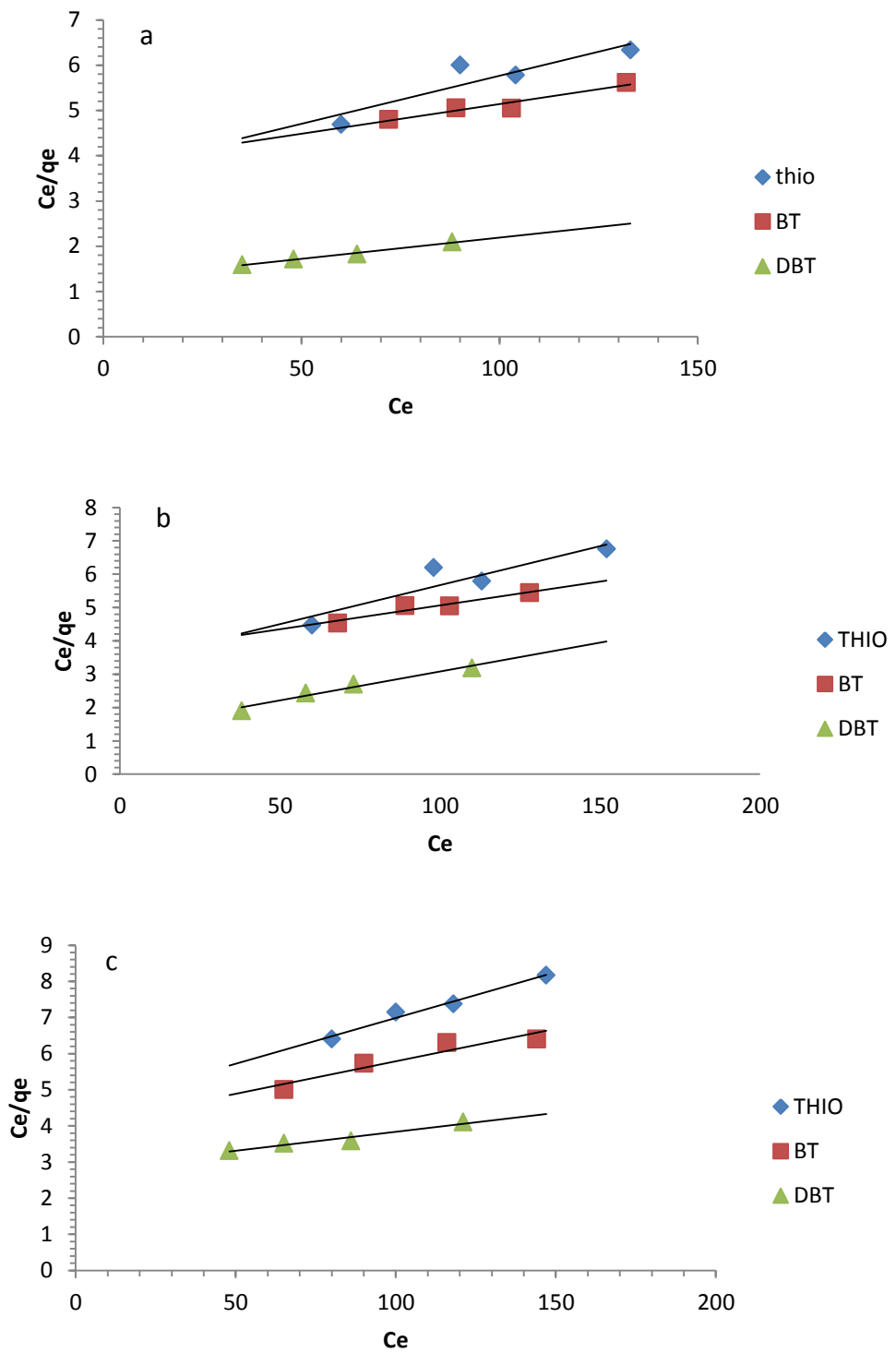


Figure 4.13: plot of Langmuir isotherm for adsorption of thiophene, BT and DBT by (a) AC/NiO/ZnO, (b) AC/ZnO and c: AC

**Table 4.3: Langmuir and Freundlich isotherm constants for Thiophene, BT and DBT onto
AC, AC\ZnO and AC\NiO\ZnO**

adsorbents	compounds	Langmuir isotherm constant				Freundlich isotherm constant			
		qm (mg/g)	b	R ²	RI	K	1/n	n	R ²
AC	THIO	39.5	0.005	0.97	0.51	2.3	0.7	1.3	0.99
	BT	55.5	0.004	0.89	0.56	2.5	0.81	1.25	0.98
	DBT	100	0.003	0.95	0.66	2.6	0.9	1.1	0.97
AC\ZnO	THIO	43	0.007	0.84	0.45	2.4	0.83	1.2	0.95
	BT	71	0.003	0.92	0.62	3	0.88	1.14	0.99
	DBT	102	0.005	0.96	0.51	3.1	0.5	2	0.99
AC\NiO\ZnO	THIO	47	0.005	0.81	0.51	2.5	0.8	1.25	0.98
	BT	76	0.003	0.93	0.64	3	0.88	1.1	0.99
	DBT	106	0.007	0.99	0.43	3.8	0.5	2	0.99

4.4.2 Freundlich isotherm

The Freundlich relation (Suna Erses et al., 2005) describes multilayer sorption and can be expressed as equation

$$\ln q_e = \ln K_f + \frac{1}{n} \ln C_e$$

Where K_f and n are the Freundlich constants related to the adsorption capacity and intensity, respectively; with K_f (mg/g) is the adsorption capacity of the sorbent and $1/n$ (g/L) giving an indication of how favorable the adsorption process [Poots 124].

To determine the constants K_f and n , the linear form of the equation may be used to produce a graph of $\ln (q_e)$ against $\ln (C_e)$ (Figures 4.14 a, b and c)).

Results in (table 4.3) showed the value of n are more than one which means that it is a favorable adsorption process. As it is shown in (table 4.3), the adsorption capacity of the three sorbents toward DBT is higher than that toward BT and thiophene. Moreover, adsorption capacity follow the order AC\NiO\ZnO > AC\ ZnO > AC. This is supported by the (percentage removal presented in Figure 4.5).

The comparison of the R^2 values from (table 4.3) indicates that Freundlich isotherm model yields a better fit to the experimental data than Langmuir isotherm.

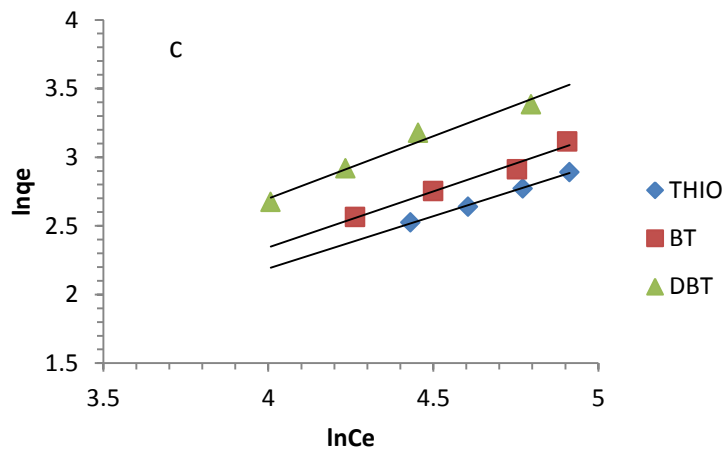
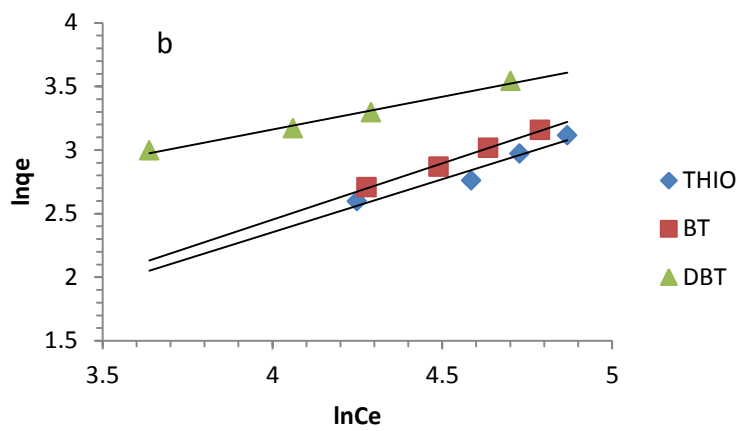
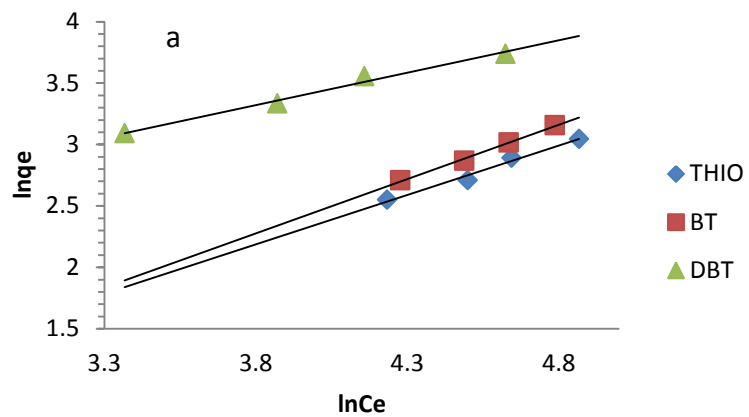


Figure 4.14: plot of Freundlich isotherm for adsorption of thiophene, BT and DBT by (a) AC/NiO/ZnO, (b) AC/ZnO and c: AC

4.5 Regeneration of spent adsorbents

Two methods; solvent followed by heating at 300 °c and thermally method which the spent sorbents were heated at 350 °c for 3h were used for regeneration of the sorbents loaded with organosulfur compounds. For the first method; Toluene was passed through the column packed with the spent sorbents by pump with constant flow rate. Aliquots of the eluent was collected in different intervals and analyzed by GC-SCD. As depicted in (Figure 4.15), the amount of thiophene and dibenzothiophene decreased with times, which indicate faster release of thiophene and BT comparing with DBT. This trend confirms the higher ability of DBT, to form π - π complex between π electrons of benzene rings and active sites on an activated carbon surface, than the BT and thiophene. It is also obvious from (figure4. 15) that the adsorbed BT and DBT on the sorbents did not desorbed completely. Thus, it was necessary to heat the spent sorbents in order completely regenerated them. These sorbents were then reused for another cycle (Figure 4.16). On the other hand, heating the spent adsorbents at 350 °c gave the same percentage of removal as depicted in figure (4.16) which means that only thermally method is effective for the regeneration process.

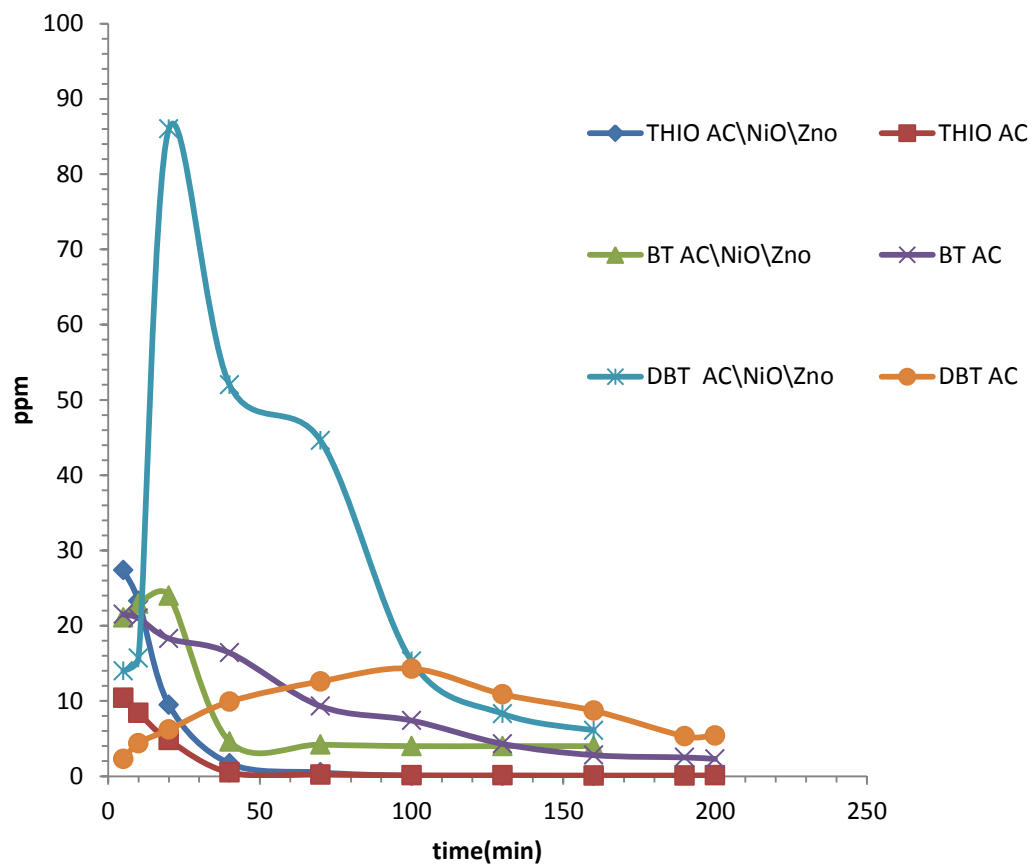


Figure 4.15: amount of thiophene, BT and DBT desorbed from AC and AC\NiO\ZnO by toluene at different times

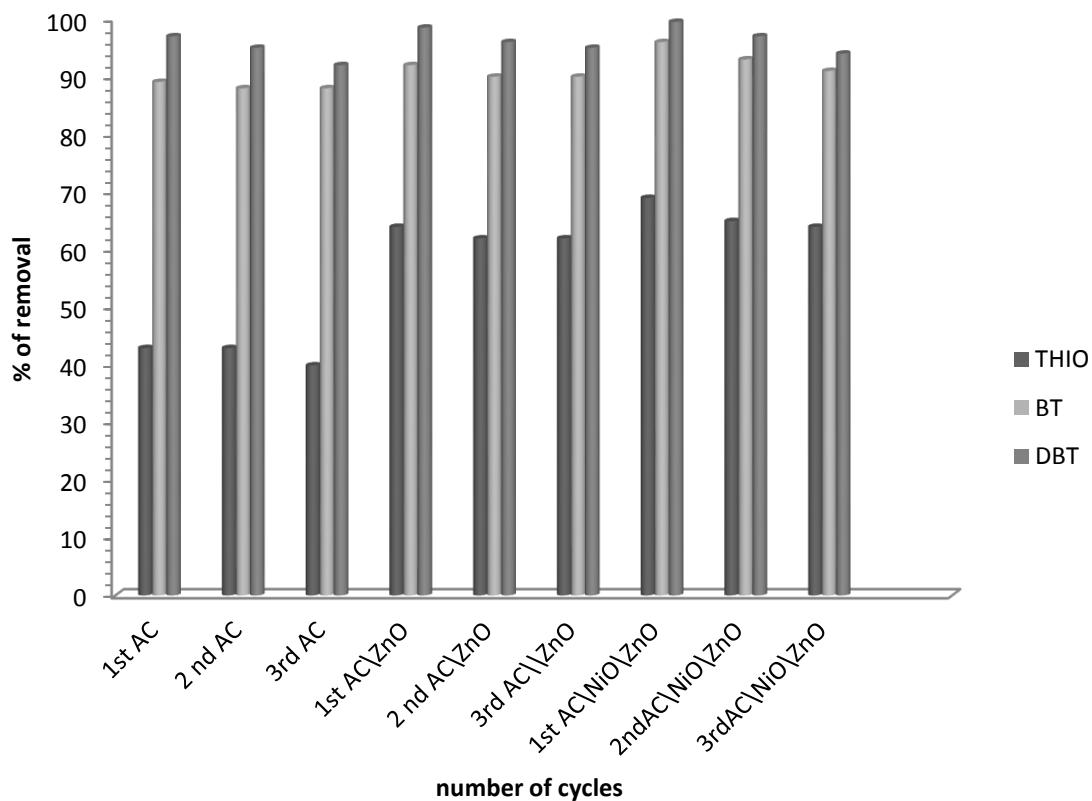


Figure 4.16: percentages of removal of thiophene, BT and DBT from model diesel by AC\NiO\ZnO, AC\ ZnO, and AC in three cycles: where 2nd is regeneration by solvent and heat, while 3rd regeneration only by heating at 350 °c for 3h. (After 10 minutes adsorption)

Conclusion

In this work, we synthesized and characterized five porous materials: AC, AC/ZnO, AC/NiO/ZnO, Al₂O₃/NiO/ZnO and Al₂O₃/ZnO. The prepared materials were examined for desulfurization at ambient conditions. Adsorptions of model fuel, contains thiophene, BT and DBT over the prepared materials were conducted in batch and fixed-bed adsorption systems. AC/NiO/ZnO has the highest adsorption capacity in both modes, which confirmed that, the adsorption capacity governs by two factors, the chemical properties as a result of interaction between the metal oxides and sulfur while the factor is the physical properties represented by the surface area and the porosity. Further, the kinetic and isotherm studies indicated that, Freundlich isotherm provided a better fit to the experimental data, while the adsorption kinetics followed the pseudo second-order. The results indicate that the metal NiO and ZnO based activated carbon adsorbents were found to possess high adsorption capacity and hence it could be employed as a low-cost adsorbent for desulfurization by adsorption as alternatives to HDS, and in particular, for the removal of BT and DBT. As well as, only thermally method is effective for the regeneration process.

Recommendation for future work

Metal oxides based activated carbon exhibited high adsorption capacity for removal of sulfur compounds from model diesel. For future work the metal oxides based activated carbon should be tested for removal of sulfur compounds in diesel fuel. Also, we recommend introducing more active sites to the activated carbon by loading another material which plays important roles like soft acidic groups

References

- [1]. B. Pawelec, et al., “Towards near zero-sulfur liquid fuels: a perspective review”, *Catal. Sci. Technol.*, 1, 23–42, 2011.
- [2]. A. Brady, “Global Refining Margins Look Poor in Short Term, Buoyant Later Next Decade”, *Oil Gas J.*, 97, 75-80, 1999.
- [3]. J. H. Gary and G. E. Handwerk, *Petroleum Refining, Technology and Economics*, Second Edition, Marcel Dekker, New York, 1998.
- [4]. C. Song, X. Ma, “New design approaches to ultra-clean diesel fuels by deep desulfurization and deep dearomatization”, *Applied Catalysis B: Environmental*, 41, 207–238, 2003.
- [5]. C. Song, et al. , “An overview of new approaches to deep desulfurization for ultra-clean gasoline, diesel fuel and jet fuel”, *Catalysis Today*, 86, 211 - 263, 2003.
- [6]. OPEC Secretariat, Helfferstorferstrasse 17 A-1010 Vienna, Austria, 2011 www.opec.org.
- [7]. O. Garba Yahaya, “Removal of Sulfur Compounds from Diesel/Crude Oil Using Extractive Liquid Membrane Contactor (ELMC) and Supported Ionic Liquid Membrane (SILM)”, *SUMMER SAUDI ARAMCO JOURNAL OF TECHNOLOGY*, 60, 2012.
- [8]. Saudi Arabia Energy Data, Statistics and Analysis - Oil, Gas, Electricity, file:///Z:/NewCABs/V6/Saudi_Arabia/Full.htm, January 2011.
- [9]. J. W. Shirokoff, M. N. Siddiqui, and M. F. Ali, “Characterization of the Structure of Saudi Crude Asphaltenes by X-ray Diffraction”, *Energy & Fuels*, 11, 561-565, 1997.
- [10]. A. D. Ahmad, et al., “Process for upgrading whole crude oil to remove nitrogen and sulfur compounds”, patent, EP 2225349 A1, 2010.

- [11]. W. L. Fang, "Inventory of U. S. Greenhouse Gas Emissions and Sinks, 1990-2003", Clean Air Markets Division, 2004.
- [12]. V. C. Srivastava, "An evaluation of desulfurization technologies for sulfur removal from liquid Fuels", *RSC Advances*, 2, 759–783, 2012.
- [13]. S.F. Venner, "EU environmental laws impact fuels' requirements", *Hydrocarbon Process*, 79, 51–71, 2000.
- [14]. P.T. Vasudevan, J.L.G. Fierro, "A review of deep hydrodesulfurization catalysis", *Catal. Rev. Sci. Eng.*, 38, 161–188, 1996.
- [15]. US EPA, Diesel Fuel Quality: Advance Notice of Proposed Rulemaking, EPA420-F-99-011, Office of Mobile Sources, May 1999.
- [16]. Y. Qingtang, "Progress and outlook on technologies for processing inferior crude oil in China", *China Petroleum Processing and Petrochemical Technology*, 3, 1-7, 2008.
- [17]. Z. C. "Mester, in Meeting Sulphur Specifications for 2000 and Beyond", San Francisco, 26–29, 2000.
- [18]. EU Fuel Regulations: <http://www.dieselnet.com/standards/eu/fuel.php>.
- [19]. Japan Fuel Regulations: <http://www.dieselnet.com/standards/jp/fuel.php>.
- [20]. Hart Energy, World Refining and Fuels Service (WRFS) and International Fuel Quality Centre (IFQC), September 2011.
- [21]. H. Schulz, W. Bohringer, F. Ousmanov, Waller P, "Refractory sulfur compounds in gas oils", *Fuel Process Technol.*, 61, 5–41, 1999.
- [22]. H. Schulz, W. Bohringer, P. Waller, F. Ousmanov, "Gas oil deep hydrodesulfurization: refractory compounds and retarded kinetics", *Catal. Today*, 49, 87–97, 1999.
- [23]. G.E. Dolbear, E.R. Skov, "Selective oxidation as a route to petroleum desulfurization", *Am. Chem. Soc. Div. Fuel Chem.*, 45, 375–378, 2000.

- [24]. R.T. Yang, A. Takahashi, F.H. Yang, A. Maldonado, "Selective sorbents for desulfurization of liquid fuels, U.S. and Foreign", Patent applications, 2002.
- [25]. R.F. Zaykina, Y.A. Zaykin, T.B. Mamaonava, N.K. Nadirov, "Radiation methods for demercaptanization and desulfurization of oil products", *Phys. Chem.*, 63, 621–624, 2002.
- [26]. G. Yu, S. Lu, H. Chen, Z. Zhu, "Diesel fuel desulfurization with hydrogen peroxide promoted by formic acid and catalyzed by activated carbon", *Carbon*, 43, 2285–2294, 2005.
- [27]. M.H. Ali, A. Al-Maliki, B. El-Ali, G. Martinie, M.N. Siddiqui, "Deep desulfurization of gasoline and diesel fuels using non-hydrogen consuming techniques", *Fuel*, 85, 1354–1363, 2006.
- [28]. H. Lu, J. Gao, Z. Jiang, F. Jing, Y. Yang, G. Wang, C. Li, "Ultra-deep desulfurization of diesel by selective oxidation with [C₁₈H₃₇N(CH₃)₃]₄[H₂NaPW₁₀O₃₆] catalyst assembled in emulsion droplets", *J.Catal.*, 239, 369–375, 2006.
- [29]. P.S. Kulkarni and C. A. M. Afonso," Deep desulfurization of diesel fuel using ionic liquids: current status and future challenges", *Green Chem.*, 12, 1139–1149, 2010.
- [30]. G. Yu, S. Lu, H. Chen, Z. Zhu, "Oxidative desulfurization of diesel fuels with hydrogen peroxide in the presence of activated carbon and formic Acid", *Energy & Fuels*, 19, 447–452, 2005.
- [31]. C. Komintarachat, W. Trakarnpruk, "Oxidative desulfurization using polyoxometalates", *Industrial & Engineering Chemistry Research*, 45, 1853–1856, 2006.
- [32]. J.K. Stanger, J.R. Angelici, "Silica-catalyzed tert-butyl hydroperoxide oxidation of dibenzothiophene and its 4,6-dimethyl derivative: a route to low-sulfur petroleum feedstock", *Energy & Fuels*, 20, 1757–1760, 2006.
- [33]. D.Wang, W. Qian, H. Amano, K. Okata, A. Ishihara, T. Kabe, "Oxidative desulfurization of fuel oil part i, oxidation of dibenzothiophenes using t-butyl hydroperoxide", *Applied Catalysis A*, 253, 91–99, 2003.

- [34]. X. Zhou, C. Zhao, J. Yang, S. Zhang, "Catalytic oxidation of dibenzothiophene using cyclohexanone peroxide", *Energy & Fuels*, 21, 7–10, 2007.
- [35]. J. Li, X. Zhou, D. Zhao, "Oxidative desulfurization of dibenzothiophene using cyclohexanone peroxide", *Energy & Fuels*, 34, 249-251, 2006.
- [36]. Yu.L. Zub, A.B. Pecheny, A.A. Chuiko, T.L. Stuchinskaya, N.N. Kundo, "Metalphthalocyanines fixed onto polyorganosiloxane matrices as oxidation catalysts for HS groups", *Catalysis Today*, 17, 31–40, 1993.
- [37]. A.H. Sun, G.C. Zhang, Y.M. Xu, "Photobleaching of metal phthalocyanine sulfonates under UV and visible light irradiation over TiO₂ semiconductor", *Materials Letters*, 59, 4016–4019, 2005.
- [38]. X. Zhou, J.Li, X. Wang, K. Jin, W. Ma," Oxidative desulfurization of dibenzothiophene based on molecular oxygen and iron phthalocyanine", *Fuel processing Technology*, 90, 317 – 323, 2009.
- [39]. J.T. Sampanthar et al., "A novel oxidative desulfurization process to remove refractory sulfur compounds from diesel fuel", *Applied Catalysis B: Environmental*, 63, 85–93, 2006.
- [40]. D. Giuseppe, , D. Angelis, Francesco, Crestini, Claudia; Saladino, Raffaele, "Efficient oxidation of thiophene derivatives with homogeneous and heterogeneous MTO/H₂O₂ systems: A novel approach for, oxidative desulfurization (ODS) of diesel fuel", *Applied Catalysis B, Environmental*, 89, 239-245, 2009.
- [41]. L. Wang, C. Hu Li, Y. F. Hou, "Phosphotungstic Acid/Semi-Coke Catalysts for Oxidative Desulfurization of Diesel Fuel", *Advanced Materials Research*, 79, 1683-1686, 2009.
- [42]. A. Srivastav, V.C. Srivastava, "Adsorptive desulfurization by activated alumina", *Journal of Hazardous Materials*, 170, 1133–1140, 2009.
- [43]. B.H. Kim, H.Y. Kim, T.S. Kim, D.H. Park, "Selectivity of desulfurization activity of *Desulfovibrio desulfuricans* M6 on different petroleum products", *Fuel Process Technol.*, 43, 87–94, 1995.

- [44]. D.J. Monticello, "Biodesulfurization and the upgrading of petroleum distillates", *Curr. Opin. Biotechnol*, 11, 540–546, 2000.
- [45]. K.A. Gray, G.T. Mrachko, C.H. Squires, "Biodesulfurization of fossil fuels", *Curr. Opin. Microbiol.*, 6, 229–235, 2003.
- [46]. S. Guobin, Z. Huaiying, X. Jianmin, C. Guo, L.Wangliang, L. Huizhou, "Biodesulfurization of hydrodesulfurized diesel oil with *Pseudomonas delafieldii* R-8 from high density culture", *Biochem. Eng. J.*, 27, 305–309, 2006.
- [47]. J. Konishi, Y. Ishii, K. Okumura y M. Suzuki, "High temperature desulfurization by microorganisms". United States Patent 5,925,560, 2000.
- [48]. N. Gupta, P. K. Roychoudhury, and J. K. Deb, "Biotechnology of desulfurization of diesel: prospects and challenges", *Appl. Microbiol. Biotechnol*, 66, 356-366, 2005.
- [49]. J. Bu et al., "Desulfurization of diesel fuels by selective adsorption on activated carbons:Competitive adsorption of polycyclic aromatic sulfur heterocycles and polycyclic aromatic hydrocarbons", *Chemical Engineering Journal*, 166, 207–217, 2011.
- [50]. A.L. Hines and R.N. Maddox, *Mass Transfer: Fundamental and Application*, Prentice-Hall, Upper Saddle River, NJ, 1985.
- [51]. R.T. Hernandez- Yang, F.H. Yang, A. Takahashi and A.J. Maldonado, Selective sorbents for purification of hydrocarbons, US patent 2004/0040891 US 2004/0044262 A1. 2004.
- [52]. M. Tymchyshyn, "Deep Desulphurization of Diesel Fuel", *Lakehead University*, 2008.
- [53]. Q. Wang, X. Liang, W. Qiao, C. Liu, X. Liu, L. Zhan, L. Ling, "Preparation of polystyrene-based activated carbon spheres with high surface area and their adsorption to dibenzothiophene", *Fuel Processing Technology*, 90, 381–387, 2009.
- [54]. J. Weitkamp, M. Schwark and S. Ernst, "Removal of thiophene impurities from benzene by selective adsorption in zeolite ZSM-5", *J. Chem. Soc., Chem. Commun.*, 1133–1134, 1991.

- [55]. D.L. King, T. Flynn, “Desulfurization of gasoline feedstock for application in fuel reforming”, *Society of Automotive Engineers, Detroit*. MI, 2000.
- [56]. S. H. Salem, “Naphtha Desulfurization by Adsorption”, *Ind. Eng. Chem. Res.*, 33, 336-340, 1994.
- [57]. J. L. Hu, Y. Wang, D. Vander Wiel, C. Chin, D. Palo, R. Rozmiarek, R. Dagle, J. Cao, J. Holladay, and E. Baker, “Fuel Processing for Portable Power Applications”, *Chem. Eng. J.*, 93, 55-60, 2003.
- [58]. C. Ngamcharussrivichai, C. Nuntang, S. Prasassarakich, “Adsorptive Removal of Thiophene and Benzothiophene Over Zeolites from Mae Moh Coal Fly Ash”, *Fuel*, 87, 2347-2351, 2008.
- [59]. K. Tang, et al., “Deep desulfurization by selective adsorption on a heteroatoms zeolite prepared by secondary synthesis”, *Fuel processing Technology*, 89,1 – 6, 2008.
- [60]. M. Muzic et al., “Evaluation of commercial adsorbents and their application for desulfurization of model fuel”, *Clean Techn Environ Policy*, 14, 283–290, 2012.
- [61]. J.G. Park et al., “Reactive adsorption of sulfur compounds in diesel on nickel supported on mesoporous silica”, *Applied Catalysis B: Environmental*, 81, 244–250, 2008.
- [62]. A.K. Bajpai, M. Rajpoot, D.D. Mishra, “Studies on the adsorption of sulfa pyridine at the solution–alumina interface”, *J. Colloid Interface Sci.*, 187 96–104, 1997.
- [63]. O. Etemadi, T.F. Yen, “Surface characterization of adsorbents in ultrasound assisted oxidative desulfurization process of fossil fuels”, *J. Colloid Interface Sci.* 313, 18–25, 2007.
- [64]. J. Wang, et al., “Alumina-supported manganese oxide sorbent prepared by sub-critical water impregnation for hot coal gas desulfurization”, *Fuel Processing Technology*, 2013.

- [65]. A. A. Adekanmi and A. Folorunsho, "Comparative Analysis of Adsorptive Desulphurization of Crude Oil by Manganese Dioxide and Zinc Oxide", *Res.J.Chem.Sci.*, 2, 14-20, 2012.
- [66]. L. Huang et al., "In situ XAS study on the mechanism of reactive adsorption desulfurization of oil product over Ni/ZnO", *Appl. Catal. B: Environmental*, 106, 26–38, 2011.
- [67]. J. Fan, G. Wang, Y. Sun, C. Xu, H. Zhou, G. Zhou, and J. Gao, "Research on Reactive Adsorption Desulfurization over Ni/ZnO–SiO₂–Al₂O₃ Adsorbent in a Fixed-Fluidized Bed Reactor", *Ind. Eng. Chem. Res.*, 49, 8450–8460, 2010.
- [68]. M. Suzuki, *Adsorption Engineering*, Kodansha Ltd., Tokyo, 1990.
- [69]. H. J. Ming, K. Ng, C. Yap, B. Saha, "Effect of pressure on the adsorption rate for gasoline vapor on pitch-based activated carbon", *J. Chem. Eng. Data*, 54, , 1504–1509, 2009.
- [70]. C. Borkar, D. Tomar, S. Gumma, "Adsorption of dichloromethane on activated carbon", *J. Chem. Eng. Data*, 55, 1640–1644, 2010.
- [71]. F. Liu, J. Wang, L. Li, Y. Shao, Z. Xu, S. Zheng, "Adsorption of direct yellow 12 onto ordered mesoporous carbon and activated carbon", *J. Chem. Eng. Data*, 54, 3043–3050, 2009.
- [72]. J.H. Kim, X. Ma, A. Zhou, C. Song, "Ultra-deep desulfurization and denitrogenation of diesel fuel by selective adsorption over three different adsorbents: a study on adsorptive selectivity and mechanism", *Catal. Today*, 111, 74–83, 2006.
- [73]. Y. Sano, K. Choi, Y. Korai, I. Mochida, "Adsorptive Removal of Sulfur and Nitrogen Species from a Straight Run Gasoil over Activated Carbons for its Deep Hydrodesulfurization", *Appl. Catal., B*, 49, 219–225, 2004.
- [74]. A. Zhou, X. Ma, C. Song, "Liquid-phase adsorption of multiring thiophenic sulfur compounds on carbon materials with different surface properties", *J. Phys. Chem. B*, 110, 4699, 2006.

- [75]. M. Seredych, J. Lison, U. Jans, T. Bandosz, "Textural and chemical factors affecting adsorption capacity of activated carbon in highly efficient desulfurization of diesel fuel", *Carbon*, 47, 2491, 2009.
- [76]. S. Kumagai et al., "Influence of solvent type on dibenzothiophene adsorption onto activated carbon fiber and granular coconut-shell activated carbon", *Fuel*, 89, 365–371, 2010.
- [77]. C. Rosas, et al., "Desulfurization of Low Sulfur Diesel by Adsorption Using Activated Carbon: Adsorption Isotherms", *Ind. Eng. Chem. Res.*, 49, 4372–4376, 2010.
- [78]. M. Muzica, K. Biondaa, Z. Gomzia, S. Podolskib, S. Telenb, "Study of diesel fuel desulfurization by adsorption", *Chemical engineering research and design*, 88, 487–495, 2010.
- [79]. G. Yu, S. Lu, H. Chen, Z. Zhu, "Diesel fuel desulfurization with hydrogen peroxide promoted by formic acid and catalyzed by activated carbon", *Carbon*, 43, 2285–94, 2005.
- [80]. Y.A. Alhamed, H.S. Bamufleh, "Sulfur removal from model diesel fuel using granular activated carbon from dates' stones activated by $ZnCl_2$ ", *Fuel*, 88, 87–94, 2009.
- [81]. B. Boulinguez, P. Le Cloirec, "Chemical transformations of sulfur compounds adsorbed onto activated carbon materials during thermal desorption", *Carbon*, 48, 1558–1569, 2010.
- [82]. D. R. Kumar, V. C. Srivastava, "Studies on Adsorptive Desulfurization by Activated Carbon", *Clean – Soil, Air, Water*, 40, 545–550, 2012.
- [83]. J. Xiao, C. Song, X. Ma, and Z. Li, "Effects of Aromatics, Diesel Additives, Nitrogen Compounds, and Moisture on Adsorptive Desulfurization of Diesel Fuel over Activated Carbon", *Ind. Eng. Chem. Res.*, 51, 3436–3443, 2012.
- [84]. L. Wang and R. Yang, "Graphene and Other Carbon Sorbents for Selective Adsorption of Thiophene from Liquid Fuel", *AIChE Letter: Separations: Materials, Devices and Processes*, 59, 29-32, 2013.

- [85]. I. Al Zubaidy, F. Bin Tarsh, N. Darwish, B.Sweidan, S. Abdul Majeed, A. Al Sharafi, and L. Abu Chacra, "Adsorption Process of Sulfur Removal from Diesel Oil Using Sorbent Materials", *Clean Energy Technologies*, 1, 66-68, 2013.
- [86]. N. Farzin Nejad et al., "Synthesis of magnetic mesoporous carbon and its application for adsorption of dibenzothiophene", *Fuel Processing Technology*, 106, 376-384, 2013.
- [87]. Z. Jiang, Y. Liu, X. Sun, F. Tian, F. Sun, C. Liang, W. You, C. Han, C. Li, "Activated Carbons Chemically Modified by Concentrated H₂SO₄ for the Adsorption of the Pollutants from Wastewater and the Dibenzothiophene from Fuel Oils", *Langmuir*, 19, 731-736, 2003.
- [88]. C.O. Ania, T. Badosz, "Metal-loaded polystyrene-based activated carbons as dibenzothiophene removal media via reactive adsorption", *Carbon*, 44, 2404-2412, 2006.
- [89]. Y. Wang, Yang, R. T. "Desulfurization of Liquid Fuels by Adsorption on Carbon-Based Sorbents and Ultrasound-Assisted Sorbent Regeneration", *Langmuir*, 23, 3825-3831, 2007.
- [90]. B. Cao, W. Shen and Y.Liu, "Adsorption desulphurization of gasoline by silver loaded onto modified activated carbons", *Adsorpt. Sci. Technol.*, 26, 595-609, 2008.
- [91]. J. Xiao et al., "Adsorption of Benzothiophene and Dibenzothiophene on Ion-Impregnated Activated Carbons and Ion-Exchanged Y Zeolites", *Energy & Fuels*, 22, 3858-3863, 2008.
- [92]. A. Zhou, X. Ma, C. Song, "Effects of oxidative modification of carbon surface on the adsorption of sulfur compounds in diesel fuel", *Appl. Catal., B*, 87, 190-199, 2009.
- [93]. V. Selvavathi et al., "Adsorptive desulfurization of diesel on activated carbon and nickel supported systems", *Catalysis Today*, 141, 99-102, 2009.
- [94]. M. Seredych and T. Badosz, "Adsorption of Dibenzothiophenes on Nanoporous Carbons: Identification of Specific Adsorption Sites Governing Capacity and Selectivity", *Energy Fuels*, 24, 3352-3360, 2010.

- [95]. M. Seredych, T. Bandoz, “Adsorption of dibenzothiophenes on activated carbons with copper and iron deposited on their surfaces”, *Fuel Processing Technology*, 91, 693–701, 2010.
- [96]. L. Xiong, X. M. Yan and P. Mei, “Synthesis and Characterization of a ZrO₂/AC Composite as a Novel Adsorbent for Dibenzothiophene”, *Adsorpt. Sci. Technol.*, 28, 341–350, 2010.
- [97]. R.N. Fallah, S. Azizian, “Removal of thiophenic compounds from liquid fuel by different modified activated carbon cloths”, *Fuel Processing Technology*, 93, 45–52, 2012.
- [98]. L. Xiong, X. Chen, X. M. Yan and P. Mei, “The adsorption of dibenzothiophene using activated carbon loaded with cerium”, *Porous Mater*, 19, 713–719, 2012.
- [99]. O. Karvan, A. Sirkeciog, H. Ataku, “Investigation of Nano- CuO/Mesoporous SiO₂Materials as Hot Gas Desulphurization Sorbents”, *Fuel Process.Technol.*, 90, 1452–1458, 2009.
- [100]. S. Maybodi, M. Teymouri, A. Vahid, A. Miranbeigi, “In Situ Incorporation of Nickel Nanoparticles into the Mesopores of MCM-41 by Manipulation of Solvent –Solute Interaction and its Activity toward Adsorptive Desulfurization of Gas Oil”, *J. Hazard. Mater*, 192, 1667–1674, 2011.
- [101]. T. Vu, T. Nguyen, H.M. Do, J.S. Park, “Fabrication of Photocatalytic Composite of Multi-Walled Carbon Nanotubes/TiO₂ and its Application for Desulfurization of Diesel”, *Mater. Res. Bull.*, 47, 308–314, 2012.
- [102]. R. N. Fallah et al., “Selective Desulfurization of Model Diesel Fuel by Carbon Nanoparticles as Adsorbent”, *Ind. Eng. Chem. Res.*, 51, 14419–14427, 2012.
- [103]. O.S. Chan, W.H. Cheung, G. McKay, “Preparation and characterisation of demineralised tyre derived activated carbon”, *Carbon*, 49, 4674-4687, 2011.
- [104]. J. V. Hinshaw, “Introduction to open–tubular column gas chromatography”, *Advanstar Communication*, 1994.
- [105]. H. M. Nair and E. J. Bonelli, Basic gas chromatography, Third Edition, Varian Inst. Group, California 1967.

- [106]. R. M. Silerstein, F. X. and Webster, Spectrometric identification of organic compounds, Sixth Edition, John Wiley & Sons, Inc. New York, 1996.
- [107]. F. W. MaLafferty, Interpretation of mass spectra, Fourth Edition, University Science books, California, 1993.
- [108]. K. Sing, D. Everett, R. Hau, L. Moscou, R. Pierotti, "Reporting physisorption data for gas solid systems with special reference to the determination of surface-area and porosity", *Pure Appl Chem*, 57, 603, 1985.
- [109]. T. Tsuchida, "Preparation and reactivity of acicular Al_2O_3 from synthetic diaspore, $\gamma\text{-Al}_2\text{O}_3 \cdot \text{H}_2\text{O}$ ", *Solid State Ionics*, 63 464-470, 1993.
- [110]. M. Zhareslu, M. Crisan, M. Preda, V. Fruth, S. Preda, "Al₂TiO₅-based ceramics obtained by hydrothermal process", *J. Optoelectron. Adv. Mater*, 5, 1411-1416, 2003.
- [111]. Y. b. Tang et al., "Preparation and characterization of activated carbon from waste ramulus mori", *Chemical Engineering Journal*, 203, 19-24, 2012.
- [112]. S. Velu, X. Ma, C. Song, "Selective adsorption for removing sulfur from jet fuel over zeolite-based adsorbents", *Ind Eng Chem Res*, 42, 5293-5304, 2003.
- [113]. E. S. Moosavi, S. A. Dastgheib and R. Karimzadeh, "Adsorption of Thiophenic Compounds from Model Diesel Fuel Using Copper and Nickel Impregnated Activated Carbons", *Energies*, 5, 4233-4250, 2012.
- [114]. X. Li, Z. Li, Q.B. Xia, H.X. Xi, "Effects of textural properties and surface oxygen content of activated carbons on the desorption activation energy of water", *Adsorpt. Sci. Technol.*, 24, 363-369, 2006.
- [115]. S. Kumar et al., "Studies on adsorptive desulfurization by zirconia based adsorbents", *Fuel*, 90, 3209-3216, 2011.
- [116]. M. Anbia, Z. Parvin, "Desulfurization of fuels by means of a nanoporous carbon adsorbent", *chemical engineering research and design*, 89, 641-647, 2011.
- [117]. S. Lagergren, "About the theory of so-called adsorption of soluble substances", *Kungliga Svenska Vetenskapsakademiens Handlingar*, 24, 1-39, 1898.

- [118]. G. McKay, Y.S. Ho, "Pseudo-second order model for sorption processes", *Process Biochem*, 34, 451–465, 1999.
- [119]. L. Wang, A. Wang, "Adsorption properties of congo red from aqueous solution onto surfactant-modified montmorillonite", *J. Hazard. Mater*, 160, 173–180, 2008.
- [120]. W. J. Weber, J.C. Morris, "Kinetics of adsorption on carbon from solution", *J. Sanit. Eng. Div. Proceed. Am. Soc. Civil Eng.* 89, 31–59, 1963.
- [121]. B.H. Hameed et al., "Equilibrium modeling and kinetic studies on the adsorption of basic dye by a low-cost adsorbent: Coconut (*Cocos nucifera*) bunch waste", *Hazardous Materials*, 158, 65–72, 2008.
- [122]. A. Suna Erses, M. Fazal, T. Onay, W. Craig, "Determination of solid waste sorption capacity for selected heavy metals in landfills", *J. Hazard. Mater*, 121, 223–232, 2005.
- [123]. K.R. Hall, L.C. Eagleton, A. Acrivos, T. Vermeulen, "Pore-and solid-diffusion kinetics in fixed-bed adsorption under constant-pattern conditions", *I&EC Fundam*, 5, 212–223, (1966).
- [124]. V.J.P. Poots, G. McKay, J.J. Healy, "Removal of basic dye from effluent using wood as an adsorbent", *J. Water Pollut. Contr. Fed.*, 50, 926– 935, 1978.

Vitae

Name :ABDULLAH ABDULLAH NAJI ALSWT

Nationality :Yemeni

Date of Birth :1976

Email :alswat99@yahoo.com

Address :Sana'a-Yemen

Academic Background :B.Sc. in Chemistry from Sana'a University in 2001